An Investigation of the Effectiveness of a Partial Cladding Pattern on Aluminum 7075 T651

by

©Evan Rendell B.Eng

A thesis submitted to the

School of Graduate Studies

in partial fulfillment of the

requirements for the degree of

Masters of Engineering

Faculty of Engineering and Applied Science

Memorial University of Newfoundland

January 2016

St. John's   Newfoundland and Labrador

Abstract

One of the primary motivations in developing new materials for the aerospace industry is maximizing specific strength.   An often conflicting goal in developing new materials is maximizing corrosion resistance. This is due to the realities of aging aircraft and the rising costs of inspection and maintenance. Currently all aluminum sheet and plate used in the aerospace industry is Alclad to increase corrosion resistance. The Alclad layer can make up 5% of the total plate thickness and does not carry any load. The goal of this work is to show that weight savings in aircraft structures can be achieved by substituting a partial cladding pattern for the continuous Alclad layer while maintaining equivalent corrosion resistance.

In this work, the corrosion resistance of aluminum 7075 T651 in the Alclad, partially clad and bare forms were compared after corrosion exposure in an acidic salt spray cabinet test. The degree of corrosion was then evaluated through visual inspection, analysis of cross-sections, tensile test and fatigue tests. Following this, single clad spot panels with varying spot sizes were produced and corroded to investigate if there is a more efficient clad spot size than what was selected for the medium sized test panel.

After corrosion exposure, severe to moderate exfoliation corrosion was observed on the unprotected medium sized test panel, light general corrosion was observed on the upper section of the partially clad panel and patches of corrosion not penetrating past the clad layer were observed on the Alclad panel. Tensile and fatigue tests showed that the Alclad and partially clad tests panes resisted degradation of mechanical properties due to corrosion similarly well while outperforming the bare test panel.

Acknowledgements

I would like to thank Memorial University for funding and for providing the facilities necessary for me to conduct my Masters of Engineering research and thesis work.

I would like to express a special appreciation and thanks to my supervisors Dr. Amy Hsiao and Dr. John Shirokoff for providing guidance and support during my research and throughout my thesis writing process.

I would also like to thank Bombardier Inc., the Research & Development Corporation of Newfoundland and Labrador (RDC) and the Province of Newfoundland and Labrador for providing a large portion of my funding.

Finally, I would like to give special thanks to my girlfriend and family for providing moral and emotional support and encouragement during my time as a Masters student.

Table of Contents

List of Figures

List of Tables

1. Introduction

One of the primary drivers for materials selection in the aerospace industry is to maximize the economic efficiency of aircraft [1]. Commercial aircraft of the past utilized the high specific strength of the high strength aluminum alloys of the 2000 and 7000 series almost exclusively for the construction of structural components [2]. These materials were selected in an effort to minimize aircraft weight resulting in maximized aircraft payloads and reduce fuel consumption. High strength aluminum alloys are susceptible to localized corrosion such as pitting, exfoliation and stress corrosion cracking. Presently, corrosion resistance of materials is also of great concern because of the cost of corrosion inspections and the high cost of unscheduled maintenance and aircraft downtime associated with replacing corroded aircraft components [3, pp. 18.8-18.9]. Corrosion as well as the ability to construct larger structural components that are more easily joined has resulted in a shift in preferred construction materials from high strength aluminum alloys to composites for new aircraft [1]. In spite of this, aluminum alloys will remain an important structural material for aircraft components, especially in compression where composites are less suitable. This shift in materials selection has caused the need for aluminum alloy innovation to maximized specific strength while maintaining acceptable corrosion resistance for aluminum to remain a competitive material choice [2].

The susceptibility of high strength aluminum alloys to corrosion requires them to be protected from corrosive environments using an anodic coating for components with complex geometries or by using Alclad products with an aerospace coating system for sheet and plate components. Alcald products are produced by the metallurgical bonding of a high strength aluminum alloy

core sandwiched between two layers of a more electronegative aluminum alloy. The outer aluminum cladding layers corrode preferentially when exposed to a corrosive environment and prevent corrosion to the core by cathodic protection. The Alclad layers can comprise up to 4% of the total sheet or plate thickness [4] and is assumed to carry no load, reducing the overall material specific strength by increasing the weight without contributing to the strength.

Sp.G. Pantelakis et al. have suggested in previous work that a continuous cladding layer may be excessive and that the application of a partial cladding pattern may provide equivalent corrosion protection for aluminum 2024 T3 alloys [5]. They have found that a partial cladding layer covering only 7% of the core aluminum substrate provides equivalent corrosion protection to the mechanical properties of Al 2024 T3 when compared to Alclad products after a 300 hour immersion exposure in a neutral 3.5% NaCl solution. However, they have also concluded that this accelerated corrosion test is likely too mild to accurately represent the corrosion environment experienced by in service aircraft.

The objective of the present work is to expand on the concept of increasing the specific strength of aerospace aluminum alloys by investigating the partial cladding corrosion resistance of Al 7075 T651. A more aggressive accelerated corrosion test, thought to better represent the aerospace corrosion environment, was selected for this investigation using a 300 hour continuous acetic acid salt spray test. First, a square test panel with single central clad spot having a total area of 100 cm^2 and a clad spot area of 1 cm^2 was exposed to the selected corrosion environment. From this test panel, the surface area effectively protected from corrosion was estimated and used to determine dimensions for a medium sized test panel with

a partial cladding pattern. The partially clad medium scale test panel was produced and compared to an Alclad test panel and a test panel with the entire cladding layer removed after exposure in the 300 hour acedic acid salt spray test. Visual observations and cross-sections were made of each of the test panels to determine the forms and extent of corrosion on each medium sized test panel. Tensile and fatigue specimens were machined from each of the corroded tests panels and produced from non-corroded aluminum alloy having undergone the same surface machining processes as the medium sized panels. These specimens were tested and compared to determine the degradation in tensile and fatigue properties of the three panel cases due to corrosion exposure. Conducted in tandem to the medium scale test panels, three single central clad spot panels were produced with varying central clad spot dimensions. The series of central single clad spot panels were exposed to the same corrosion environment and the extent of corrosion relative to the clad spot was determined. The goal of this test was to determine if there was a relationship between the central clad spot size and the area and extent of corrosion protection provided by the clad spot.

Some limitations in this work include that the primary loads applied to Al 7075 T651 in aircraft structures are compressive while the tests conducted in this experiment after corrosion exposure are in tension. This decision was made primarily due to testing equipment available at Memorial University.

The effectiveness of partial cladding patterns for the protection of high strength aluminum in combination with aerospace coating systems has not been directly addressed in this work. For a sacrificial cladding layer to be successful in protecting a high strength aluminum core, the

cladding layer needs to be exposed to the corrosion environment and electrically connected to the core. Aerospace coating systems effectively isolate the protected aluminum. The cladding layer acts as a safeguard if the coating system is flawed or damaged. If a flaw or damage to the coating system does not expose a clad spot, it will likely not be effective in protecting the exposed aluminum core.

For partial cladding to become a viable alternative to Alclad products in the aerospace industry consideration needs to be made on how the cladding layer will be commercially produced. Any increase in production costs would need to be shown to be surpassed by fuel savings in aircraft operations due to decreased aircraft weight.

2. Statement of Objectives

The funding for this research was made available through the purchase of Bombardier 415 "Superscooper" aircraft by the Government of Newfoundland and Labrador and the Industrial Regional Benefits Program. The Bombardier 415 "Superscooper" is an amphibious water bomber that is used worldwide in firefighting operations. While fulfilling this roll, the Bombardier 415 is exposed to corrosion environments above and beyond those of regular aircraft. The "Superscooper" is routinely in intimate contact with marine environments while collecting fresh or salt water for firefighting operations and is capable of landing in bodies of water or unpaved runways when operating in remote locations [6].

This funding provided an opportunity to conduct corrosion research on aircraft materials used in the construction of the Bombardier 415 that are exposed to harsh marine environments and the coating systems designed to protect them from corrosion. Currently all of the high strength aluminum plate or sheet used in the construction of aircraft is protected from corrosion by a continuous cladding layer known as Alclad. This cladding layer does not support any load but acts as a sacrificial anode protecting the corrosion susceptible high strength aluminum core through cathodic protection [5]. The goal of this research is to investigate the feasibility of reducing the amount of cladding used to protect aerospace sheet and plate from a continuous layer to a discontinuous partial cladding pattern. If it could be determined that the corrosion protection provided by a partial cladding is equivalent to Alclad it could benefit the Bombardier 415 by reducing the weight of aluminum structural components. This would in turn reduce fuel

costs and increase the payload capabilities of the Bombardier "Superscooper" and of all other

aircraft using aluminum for major structural components.

3. Literature Review

3.1 Aerospace Corrosion Environment

The commercial aerospace environment can present many challenges for the corrosion protection of the high strength aluminum alloys used in this industry [7]. Aircraft are exposed to a variety of outdoor atmospheres depending on the region where they are operating. In these environments the exterior of aircrafts can be exposed to many corrosive substances such as air pollutants from local industry and salt from maritime environments. The aircraft exteriors are also exposed to cyclic temperatures from the transition between colder high altitudes to warmer low altitudes. These cyclic temperatures can lead to embrittlement and damage to protective coatings that exposed the underlying aluminum alloy to corrosion. The landing and taking off process also results in cyclic stresses in components such as the wing skins and landing gear that can result in stress corrosion cracking or corrosion fatigue if corrosion protection on these parts is insufficient or flawed. Condensation can also be formed within crevices such as the wing interiors or wheel wells, this moisture can cause crevice corrosion.

Within the aircraft there are again many opportunities for corrosion to occur. Spills from the galley, the lavatory or leaks from onboard batteries or hydraulic fluid can cause highly corrosive environments if not properly drained. Condensation often forms within the aircraft due to the pressurized cabin.

The design of aircraft can also lead to many corrosion issues as there are often areas that are difficult to inspect such as lap joints that can promote crevice corrosion if exposed to moisture.

Contact of dissimilar metals is sometimes unavoidable in aircraft construction and can cause galvanic corrosion if the dissimilar metals are not properly isolated from each other [7].

To protect against these forms of corrosion, susceptible aluminum alloys are protected by either a corrosion resistant coating system or by anodizing parts. Crevices can be treated with corrosion inhibitors and sealants can be used where dissimilar metals are in contact. These forms of protection can be damaged or flawed requiring constant corrosion monitoring to ensure the safety of commercial aircraft.

3.2 Corrosion of Aluminum Alloys

Aluminum is highly reactive metal that quickly forms aluminum oxide when exposed to oxygen. This oxide layer has excellent adhesion to the aluminum substrate when it is formed, is resistant to many forms of chemical attack, is a good electrical insulator and will quickly reform if damaged. This combination of properties results in aluminum exhibiting passivation behavior in many environments. This means that the rate of corrosion of aluminum will quickly decrease over a very short period of time and will be protected from general corrosion in many corrosive environments such as in the atmosphere or in sea water [8, p. 1986].

Although aluminum is very resistant to general corrosion, some alloys are susceptible to localized corrosion, primarily those that have copper as a major alloying element (2000 and 7000 series alloys). The forms of localized corrosion that most commonly affect aluminum alloys are: pitting, crevice corrosion, intergranular corrosion, environmentally assisted cracking and filiform corrosion. These forms of corrosion can be divided into two major categories. The first category including pitting, crevice corrosion and filiform corrosion depend on a local

environment being formed that is aggressive to the passive oxide layer and allows corrosion to take place. While intergranular corrosion and environmentally assisted cracking are more dependent on the metallurgical composition and thermal history of the aluminum alloy.

Pitting corrosion is the most common form of corrosion observed on aluminum alloys. Pitting occurs at near neutral pH where the passive film is the most stable. Pit initiation occurs at locations when there is a flaw in the passive oxide layer. This flaw can be the result of a discontinuity in the oxide film, mechanical defects in the aluminum substrate or a weakening of the film caused by second phase particles in the aluminum alloy. Pitting will occur in the presence of a halide ion in solution, most often chlorine, which helps to break down the oxide layer. Once the pit growth has initiated it will progress due to the formation of hydrogen ions at the pit base creating an intensely acidic environment aggressive to the reformation of the oxide layer. Generally pit growth for aluminum alloys is self-limiting and will stop once the pit has reached a certain size and the pit will repassivate.

Crevice corrosion is the result of a small confined space created by the physical arrangement of an aluminum structure or by the arrangement of aluminum and a non-metal. When this crevice is exposed to a fluid, a gradient in the concentration of oxygen ions can be formed with oxygen depletion at the base of a crevice and an oxygen rich area at the opening of the crevice. This oxygen ion distribution will create a local galvanic cell that will corrode the aluminum alloy at the base of the crevice. The pH at the base of the crevice becomes more acidic and chloride ions become more concentrated if present in the electrolyte [9, pp. 578-582].

Filliform corrosion is similar to crevice corrosion but it occurs in the atmosphere when a coating is applied to the aluminum substrate and relative humidity is between 55% and 95%. Corrosion initiates at a flaw in the coating and propagates under the coating in wormlike filaments. Like crevice corrosion, there is a region of oxygen depletion where new aluminum oxide film is being formed at the "head" of corrosion filament and a region of higher oxygen concentration at the "tail" of the filament where oxygen is replenished by the atmosphere. This gradient in oxygen concentration causes a local galvanic cell driving the corrosion process. The pH at the "head" of the corrosion filament drops drastically as it grows weakening any newly formed oxide film. The corrosion products at the "tail" of the filament swell and cause cracking and delamination to the coating, allowing oxygen concentrations to rise at the "tail" and continue the corrosion process.

Intergranular corrosion is a form of corrosion that is the result of aluminum alloy microstructure. In the case of alloys with copper as a major alloying element, second phase copper rich particles (Al_2Cu) are formed at the grain boundaries during the cooling process after formation. The precipitation of these copper rich particles deplete copper from the region adjacent to the grain boundaries and make them more electronegative when compared to the alloy grains that still have copper is solid solution. A galvanic cell is formed between the anodic region adjacent to the grain boundaries and the cathodic grains resulting in corrosion at the grain boundaries. Aluminum alloys with magnesium as a major alloying element have magnesium rich second phase particles (Mg_2Al_3) forming at the grain boundaries. These particles are anodic relative to the alloy grains and intergranular corrosion becomes a problem when an alloy is heated for an extended period of time and the magnesium rich particles grow

and coalesce creating a continuous path for the intergranular corrosion to propagate. The sensitivity of aluminum alloys to intergranular corrosion is largely dependent on the heat treatments applied because this dictates the abundance and distribution of the second phase particles that are the root cause. For copper containing aluminum alloys, overaging tempers (T7) can be used. This allows second phase copper containing particles to precipitate within the alloy grains, mitigating the potential difference between the grains and the copper depleted regions adjacent to the grain boundaries. Overaging tempers come at the cost of reduced alloy strength of up to 20% [10]. Magnesium containing alloys can be protected from intergranular corrosion by avoiding elevated temperatures for extended periods of time, preventing the Mg_2Al_3 particles from forming a continuous path along the grain boundary. Intergranular corrosion is often aggravated by pitting corrosion that develops first and exposes large numbers of grain boundaries to the corrosive environment. Inergranular corrosion has a larger detrimental effect on the fatigue resistance of aluminum alloys when compared to pitting corrosion because the corroded area is much sharper resulting in higher stress concentrations under cyclic loading. Like pitting corrosion, the penetration of intergranular corrosion is generally limited by oxygen depletion at the final depth of the corroded grain boundaries. Once this depth is attained, the intergranular corrosion will spread laterally over surface of the affected aluminum alloy.

Environmentally assisted cracking is an umbrella term that refers to hydrogen embrittlement, corrosion fatigue and stress corrosion cracking. Each of these three forms of aluminium corrosion cracking can cause premature failure of an aluminum structure in many environments but it is also possible that they are working in tandem. It is not always clear which cracking

mode is dominant as one may be playing a larger role in crack initiation, while another in crack propagation. Hydrogen embrittlement can aggravate or may be a key mechanism in both corrosion fatigue and stress corrosion cracking [11, pp. 297-299].

Hydrogen embrittlement is the brittle crack propagation of an aluminum structure caused by hydrogen absorption into the solid metal solution. The source of the hydrogen can be during the aluminum forming process or during aluminum corrosion. Hydrogen absorption at existing crack locations can be facilitated by stress assisted diffusion and dislocation transport. The presence of the hydrogen at cracks can cause local plasticity resulting in the brittle behavior of the aluminum alloy [11, pp. 292-293].

Corrosion fatigue is the failure of an aluminum structure in a corrosive environment at cyclic loadings below the yield strength for the material. The precise mechanisms for corrosion fatigue initiation and propagation are topics currently being studied. Corrosion fatigue has been observed commonly initiating at pits or intergranular corrosion created due to localized corrosion and propagating under cyclic loading once the surface flaw has reached a critical size [9, pp. 586-587]. Corrosion fatigue in aluminum is typically transgranular, and is characterized by an "oyster shell" fracture surface formed from numerous plastic deformations or crack "jumps" caused by the combined effect of a corrosive environment and cyclic loading [11, pp. 278-279].

Stress corrosion cracking (SCC) is a brittle intergranular cracking phenomenon that occurs to a metallurgical susceptible alloy in the presence of a corrosive environment and a sustained stress. The aluminum alloys susceptible to SCC are those that are susceptible to intergranular

corrosion, meaning they form second phase intermetallic particles during their heat treatment that cause the grain boundaries or the area adjacent to the grain boundaries to become anodic relative to the majority off the alloy. SCC of aluminum alloys occurs in humid or aqueous environments and is aggravated by the presence of halides, most commonly chloride. The sustained static stresses that lead to SCC can be residual tensile stresses at the structure surface from the aluminum production process as well as static loads applied to aluminum structures. The tensile stresses that cause SCC are much lower than the yield strength of the affected material. The main mechanisms believed to explain SCC are based on either anodic dissolution in the presence of a sustained tensile stress or hydrogen embrittlement at grain boundaries during a sustained tensile stress [12]. SCC progression is greatest at acidic pH values and decreases with decreasing pH. Heat treatments that reduce an aluminum alloys susceptibility to intergranular corrosion will also reduce the susceptibility to SCC but the optimal heat treatment for protection against both forms of corrosion is rarely the same. Thinner aluminum products such as aluminum sheet are not susceptible to SCC and Alclad aluminum products are generally immune. Thicker aluminum alloy plate products can be stretched to relieve internal stresses and increase resistance to SCC [13, pp. 102-103].

3.3 Corrosion Specific to Al 7075 T651

Aluminum 7075 T651 is among the strongest aluminum alloys but is also among the most susceptible to general and pitting corrosion; only alloys from the 2000 series are less resistant to these forms of corrosion [13, pp. 33-35]. The susceptibility of Al 7075 T651 to pitting and general corrosion is primarily due to the addition of copper as an alloying element, copper

containing intermetallic particles can have a detrimental effect on the alloy's protective oxide film [13, p. 35].

The forms of corrosion that are the most detriment to the service life of Al 7075 T651 are intergranular in nature. Al 7075 T651 is susceptible to stress corrosion cracking and intergranular corrosion. In the case of Al 7075 T651, second phase precipitates consisting of Mg_2Al_3 and $MgZn_2$ form at the alloy grain boundaries during the aging process. These particles are anodic relative the bulk of alloy and provide an anodic path to facilitate intergranular corrosion [11, pp. 218-222].

For Aluminum 7075 T651 plate, intergranular corrosion generally takes the form of exfoliation corrosion. Exfoliation is a special case of intergranular corrosion where in addition to the alloy having an anodic path along the grain boundaries, the grain boundaries are elongated from the aluminum plate rolling process. Exfoliation is generally initiated at the large number of grain boundaries exposed at the cut edges of the alloy plate or at rivet holes. Exfoliation can also be initiated from pitting over the alloy surface. Exfoliation differs from other forms of intergranular corrosion because the elongated grain boundaries allow large thin non-corroded "sheets" to be lifted away from the aluminum alloy substrate by the wedging action of corrosion bi-products within the corroded grain boundaries [11, pp. 224-225].

The exfoliation and stress corrosion cracking resistance of Al 7075 can be improved by applying overaging tempers (T7) to the alloy. These heat treatment processes allow second phase precipitates to form within the alloy grains, reducing the potential difference between the

grains and grain boundaries. Overaging tempers reduce the alloy susceptibility to intergranular corrosion but also reduces the mechanical strength of the alloy by up to 20% [10, p. 69].

Aluminum 7075 T651 should only be used when appropriately protected from corrosion. This corrosion protection generally comes in the form of applying an anodizing process which artificially thickens the passive oxide layer or by applying a cladding layer which acts as a sacrificial anode, protecting the Al 7075 core from corrosion.

3.4 Cladding of Aerospace Aluminum

Aluminum is generally considered to be very resistant to corrosion in most situations. This resistance to corrosion is attributed to a rapidly forming aluminum oxide layer that forms on the outer surface of the metal when exposed to oxygen. This layer is not easily dissolved in neutral pH and is a good electrical insulator [8, p. 1986].

The aluminum alloys most widely used in the aerospace industry are the 2000 and 7000 series alloys due to their high strength to weight ratios. These alloys are however prone to localized corrosion. Zero tolerance for corrosion in the aerospace applications due to safety concerns makes reliance on corrosion protection from the aluminum oxide layer insufficient. Simply adding protective coatings to these alloys is also insufficient because any damage or defects will allow localized corrosion to initiate.

In 1927 Alcoa produced the first commercially viable solution to this problem by developing Alclad aluminum sheet and plate products. Alclad products are produced by hot rolling two thin sheets of pure aluminum with a core of high strength aluminum, metallurgical bonding the layers into a composite sheet. Initially, the objective was to simply combine the excellent

corrosion resistance of pure aluminum with the desirable mechanical properties of high strength 2000 series alloys. However, after conducting corrosion experiments, it was discovered that the unprotected edges of the 2000 series aluminum alloys were also not affected by corrosion. It was then determine that the pure aluminum layer was not simply acting as a corrosion resistant barrier but was also providing cathodic protection to the high strength aluminum alloy core [14].

Since this discovery, two main aluminum alloys have been developed as the Alclad layer used in the aerospace industry. Al 1050A alloy is generally used for cladding 2000 series alloys and Al 7072 alloy is generally used for cladding 7000 series alloys. The Alclad plate and sheet used in the aerospace industry has the cladding layer applied to both sides with an average thickness of 2-5% of the total sheet or plate thickness per side [10, pp. 197-198].

3.5 Previous Work in Justifying Partial Cladding Patterns

In previous works, Sp.G. Pantelakis et al. explored the concept of protecting aerospace aluminum plate and sheet with a localized cladding pattern rather than a continuous Alclad layer [15], [5]. The primary objective of these works was to investigate if a localized cladding pattern is able to provide equivalent corrosion protection when compared to Alclad. The stated benefits of using a localized cladding pattern is weight savings on aircraft structures and possibly improving the fatigue characteristics of the material.

In the first paper [15], the authors set up the premise for a localized cladding pattern by investigating the roll of the cladding layer in the corrosion protection of 2024 T3 aerospace aluminum plate. The aluminum plate used in this experiment was 3.2 mm thick with a cladding

layer 0.15 mm thick composed of 1230 aluminum on each face. A series of tensile specimens were produced in accordance to ASTM E8M-94a [16] with a range of the cladding layer surface area removed. The cladding layer of the prepared tensile specimens was mechanically removed through milling such that 75%, 70%, 68.5%, 65%, 30%, 10% and 3% of the cladding layer remained on both faces. The corrosion environment chosen for the experiment was ASTM G34 the Standard Test Method for Exfoliation Corrosion Susceptibility in 2XXX and 7XXX Series Aluminum Alloys (EXCO test) for a duration of 36 hours. The EXCO exfoliation test is an immersion test where the corrosion solution is composed of 18 wt% NaCl, 3.9 wt% KNO_3 and 0.47 wt% HNO_3 with the remainder distilled water [17]. After the corrosion exposure, mild pitting was observed on or in close proximity to the cladding layer. The pitting occurring on the cladding layer penetrated to the 2024 core and the pits widened leaving the core unaffected. This confirmed that the cladding layer was providing cathodic protection for the high strength aluminum core. The results of the tensile tests showed a gradual reduction in material tensile strength with a reduction of the cladding surface area. The authors observed a drastic drop in elongation to failure between the 30% and 10% cladding surface area samples. Similar fracture surfaces were observed between the non-corroded and the 36 hour EXCO exfoliation test for the fully clad and partially clad samples. The authors concluded that a 30% cladding surface area is sufficient when compared to the fully clad samples to protect the mechanical integrity of 2024 T3 aluminum plate when exposed to a 36 hour EXCO exfoliation test.

The second paper [5] attempts to build on the work of the first in providing further evidence that a localized cladding pattern could provide equivalent corrosion protection when compared to a continuous cladding layer. The material selected in the second paper is 2024 T351

17

aluminum; the cladding material and the overall thickness of the aluminum plate were not reported by the authors. The corrosion environment used in the following experiments was a 3.5% NaCl neutral (pH 5.8-6.1) immersion test. This test is significantly less aggressive than the EXCO exfoliation test. The authors first, for comparison, corroded a bare 2024 aluminum sample for 100 hours followed by cleaning by immersion in HNO_3. The surface of the sample exhibited signs of general corrosion with pitting of an average depth of 5 µm and a maximum pit depth of 15 µm.

Three 40 mm diameter circular panels were then then prepared with a varying diameter (2, 3 and 4 mm) central clad spot by removing the clad layer through mechanical milling. These samples were corroded similarly to the bare samples with the exception that back clad face was isolated from the corrosion environment with natural wax. Four major observations were the result of this experiment:

1. The type of corrosion changed from general corrosion to pitting corrosion for samples with the central clad spot. The surface of the samples remained non-corroded with the exception of the 2 mm panel that did have some surface roughness indicating some general corrosion.
2.   The average depth of pitting increased with increasing distance from the central clad spot. The rate of increase was larger as the clad spot area decreased.
3. There was no relationship between distance from the clad spot and maximum pit depth.
4. Pitting density increased with distance from the clad spot for the 2 and 3 mm clad spot samples while it remained constant for the 4 mm sample.

From these observations the authors decided to produce a larger test panel with the cladding

ratio of the 4mm clad spot sample to test the effect of increasing the sample scale. The larger

test panel had a square shape and dimensions of 100x100 mm with a square central clad spot

of 10x10 mm. Average pit depth remained constant throughout the panel (30 µm) but the

authors found that there was a higher probability of deeper pits (30-70 µm) at larger distances

from the clad spot. Using the Vallellano notch model [18] and calculating stress concentration

factors relative to distance from the clad spot, a region of acceptable pitting damage was

determined as 27.5 mm from the clad spot.

Three larger test panels (400x400 mm) were then produced having an unclad, fully clad and

spot clad pattern surface. The spot clad pattern having the dimensions determined above of

10x10 mm clad spots arranged in an two dimensional array separated by 27.5 mm, the cladding

layer removed from the panel between the clad spots by mechanical milling. These panels

were exposed to the corrosion environment for a 300 hour period and cleaned in the methods

described above. Tensile and fatigue test specimens were then machined from the test panels

in accordance to the ASTM E8 [19] and the ASTM E466 [20] standards and tested. In the unclad

tensile samples, there was a reduction in the tensile strength and yield strength of 13% and

12% respectively after corrosion exposure. Also, in the fully clad tensile samples, there was a

reduction in the tensile strength and yield strength of 10% each. For the spot clad tensile

samples, there was a negligible reduction in the tensile strength and a reduction in the yield

strength of 10%. The authors do not provide an explanation as to why the tensile strength of

the spot clad panels is not affected by the corrosion environment but suggested that the

corrosion environment was too mild for definitive results. The authors also reported that the

elongation to failure for the three panels increased after being corroded and suggested further investigation was necessary.

The fatigue behavior of the unclad panel was better than the fully clad and spot clad panels. This was explained by the fact that under cyclic loading, the softer cladding layer cracks prematurely relative the much harder core and the cracks propagate into the core. There was no difference observed in the fatigue behavior between the fully clad and the partially clad panels. The authors again conclude that the chosen corrosion environment is too mild to differentiate between the two cases.

4. Experimental Setup

4.1 Experimental Objectives and Summary

The goal of the following series of experiments was to test the use of a partial cladding pattern on aerospace aluminum alloys for corrosion resistance when compared to Alclad aluminum. If a partial cladding pattern is found to be sufficiently resistant to corrosion it could lead to a significant reduction in aircraft weight through the use of a partial cladding pattern or by showing that the cladding currently used in the aerospace industry is excessive and can be reduced to optimize aircraft weight and corrosion resistance.

This objective was to be accomplished by building on the previous work conducted by Sp.G. Pantelakis et al. [5], [15] in several ways. The authors in the previous work concluded that the corrosion environment they selected was not aggressive enough to produce definitive results. In this work, the selected corrosion environment was an acetic salt spray cabinet test. This corrosion environment is more aggressive than the neutral salt immersion test used by Sp.G. Pantelakis et al. [5] and may be considered more representative of the corrosion environments experience by in service aircraft. The aluminum alloy selected in this experiment is also notably different than the aluminum 2024 T351 selected in the previous work [5], [15]. The selected aluminum 7075 T561 is also commonly used in aircraft construction but has significantly different alloying elements than 2024. The primary differences are that aluminum 7075 includes zink as the major alloying element and has a larger weight percent of magnesium with a smaller weight percent of copper when compared to aluminum 2024. These differences in alloying elements result in different mechanical properties and corrosion behavior.

Three sets of tests were performed to investigate the effectiveness of a partial cladding pattern for the corrosion protection of Al 7075 T651. First, to determine reasonable dimensions for a partial cladding pattern to be applied to a medium sized panel, a 1 cm^2 single clad spot panel was machined and exposed to the acetic salt spray environment. A 2.5 mm grid was applied to the corroded surface of this panel and the degree of surface corrosion was evaluated relative to the clad spot. To investigate the depth of corrosion penetration, 0.17 mm was milled from the panel thickness and the corrosion relative to the clad spot penetrating this depth was evaluated.

From the results of the initial single clad spot test, a medium sized test panel with a partial cladding pattern was machined. To show that a partial cladding pattern provides equivalent resistance when compared to a fully clad panel, a fully clad panel and a panel with the cladding removed were produced for comparison. All three panels were exposed to the same acidic salt spray environment. After exposure, the corrosion on the test panels was visually characterized and compared. Representative cross-sections were cut from the panels and analyzed with a microscope. To determine the degradation in mechanical properties due to corrosion, un-corroded tensile and fatigue specimens were machined and tested to compare to the tensile and fatigue specimens produced from the three corroded panels.

The third test was conducted to investigate the relationship between clad spot size and the size and effectiveness of the area protected by the clad spot. This was also done to validate choice for a 1 cm^2 clad spot in the partial cladding pattern and check for a more optimal clad spot size. For this experiment, three central clad spot panels were machined with various clad spot sizes

of 0.5 cm^2, 1 cm^2 and 2 cm^2. After corrosion exposure, the extent of corrosion damage relative to the clad spot was evaluated on the panel surfaces and at a depth of 0.17 mm using a 2.5 mm grid.

4.2 Materials Selection

Aluminum 7075 T651 has found extensive use in the aerospace industry due to the alloy's combination of high strength, moderate toughness and corrosion resistance. In commercial aircraft, Al 7075 T651 is commonly selected for applications requiring high strength such as upper wing skins, wing tension members and fuselage skins [1]. In these applications, Al 7075 T651 plate and sheet is clad with Al 7072 to improve corrosion resistance.

The major alloying elements in Al 7075 are zinc, magnesium and copper. The acceptable composition ranges and the composition of the aluminum plate used in this research can be seen in Table 4.1. The primary source of strengthening for the Al 7075 alloy is precipitation hardening where second phase particles of $MgZn_2$ are formed and impede the motion of dislocations. The addition of copper to the alloy improves strength and reduces susceptibility to stress corrosion cracking. Chromium is also added to improve resistance to SCC by promoting precipitate formation within grain boundaries. Chromium has the added benefit of reducing grain recrystallization, promoting retention of elongated grain structures formed during cold working. Iron and silicon are impurities that can reduce the alloy fracture toughness if their concentrations are not minimized [21, pp. 185-194].

Table 4.1: Literature and received Alclad aluminum 7075 T651 alloy compositions measured by energy-dispersive X-ray spectroscopy

	Al	Zn	Mg	Cu	Fe	Si	Mn	Cr	Ti	Other (total)	Other (each)
7075 Lit [4]	Balance	5.10-6.10	2.10-2.90	1.20-2.00	0.0-.50	0.0-0.40	0.0-0.30	0.18-0.35	0.0-0.20	0.0-0.15	0.0-0.05
7075	90.78	4.43	2.86	1.50	0.10	0.0	0.03	0.30	0.0	0.0	0.0
7072 Lit [22, p. 330]	Balance	0.8-1.3	0.0-0.10	0.0-0.10	0.0-0.70 Fe+Si		0.0-0.10	-	-	0.0-0.15	0.0-0.05
7072	98.06	0.79	0.33	0.0	0.80		0.0	0.01	0.01	0.0	0.0

The T651 temper maximizes the strength of Al 7075 but increases the alloys susceptibility to exfoliation and SCC. The T6 temper designation means that the alloy was solution heat treated, followed by a water quench and artificially aged. The Tx51 temper designation means that the alloy was stress relieved through stretching to improve SCC resistance.

4.3 Accelerated Corrosion Environment

The corrosion environment selected for this experiment was a continuous acidic salt fog cabinet test in accordance to ASTM G85 Annex A1 [23]. The test cabinet used was the 120 liter, bench top, Ascott S120ip salt spray chamber. The length of the corrosion exposure was selected as 300 hours for all of the experiments.

The acidic salt spray solution used during the testing had a pH of between 3.1 and 3.3, with a 4-6 weight percent sodium chloride concentration. The water used for the bulk solution was in accordance to ASTM D1193 [24] and was prepared using a Purite DC9 water deionising cylinder. The pH of the salt spray solution was adjusted by adding 99.7+% ACS reagent grade acetic acid to the bulk solution. The pH was measured using an Oakton pH tester. The salt used in the

experiment was "Corro-Salt" purchased from Ascott. This salt was selected because it conforms to the impurity limits outlined in ASTM B117 [25], namely: total impurities less than 0.3%, a halides composition (excluding chloride) of less than 0.1%, a copper content of less than 0.3 ppm and no added anti-caking agents. The salt content of the salt spray solution was measured using a hydrometer to determine the solution density in combination with data relating solution density and salt content provided in ASTM G85 [23].

The samples were arranged in the salt spray cabinet at an angle of 10° and spaced out in such a way that the acetic salt fog collected on a sample would not drip onto other samples. An example of such an arrangement can be seen in Figure 4.1. The cabinet temperature was kept at 36°C. The rate of fog deposition within the salt spray chamber was adjusted to 1.0 to 2.0 mL per hour per 80 cm^2 horizontal area by varying the acetic salt spray solution flow rate and the air supply pressure to the fog atomizer. The rate of fog deposition was measured with two 10 cm diameter circular fog collectors, one placed near the fog atomizer and the other furthest possible away. The volume of collected fog was measured every 24 hours during the test (excluding weekends and holidays) and the pH and density were determined to ensure proper corrosion environment conditions in the salt spray chamber.

Figure 4.1: Inside of the salt spray chamber

4.4 Test Specimens

The test specimens used in the experiment were machined from one continuous piece of 6.35 mm thick Alclad aluminum 7075 T651 plate. All of the samples had the back surface, cut edges and a 1 cm strip along the perimeter of the front surface isolated from the corrosion environment with 0.54 mm polyvinyl chloride corrosion resistant tape. The seams between the strips of tape were sealed with super glue gel. These surfaces were isolated from the corrosion environment to prevent electrical interaction between the clad back surface of the samples and the corroding front surface where the cladding was partially or fully removed for many of the samples. The samples were cleaned after machining with low-lint wipes and 99.7% acetone.

4.4.1 Initial 1 cm^2 Central Clad Spot Panel

The goal of the first corrosion test was to produce a test specimen to determine appropriate

dimensions for a partial cladding pattern that will provide equivalent corrosion protection when

compared to a continuous cladding layer. A 12x12 cm square test specimen was machined with

a 1x1 cm square central clad spot. The cladding layer was removed over the remainder of the

front surface by mechanically milling 0.19 mm from the thickness. The milling marks were

removed by sanding the milled surface by hand. The area of the surface exposed to the

corrosion environment was 10x10 cm after the corrosion resistant tape was applied.

4.4.2 Medium Sized Test Panels

The goal of the medium sized test panels was to compare the corrosion resistance of fully clad,

spot clad and bare aluminum 7075 T651 alloy in an acidic salt fog environment. The fully clad

panel, seen in Figure 4.2, was cut from the original Alclad aluminum plate and was left in the as

delivered condition.
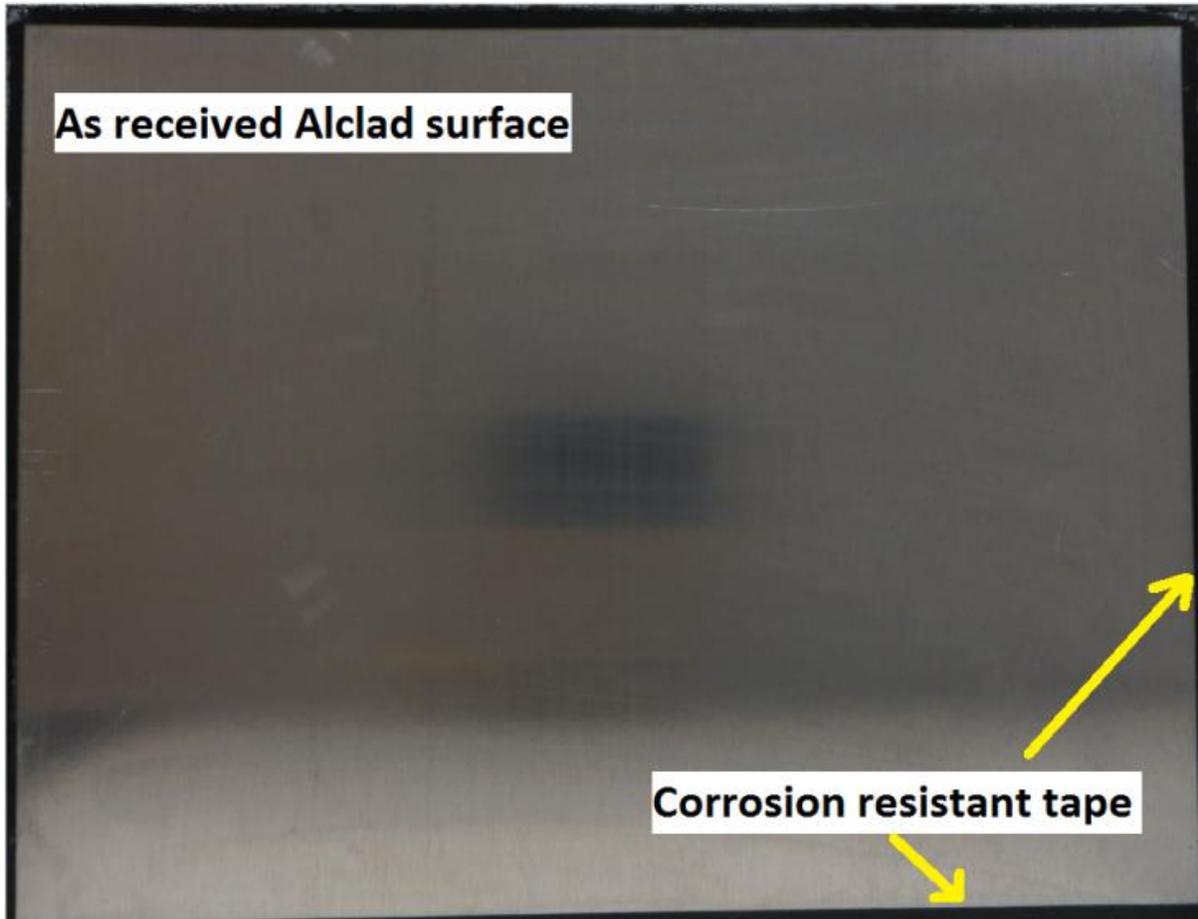
Figure 4.2: Fully clad medium sized test panel with corrosion resistant tape

The front surface of the spot clad panel, seen in Figure 4.3, was machined by removing 0.19 mm from the plate thickness with a CNC milling machine to produce an array of 1x1 cm square clad spots spaced 2 cm from each other. The dimensions used in the spot clad pattern were determined from the first 1 cm^2 central clad spot corrosion experiment. Milling marks were not removed from the partially clad test panel.
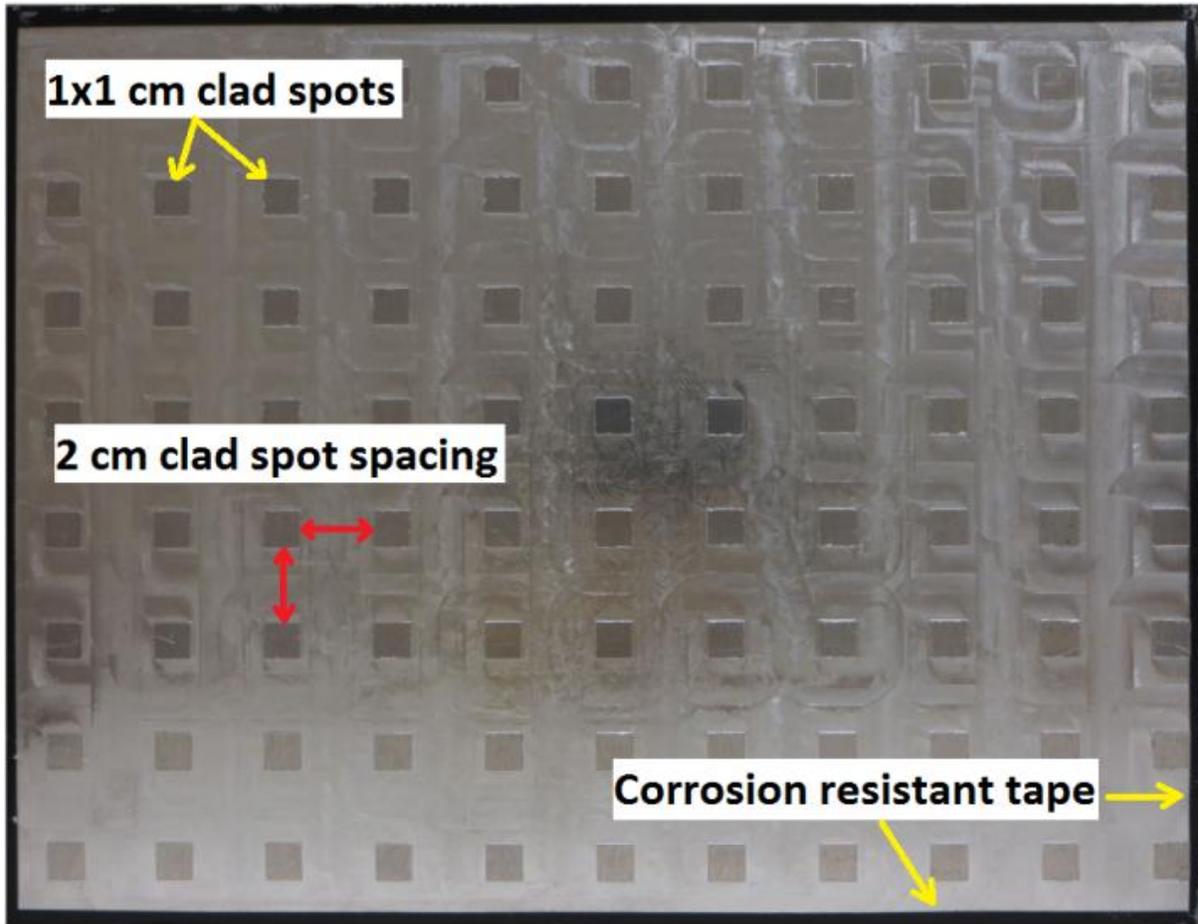
Figure 4.3: Partial cladding pattern medium sized test panel with corrosion resistant tape

The bare aluminum 7075 T651 panel, seen in Figure 4.4, was produced by mechanically milling 0.19 mm from the entire plate thickness. Milling marks were not removed from the bare aluminum panel. All three panels have an exposed surface area of approximately 30x25 cm after the application of the corrosion resistant tape. After the 300 hour exposure to the acidic salt fog corrosion environment, tensile test specimens, fatigue test specimens and representative cross-sections were cut from each the medium sized test panels.
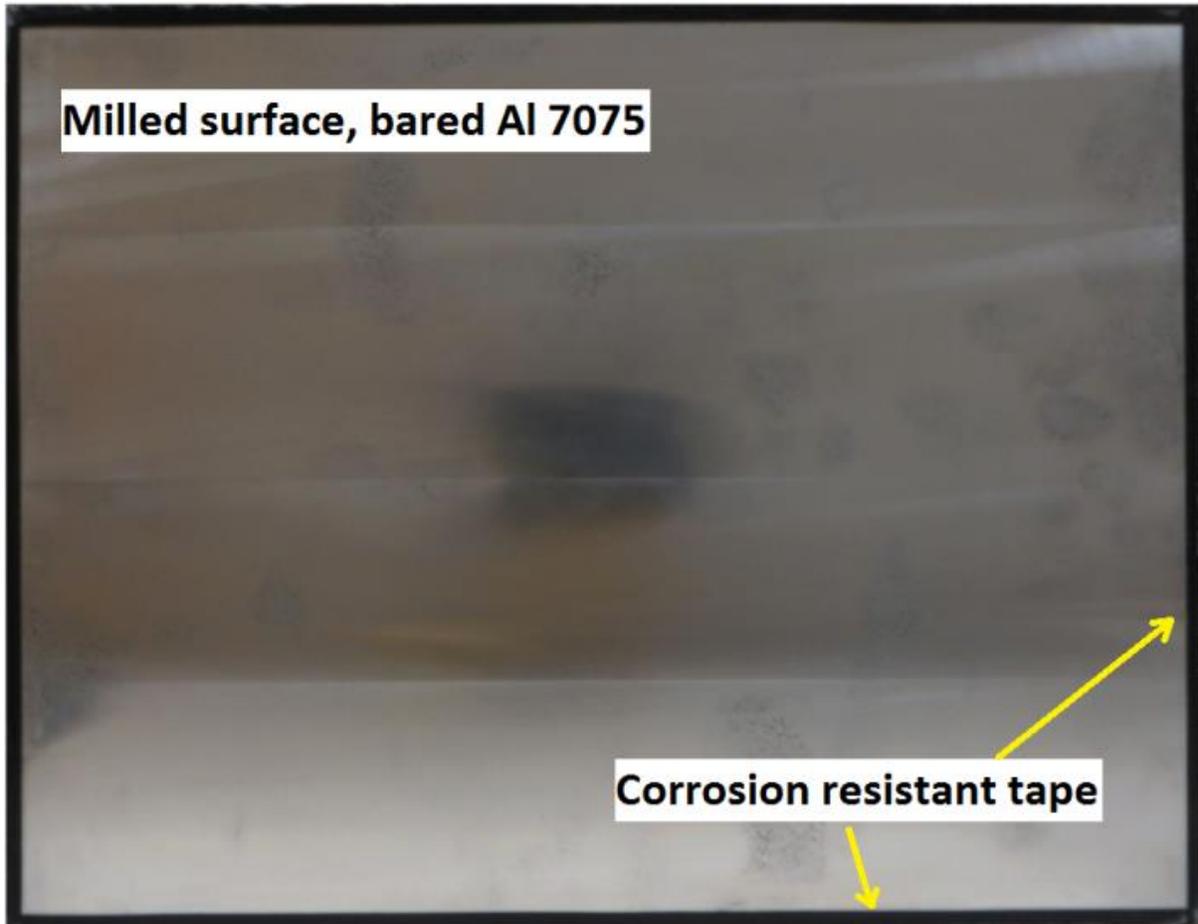
Figure 4.4: Cladding removed medium sized test panel with corrosion resistant tape

4.4.3 Varying Central Clad Spot Size Panels

The goal of the varying central clad spot size panels was to determine if varying the central clad spot dimensions would affect the size of the area protected by the clad spot and the severity of the corrosion damage in the protected area. Three 11x11 cm square test panels were machined with varying central square clad spots sizes of 0.5 cm^2, 1 cm^2 and 2 cm^2. The varying central clad spot size panels can be seen in Figures 4.5, 4.6 and 4.7. The Alclad layer was removed by mechanically milling 0.19 mm from the thickness of the front surface, leaving the

cladding at the central clad spot. The milling marks were not removed from these samples.

This step was omitted because removing the milling marks from the medium scale, partially

clad, test panel was considered impractical and it was decided to keep the set of central clad

spot panels consistent with this. It is known that the presence of the milling marks will increase

the corrosion susceptibility of the aluminium surface due to the increased surface area

available for corrosion to initiate [26]. The area of the surface exposed to the corrosion

environment was 10x10 cm after the corrosion resistant tape was applied.

Figure 4.5: 0.5 cm^2 central clad spot panel with corrosion resistant tape
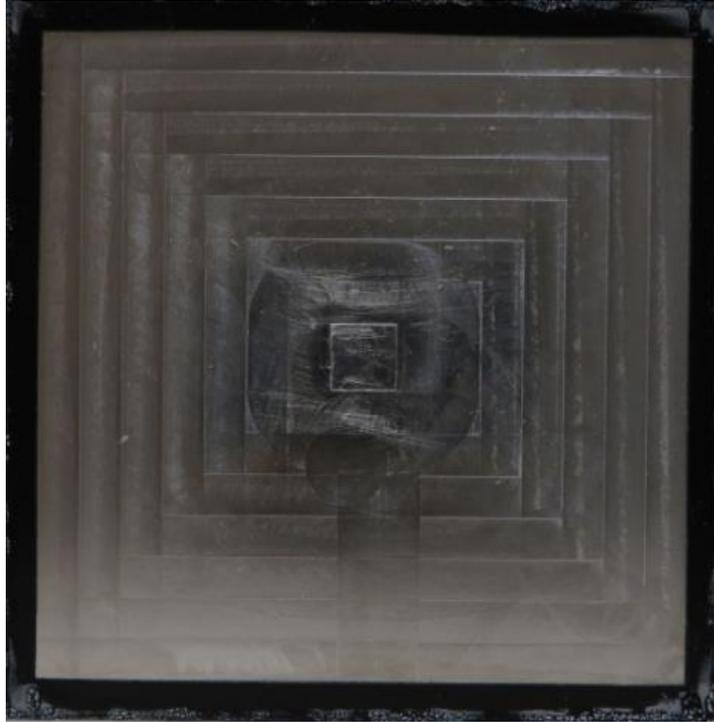
Figure 4.6: 1 cm^2 central clad spot panel with corrosion resistant tape

Figure 4.7: 2 cm^2 central clad spot panel with corrosion resistant tape

4.5 Evaluating Extent of Corrosion on Single Clad Spot Panels

After corrosion exposure of the single clad spot panels, a 2.5 mm grid was affixed to the corroded surfaces. The grid was produced by printing lines spaced 2.5 mm apart on transparency film. Each grid section was then evaluated for the amount of corrosion visible within the section by giving it a rating between 0-100 in increments of 5 for the total percentage of corroded surface area. The corrosion rating of each grid section was visually estimated in increments of 5, because this was not an exact measurement it is likely that the error in producing the surface plots for the corroded single clad spot panels was at least ±5%.

To investigate the depth of the corrosion penetration, approximately 0.17 mm was mechanically milled from the surface of each of single clad spot panels and the grid was reapplied. The extent of corrosion damage over the surface penetrating this depth was then evaluated.

4.6 Representative Cross-Sections

Representative cross-sections were cut from the three medium sized test panels after corrosion exposure with an Isomet 11-1180 low speed saw. The cross-sections were then mounted in SamplKwick fast dry acrylic, hand polished with successively finer grit sand paper (P280 to P1200) and given a final polish with 6 and 1 μm diamond suspension with a Buehler grinder polisher.

The cross-sections were then viewed at 100x magnification with a Nikon Eclipse 50i optical microscope and images were captured with an Infinity 1 microscopy camera.

4.7 Tensile Tests

Four rectangular tensile specimens were machined from each of the medium sized test panels after corrosion exposure in accordance to ASTM B557 [27]. For comparison, six rectangular test specimens were machined from un-corroded Al 7075 T651. Of the six un-corroded test specimens, two were fully clad, two had the cladding removed and two were machined from a partially clad section, representing each of the medium sized test panels. The tensile tests were performed in accordance to ASTM B557 with an Instron 5585H load frame using wedge type grips. The crosshead speed of all the tensile tests was 5 mm/minute and the strain during the elastic section of the tests was measured using an Instron 2630-106 clip on extensometer with a gauge length of 25 mm.

4.8 Fatigue Tests

Four fatigue specimens with tangentially blending fillets between the uniform test section and the ends were machined from each of the medium sized test panels after corrosion exposure in accordance to ASTM E466 [20]. For comparison, six test specimens were also machined from un-corroded Al 7075 T651. Of the six un-corroded test specimens, two were fully clad, two had the cladding removed and two were machined from a partially clad section, representing each of the medium sized test panels.

The constant amplitude fatigue tests had a tension-tension stress ratio of 0.1 and two corroded specimens from each medium sized test panel were tested at maximum stresses of 535 and 490 MPa. The maximum stresses selected were fairly high, 535 MPa is slightly above the yield stress of all the corroded test panels while 490 MPa is slightly below the yield stress. High

maximum stresses were selected because of the low crosshead speed of the Instron 5585H load frame used for this experiment. A larger range of maximum stresses, suitable for producing an S-N curve, was not selected because of limitations on the number of specimens that could be produced from the test panels. The un-corroded test specimens were tested only at the lower 490 MPa maximum stress.

The waveform used during the fatigue tests was triangular. One deviation from the test standard was that the fatigue tests were not controlled at a constant rate of change in force. This would ensure a constant test frequency. This was not possible with the load frame that was used because the load cell was excessively large and did not produce a consistent cycle maximum stress. A constant rate of change in elongation was chosen instead and the uniformity of cycle maximum stresses improved greatly. The rate of change in force remains approximately constant throughout the test but gradually increases during the early part of the test as the test specimen elongate and then gradually decreases during the final parts of the test as the specimens become stiffer due to work hardening. The test frequency for the larger maximum stress (535 MPa) was approximately 0.168 Hz while the test frequency for the lower maximum stress (490 MPa) was approximately 0.186 Hz. The small variation in test frequency was considered acceptable because fatigue strength is not sensitive to the test frequency between 10^{-2} and 10^{2} Hz for most metallic materials [20].

5. Results

5.1 Central Clad Spot Panels

5.1.1 Initial 1 cm^2 Central Clad Spot Panel

After 300 hours of acidic salt spray exposure the central clad spot panel was cleaned in accordance to ASTM G1 [28]. Initially the panel was cleaned with water and a stiff brush to remove deposited salt and some of the bulk corrosion products. This was followed by immersing the panel in nitric acid for four minutes at room temperature.

As shown in Figure 5.1, it appears that a fairly well defined circular area is protected from corrosion by the central clad spot. The remainder of the panel shows corrosion that could be described as moderate exfoliation [17] or as poorly defined pitting with a large degree of horizontal propagation and delamination [28].

In an effort to quantify the severity and location of the corrosion damage relative to the clad spot, the machining method for determining pit depth described in ASTM G46: Standard Guide for Examination and Evaluation of Pitting Corrosion [29] was adapted to be used with corrosion that more closely resembles exfoliation. As shown in Figure 5.2, a 2.5 mm grid was applied to the corroded surface of the panel and the percent area of the panel surface affected by corrosion was visually estimated in each grid section.

Figure 5.1: Cleaned central clad spot panel
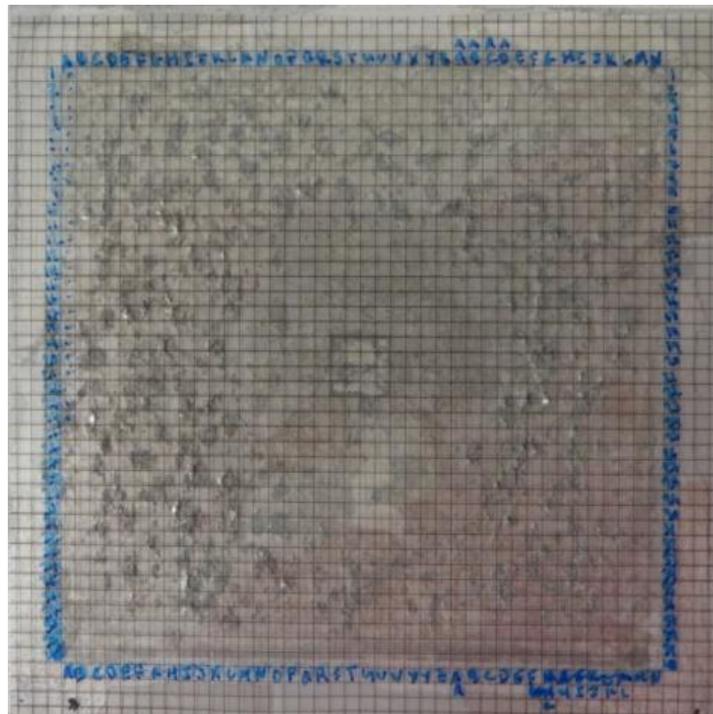
Figure 5.2: Cleaned central clad spot panel with the application of a 2.5mm grid

These values were then graphically represented in a surface plot, shown in Figure 5.3. This was

done for two reasons. The first was to better visualize the extent of corrosion damage relative

to the central clad spot. Using the surface plot, the area of the panel protected by the clad spot

was estimated as a 3x3 cm square, shown in Figure 5.4. These dimensions were then used to

produce the medium sized test panel with a clad spot pattern. It was estimated that a two

dimensional array of 1 cm^2 clad spots spaced 2 cm from each other would be sufficient to

protect the panel surface from corrosion after a 300 hour exposure in the acidic salt spray

environment.
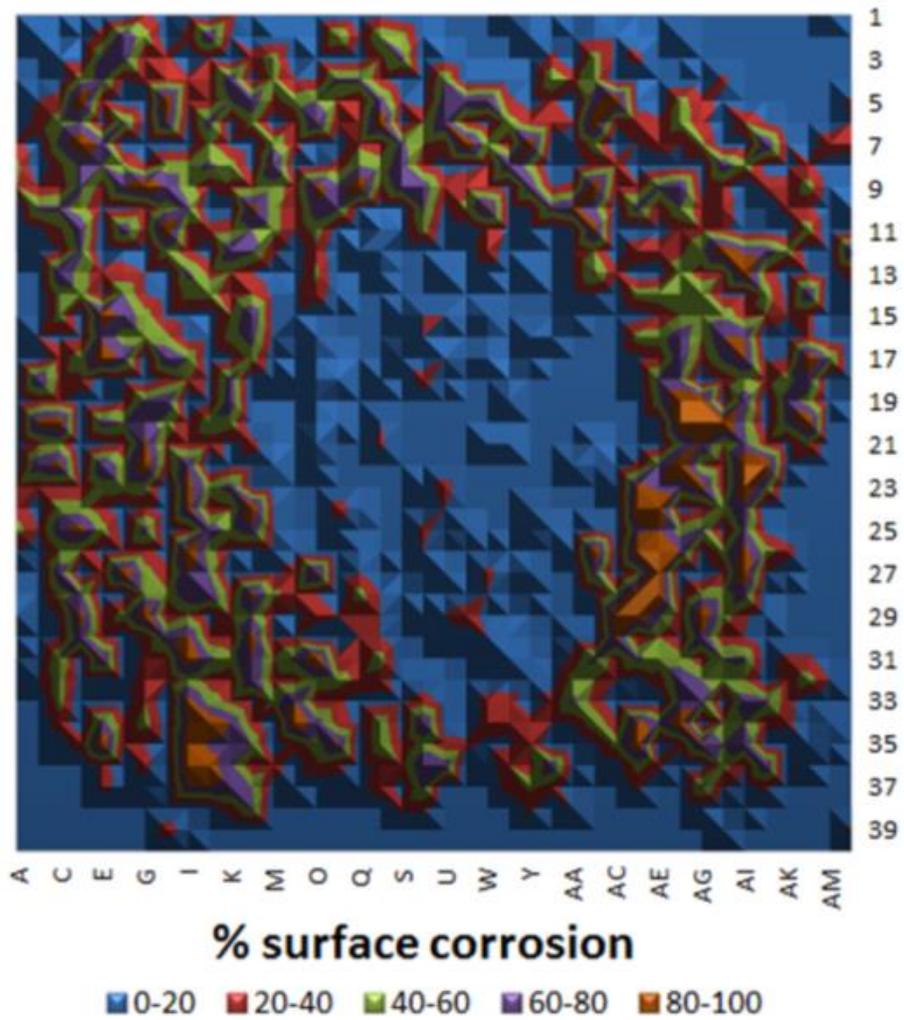
Figure 5.3: Surface plot of the 1x1 central clad spot panel (no milling), 24% of the surface exhibits signs of corrosion
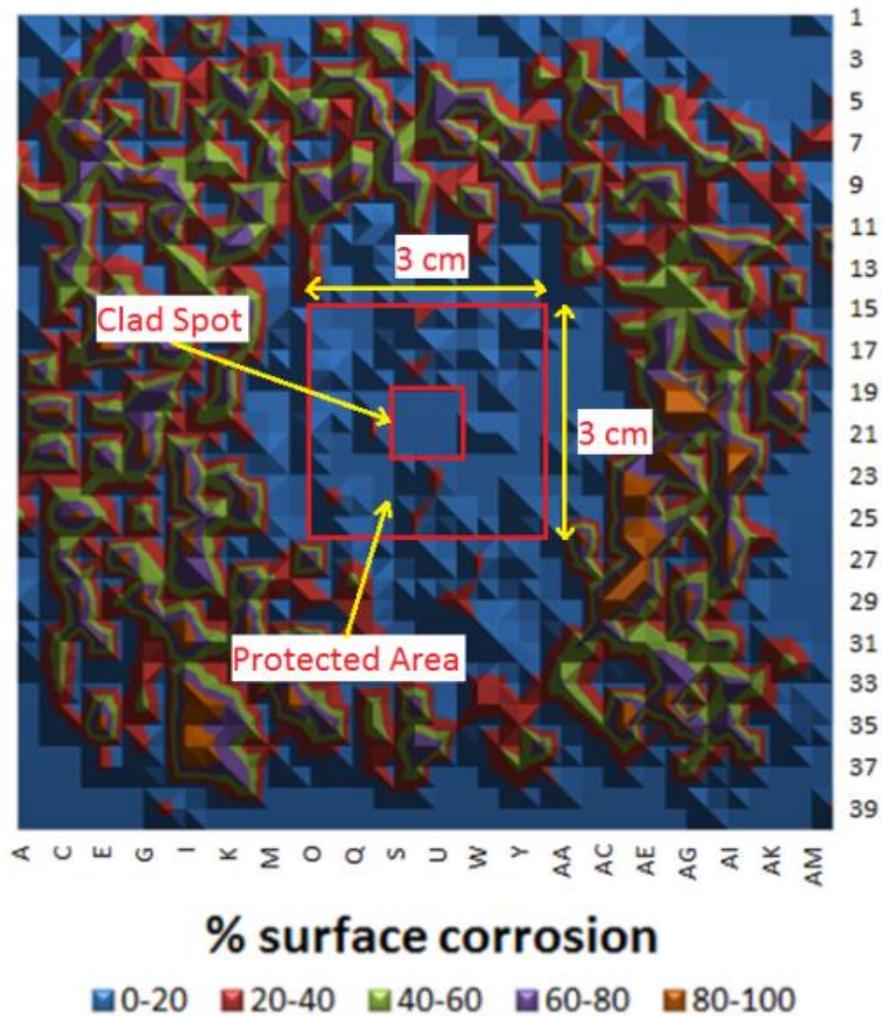
Figure 5.4: Estimation of area protected by clad spot

The second purpose of the surface plots was to maintain a record of the observed corrosion damage while the depth of the exfoliation was determined through destructive means. Non-destructive methods such as use of a micrometer or a microscope were considered impractical due to the nature of the corrosion. The base of the corrosion penetration was not accessible due to the blistering and raised layers of aluminum obscuring the corrosion opening. Instead, successive thin layers were milled from the surface of the test panel and a new surface plot was

41

produced for each stage. In this way, the minimum corrosion depth and relative location to the clad spot could be determined. The results of the milling process for the central clad spot panel can be seen in Figures 5.5 and 5.6.
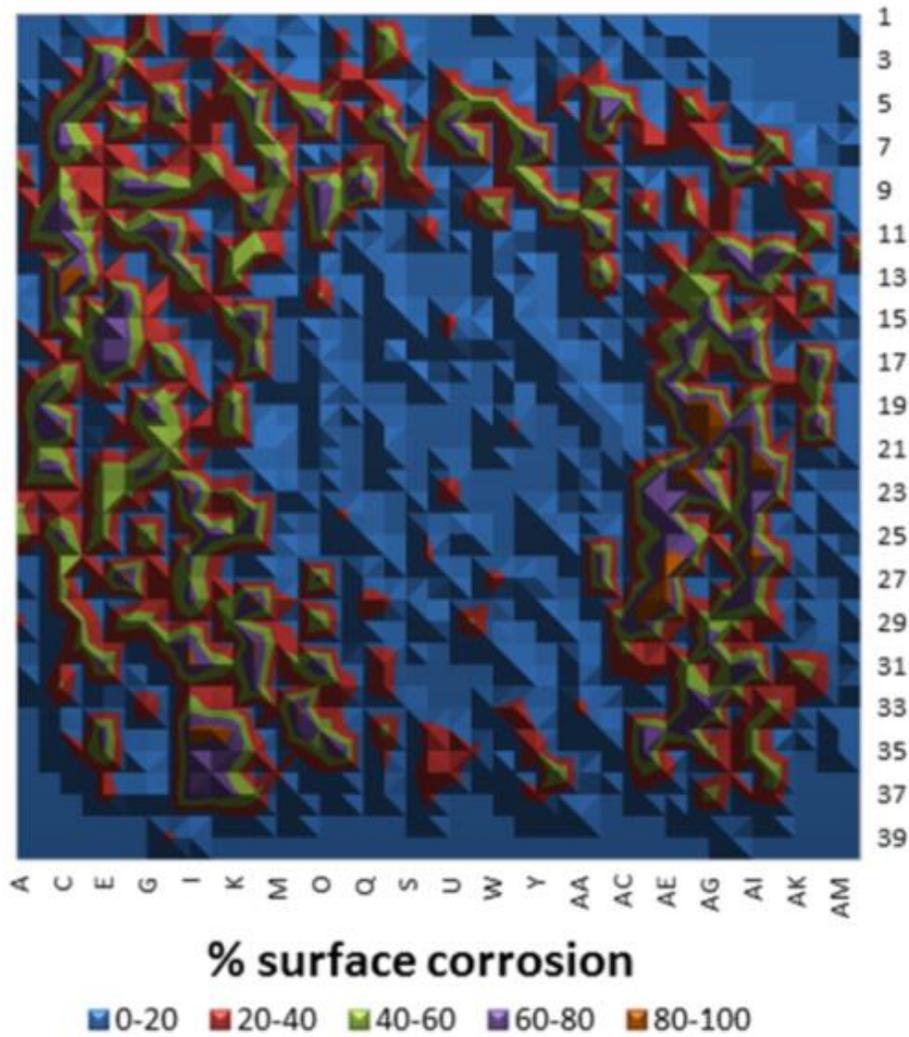
Figure 5.5: Surface plot of the central clad spot panel, 0.02 mm milled, 19% of the surface exhibits signs of corrosion
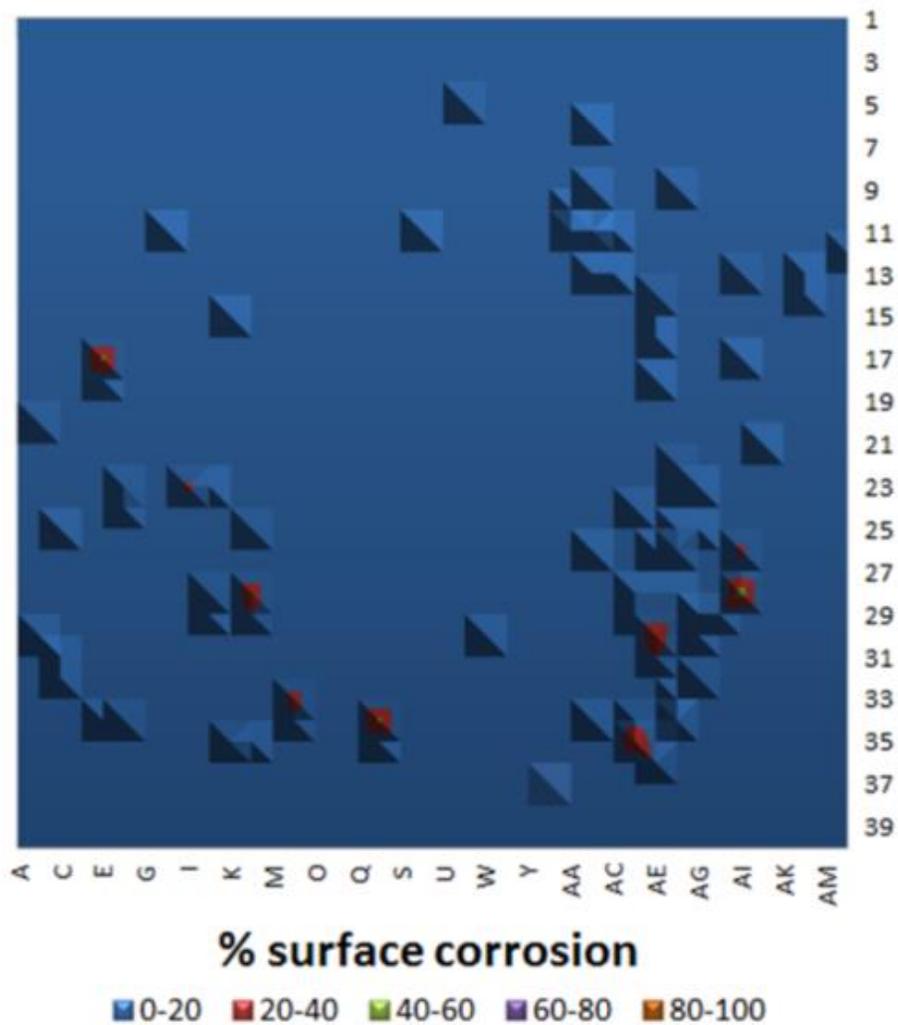
Figure 5.6: Surface plot of the central clad spot panel, 0.17 mm milled. 0.6% of the surface exhibits signs of corrosion

5.1.2 Varying Central Clad Spot Dimensions

The three varying central clad spot dimension panels were machined in a similar fashion and

exposed to the same corrosion environment as the initial 1 cm^2 central clad spot panel. The key

difference between the procedures for preparing the varying central clad spot dimension

panels was that the milling marks were not removed. After corrosion exposure, a 2.5 mm grid

was applied to the panel surface and the percentage of corroded surface in each grid section was determined, the surface plots generated by this procedure can be seen in Figures 5.7, 5.8 and 5.9. From these surface plots it can immediately be seen that the presence of milling marks has had a detrimental effect on the corrosion resistance of the panels. If the initial 1 cm^2 central clad spot panel seen in Figure 5.3 is compared to the 1 cm^2 clad spot panel from the varying spot dimensions test seen in Figure 5.8, it is apparent that the clad spot is less effective at protecting the test panel. The milling marks acted as sites to facilitate the initiation of corrosion. In Figure 5.8 the region of the test panel protected by the clad spot is less defined, the overall corrosion over the surface is more uniform and more severe. The percentage of the panel surface showing signs of corrosion for the initial 1 cm^2 clad spot panel was 24% while it was 29% for the second test.

When comparing the surface plots of the 0.5 cm^2, 1 cm^2 and the 2 cm^2 clad spot panels, increasing panel protection with increasing clad spot dimensions is not immediately apparent. The percentage of corroded surface area for the 1 cm^2 and 2 cm^2 clad spot panels were the same at 29% while the 0.5 cm^2 clad spot panel had a lower percentage of corroded surface area at 23%. This was not the expected result. The explanation for the lower corroded surface area of the 0.5 cm^2 clad spot panel may be that there was some interaction between the clad back surface of the panel and the front surface. This explanation is supported by the observation that the majority of the surface less affected by corrosion for the 0.5 cm^2 clad spot test panel is around the edges. This suggests that the taping procedure used to isolate the back surface of the test panels may not have always been effective.

If we only consider the 3x3 cm central regions of the panel, the area considered protected by

the clad spot in the initial clad spot test, the protective effect of the clad spots is more evident.

The percentage of surface corrosion in this area for the 0.5 cm^2, 1 cm^2 and 2 cm^2 clad spot

panels is 31%, 19% and 21% respectively. This shows a similar protective effect from the 1 cm^2

and 2 cm^2 clad spots where less corrosion is observed in the central region than on the overall

panel; while the corrosion observed in the central region of the 0.5 cm^2 clad spot panel is more

severe than on the overall panel.
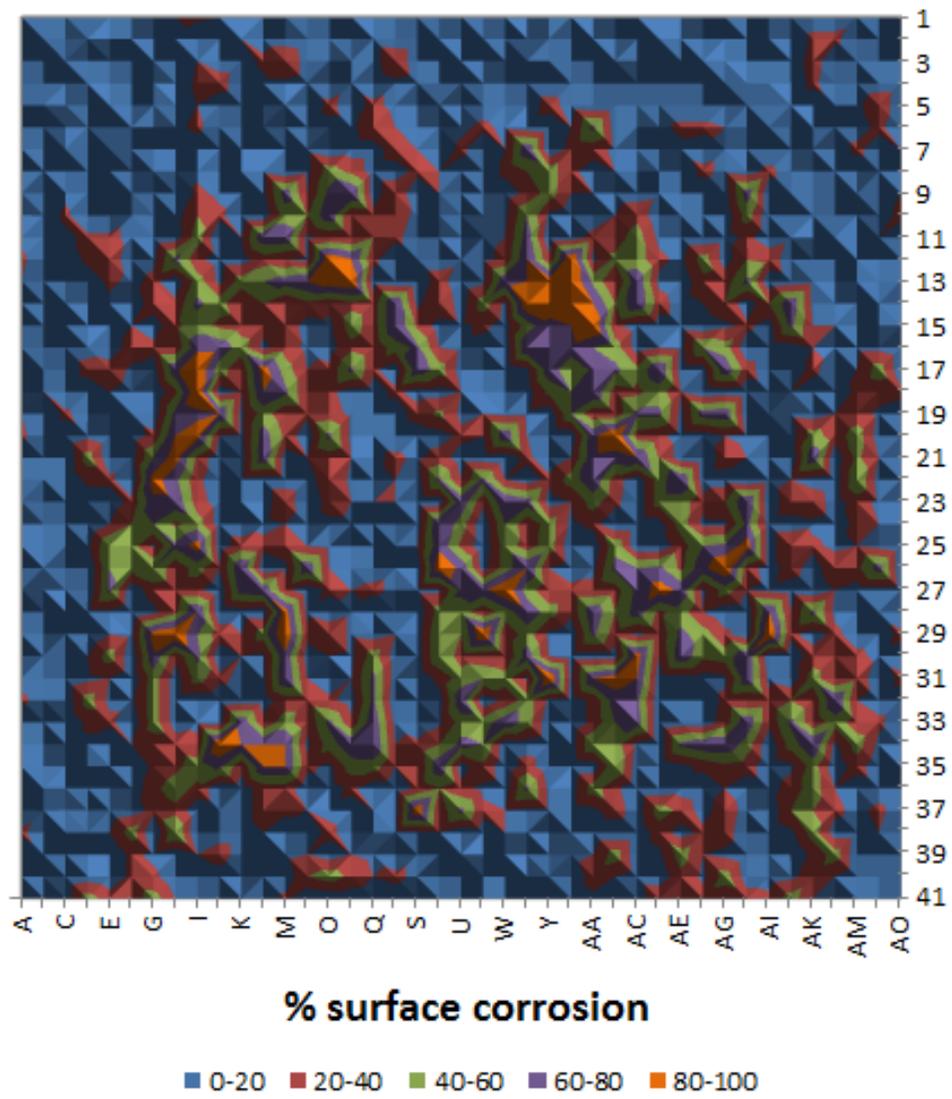
Figure 5.7: Surface plot of the 0.5 cm^2 central clad spot panel, no milling
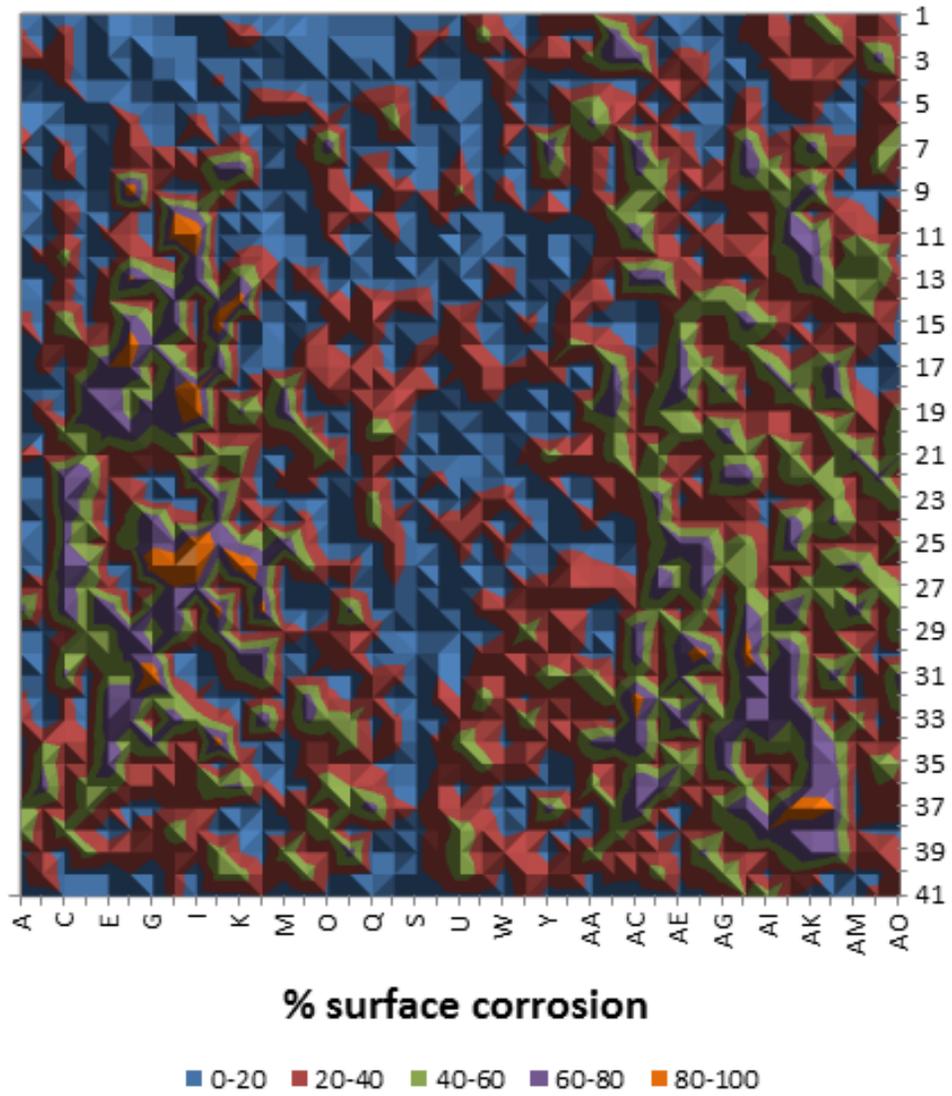
Figure 5.8: Surface plot of the 1 cm^2 central clad spot panel, no milling
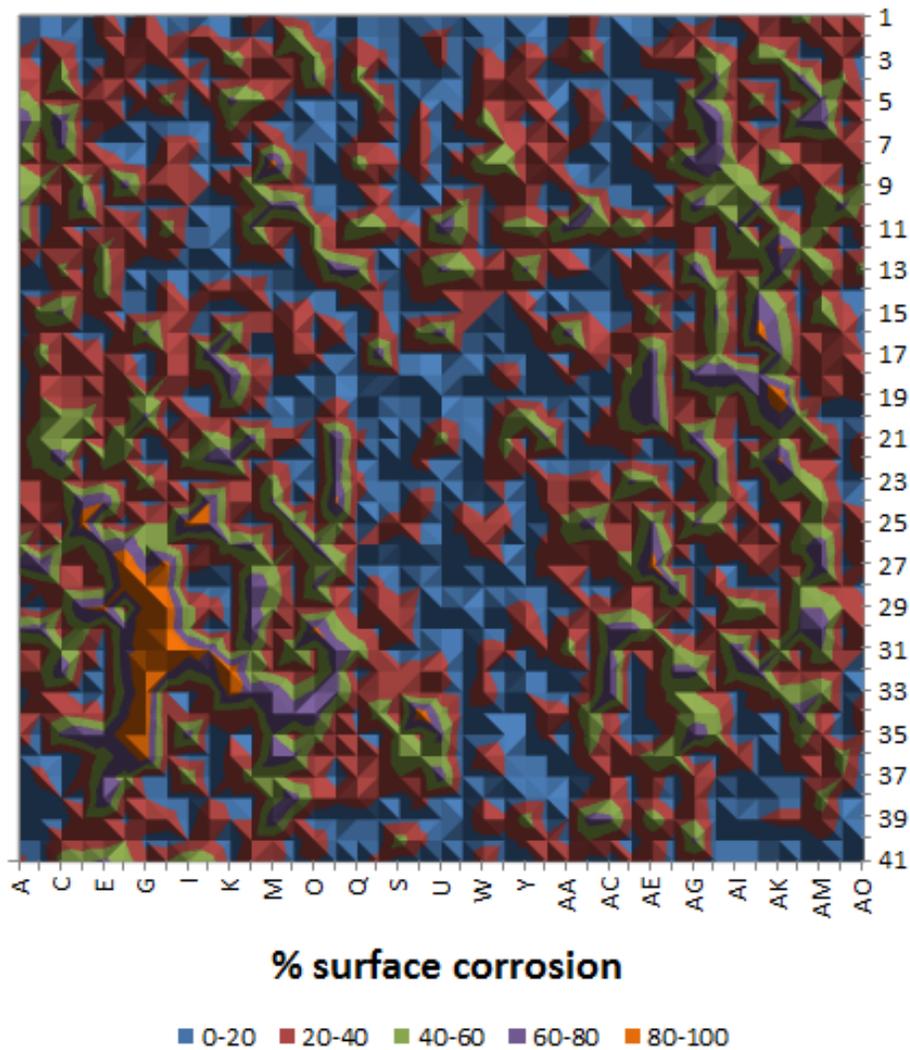
Figure 5.9: Surface plot of the 2 cm^2 central clad spot panel, no milling

The surfaces of the three varying clad spot size panels were then milled to a depth of approximately 0.17 mm to investigate the penetration of corrosion. It can be seen in Figures 5.10, 5.11 and 5.12 that in all three cases the corrosion occurring at this depth has a higher concentration on either side of the clad spot with a "strip" of protected area in the middle of the panel. Overall the percentage of surface corrosion for the 0.5 cm^2, 1 cm^2 and 2 cm^2 test

panels was 2.6%, 2.2% and 1.3% respectively. This shows that a larger clad spot will provide

increased corrosion penetration protection.

% surface corrosion

■ 0-20 ■ 20-40 ■ 40-60 ■ 60-80 ■ 80-100
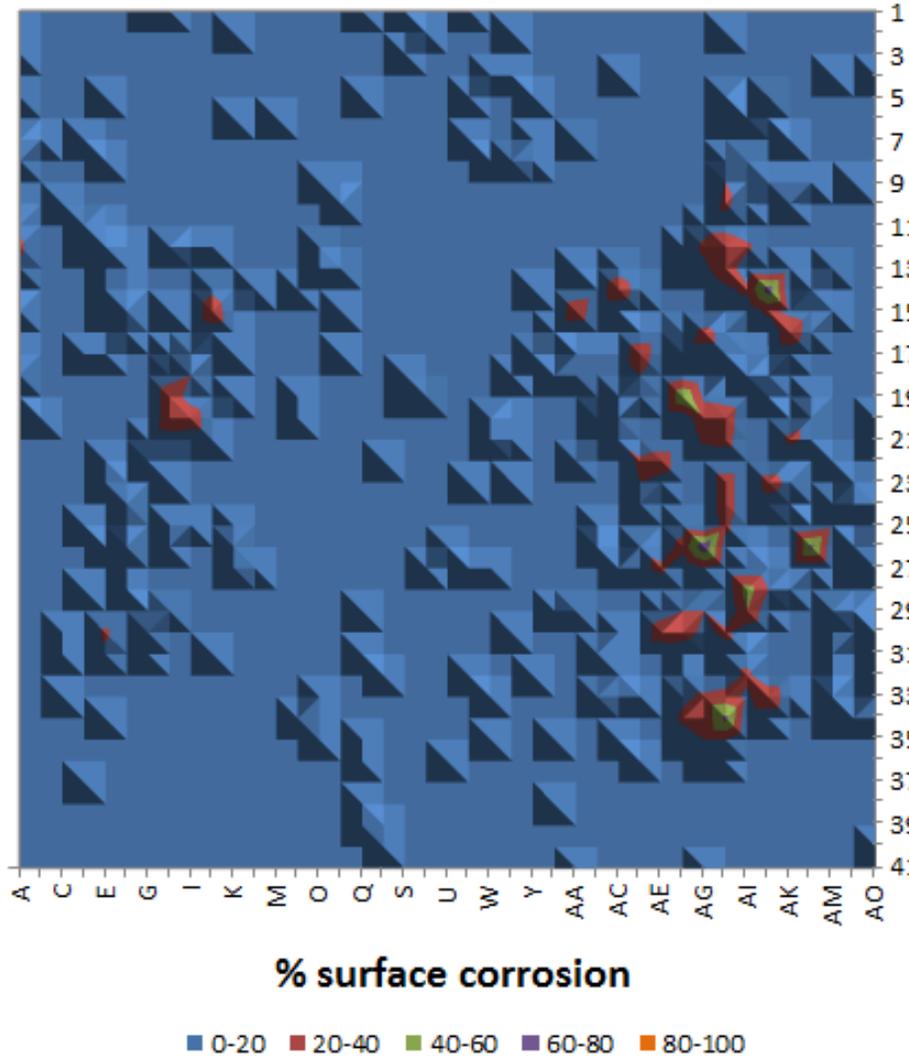
Figure 5.10: Surface plot of the 0.5 cm^2 central clad spot panel, 0.17 mm milled
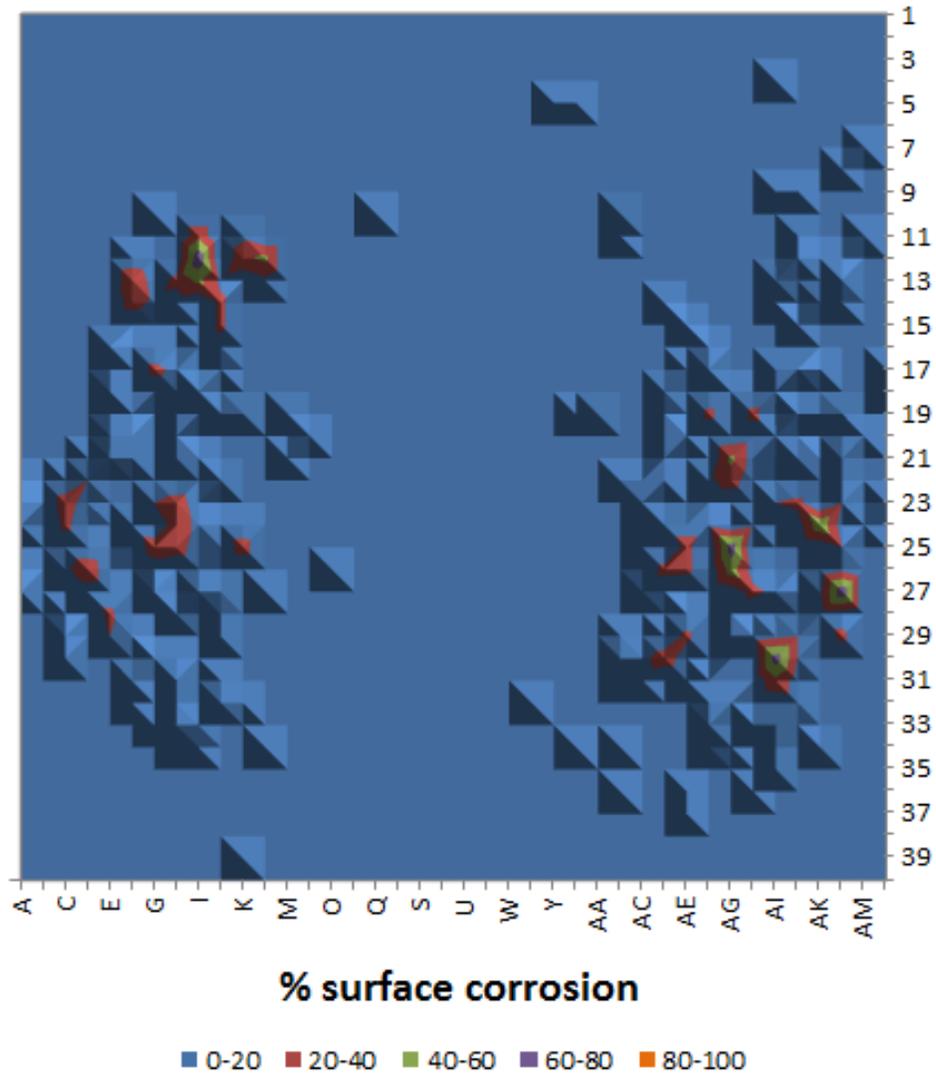
Figure 5.11: Surface plot of the 1 cm^2 central clad spot panel, 0.17 mm milled
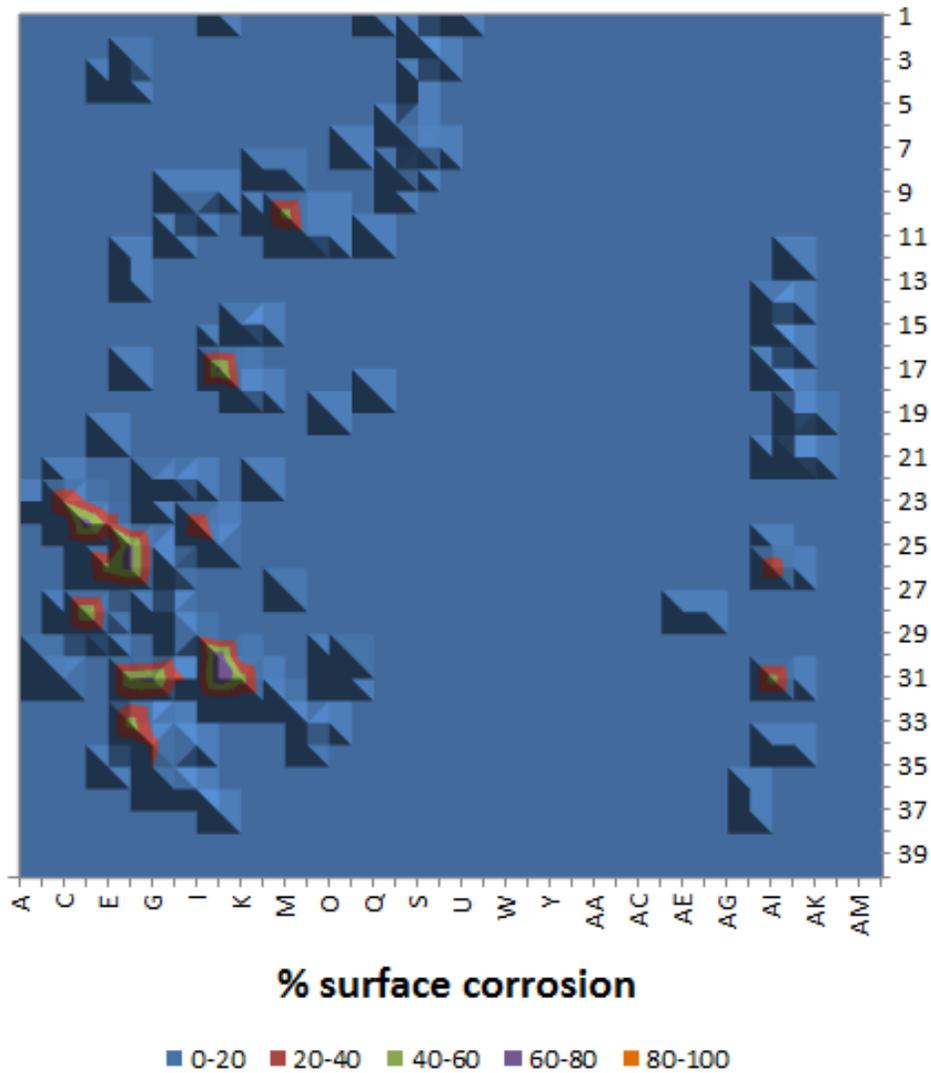
Figure 5.12: Surface plot of the 2 cm^2 central clad spot panel, 0.17 mm milled

If only the 3x3 cm central region of the panels is considered, the percentage of surface

corrosion for the 0.5 cm^2, 1 cm^2 and 2 cm^2 test panels was 1.1%, 0.07% and 0.07% respectively.

The 0.5 cm^2 clad spot is insufficient to protect the central region of the test panel when

compared to the similar protection provided by the 1 cm^2 and 2 cm^2 clad spots. A summary of

51

all of the values for the percentage of corrosion observed on the varying clad spot size panels

can be seen in Table: 5.1.

Table 5.1: Percentage of surface corrosion observed on the varying clad spot size panels at the surface of the panel and at a depth of 0.17 mm

	$0.5\ cm^2$ clad spot		$1\ cm^2$ clad spot		$2\ cm^2$ clad spot	
	No milling	0.17 mm milled	No milling	0.17 mm milled	No milling	0.17 mm milled
Overall surface	23%	2.6%	29%	2.2%	29%	1.3%
3x3 cm square central area	31%	1.1%	19%	0.07%	21%	0.07%

5.2 Medium Scale Test Panels with Partial Cladding Pattern

5.2.1 Visual Observations of Corroded Panels

After removing the residual salt buildup on the clad medium sized panel with water and a stiff brush a fairly uniform distribution of large irregular shaped corrosion spots were exposed, this is shown in Figure 5.13. Upon closer inspection, small pits were also evident, distributed throughout the cladding layer. The depth of the observed corrosion was very shallow. From these observations, it can be inferred that in the acidic salt spray environment, pitting occurred and progressed in the cladding layer until reaching the core material. At this point, the pits stopped growing in depth because the Alclad layer is more electronegative than the core and acts as a sacrificial anode. Once the pit depth reached the aluminum core, the pits widened as the cladding layer continued to corrode preferentially relative to the core material. Multiple widening pits then connected to form the large irregular corrosion spots and continued to expand as the corrosion of the panel progressed. This corrosion behavior is what is expected and desired from aluminum protected by an Alclad layer. The cladding layer corrodes preferentially and the localized corrosion remains superficial, protecting the core material.
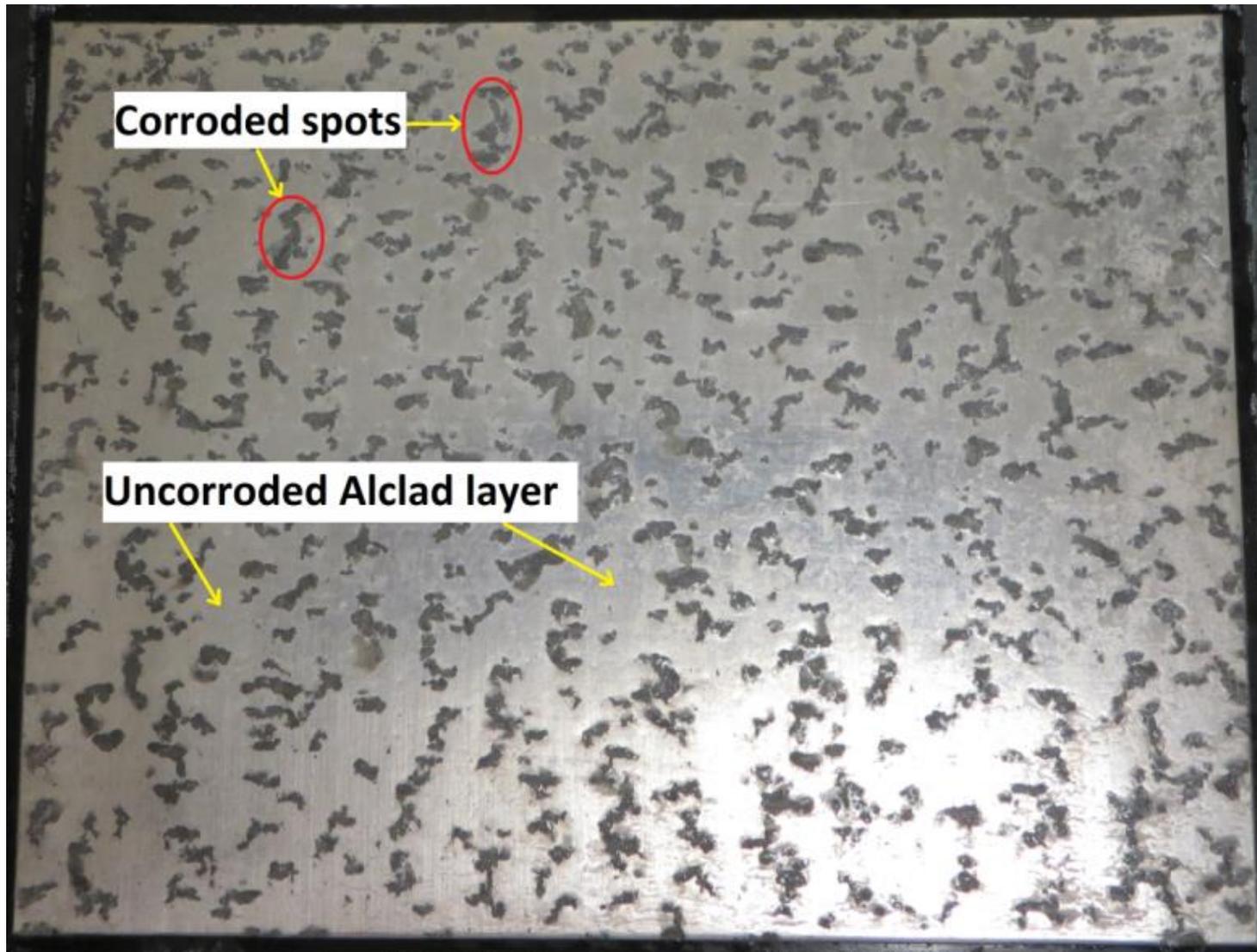
Figure 5.13: Fully clad test panel after corrosion exposure, before nitric acid cleaning, shallow corrosion spots are uniformly distributed over the panel surface

The unclad panel is show in Figure 5.14 after the residual salt buildup was removed in the same method described above. After exposure to the acetic salt spray environment, exfoliation corrosion was observed uniformly throughout the panel surface. Using the exfoliation corrosion rating system described in ASTM G34, the observed corrosion could initially be described as in between pitting and moderate exfoliation. Distinct pit-blisters were observed but with more lifting of the aluminum along the pit edge than is described in the standard. The more severe lifting of the aluminum into blisters and slivers resembles more closely a moderate exfoliation rating but with less layering than is described in the standard. The observed corrosion can be best described as pit-blisters that have exposed the grain boundaries, allowing intergranular corrosion to occur in tandem. This caused moderate exfoliation, especially where multiple pits interacted to lift continuous sheets of the aluminum.

The red colored corrosion products observed over the majority of the corroded bare test panel is believed to be copper alloyed within the 7075 alloy that has dissolved into the corrosive electrolyte from a dealloying process and replated on the aluminum surface. This process is further discussed in Section 6.2.
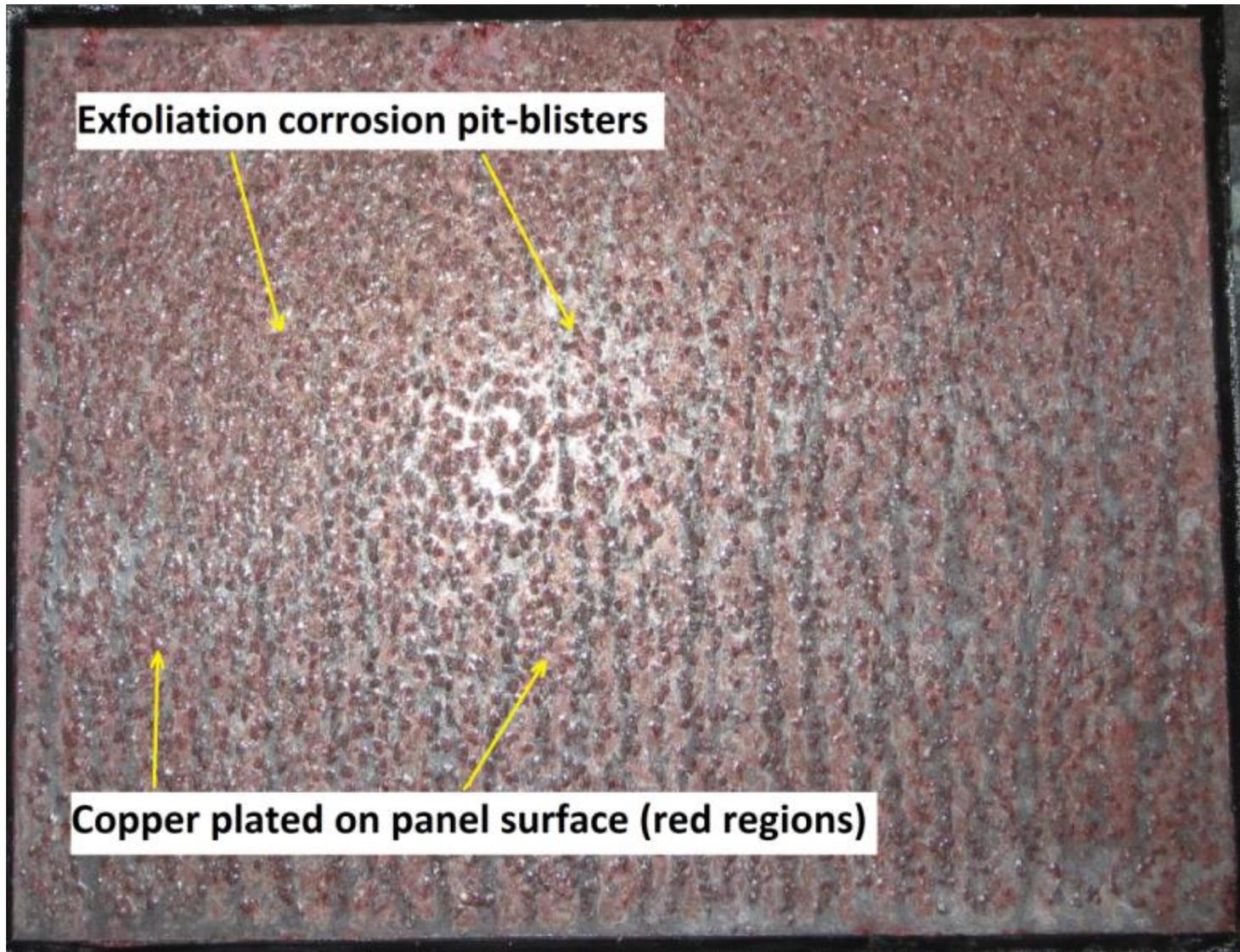
Figure 5.14: Cladding removed test panel after corrosion exposure, before nitric acid cleaning, exfoliation corrosion is observed over the panel surface

The residual salt buildup was removed from the spot clad panel in the same method described above. The corrosion observed on the surface of the spot clad panel was much less uniform than the fully clad and unprotected panels. In Figure 5.15, five distinct regions of corrosion behavior can be observed. (1) The surface of the clad spots experience general corrosion, depleting the sacrificial cladding layer while protecting the overall panel surface. (2) The majority of the panel surface was successfully protected by the partial cladding pattern. This is evident in the lower three quarters of the panel where the surface retained the shiny appearance and milling marks from the machining process. (3) On the upper edge of the panel there is a region of general corrosion with red coloring resembling what was observed on the unprotected test panel. Again, the explanation for this coloring is likely alloyed copper from the aluminum 7075 core deposited onto the panel surface from a dealloying process. The presence of the copper would have the opposite effect as the sacrificial cladding layer, creating a galvanic couple and aggravating corrosion. The effect of the copper is likely the cause of (4) the region of light general corrosion located between the red colored region and the shiny non-corroded region. Finally, (5) there are small patches of corrosion distributed throughout the non-corroded region of the panel. These patches are generally located adjacent to the clad spots. These patches of corrosion can possibly be explained by the acidic salt solution stagnating in the edges of the clad spots or within milling marks and leading to crevice corrosion.
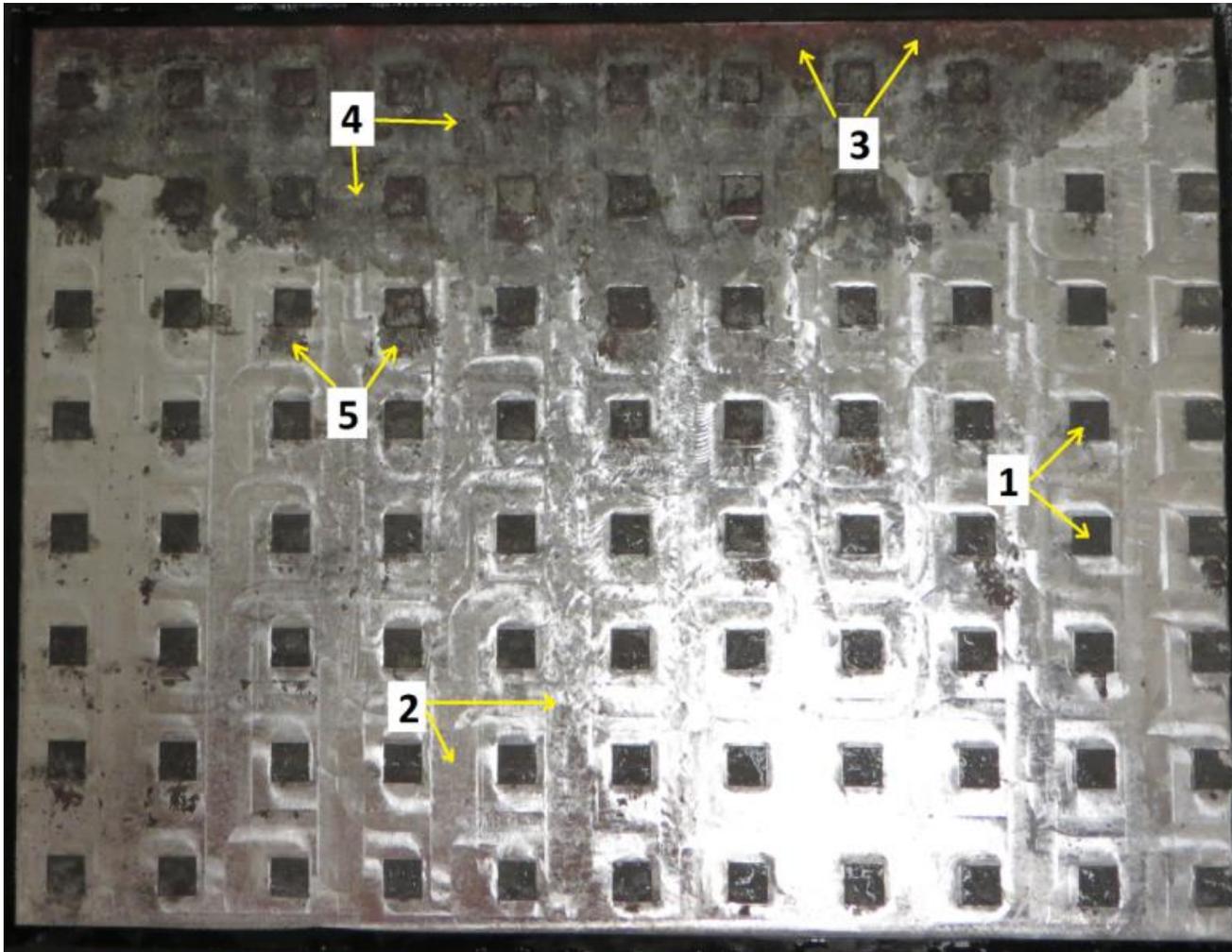
Figure 5.15: Spot clad test panel after corrosion exposure, before nitric acid cleaning, five areas of corrosion behavior are observed: 1. Uniform corrosion on the clad spots 2. No corrosion over the majority of the panel surface 3. Light uniform corrosion with red coloring on the top edge of the panel 4. Light uniform corrosion between the red colored uniform corrosion and the non-corroded surfaces 5. Small patches of light uniform corrosion within the non-corroded area, usually adjacent and below the clad spots

5.2.2 Mass Loss of Medium Scale Test Panels after Corrosion Exposure

It is known that mass loss is not an accurate representation of the extent of corrosion damage for materials, such as aluminum 7075 T651, that are susceptible to localized corrosion [30]. The initial and after corrosion masses were measured and tabulated in Table 5.2. As expected, the mass lost due to corrosion of the test panels was very low, confirming that uniform corrosion is not taking place at a substantial rate.

Table 5.2: Mass loss of medium scale test panels after corrosion exposure

	Initial mass (g)	Mass after corrosion exposure and cleaning (g)	Mass lost due to corrosion (g)
Cladding removed	1410.45	1407.55	2.90
Spot Clad	1337.15	1334.40	2.75
Fully Clad	1471.45	1469.20	2.25

5.2.3 Cross-Sections of the Corroded Panels

Representative cross-sections of the medium sized test panels were cut, mounted, polished and analysed with an optical microscope at 100x magnification. This was done to confirm the visual observations made about the test panels and investigate the penetration of the corrosion damage.

Figures 5.16 and 5.17 are representative cross-sections of the fully clad test panel. Figure 5.16 shows the region of the clad test panel unaffected by corrosion. The surface is smooth, the lack of any corrosion penetration confirms that the surface was fully protected from the corrosion environment. The cladding layer is distinguishable from the aluminum core; the thickness was measured as approximately 0.08 mm.

Figure 5.17 shows a cross-section of a corroded spot on the Alclad test panel. Dense pitting can

be seen penetrating through the cladding layer up to the aluminum 7075 core. Once reaching

the core, the pits progress laterally, widening the pit and merging with other pits, consuming

the cladding layer. This corrosion behavior is what was expected from the Alclad 7075 alloy and

represents the clad layer successfully protecting the core from corrosion damage.
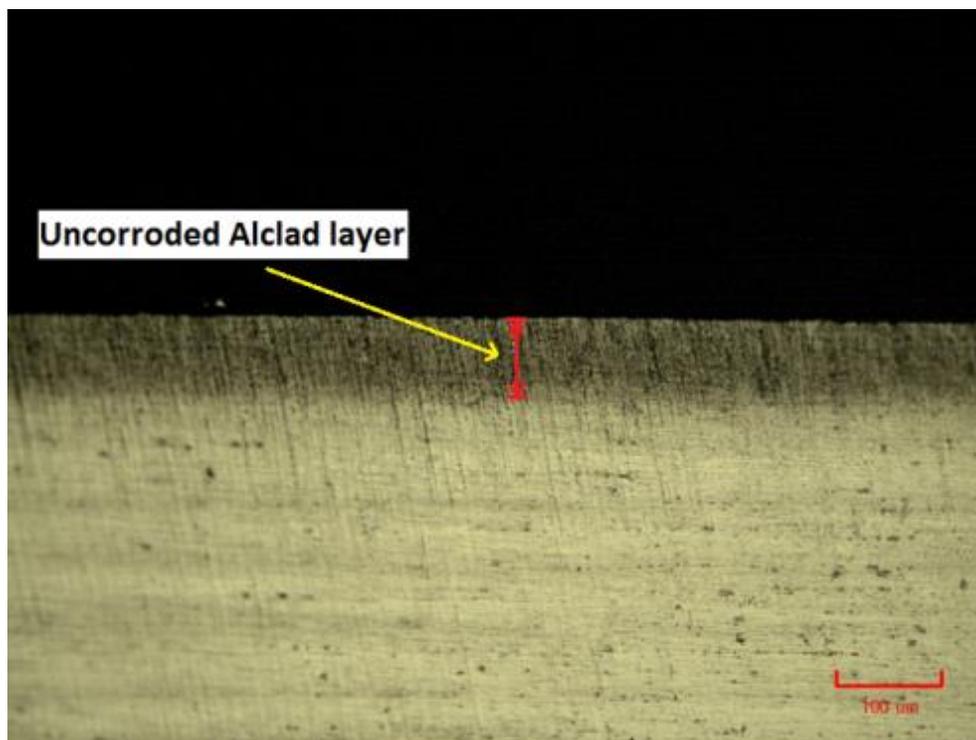
Figure 5.16: Clad panel, region with no corrosion, 100x magnification
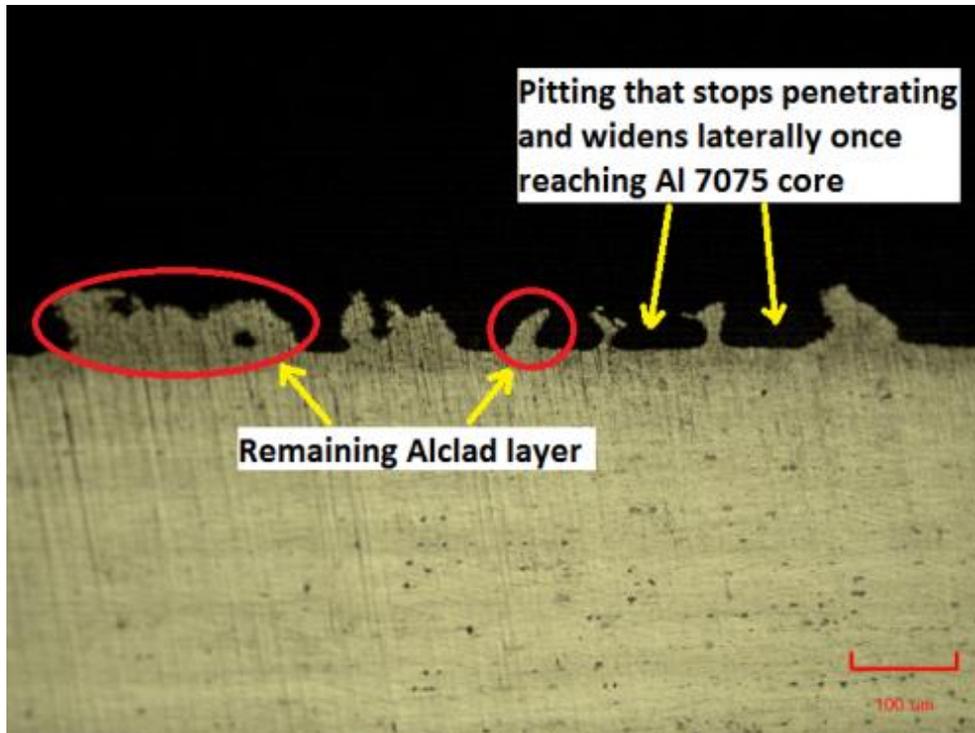
Figure 5.17: Clad panel, region with corrosion, 100x magnification

Figures 5.18, 5.19, 5.20 and 5.21 are representative cross-sections of the test panel with the cladding removed. Figure 5.18 shows a corrosion blister confirming severe intergranual attack leading to exfoliation corrosion. It is apparent that the expanding corrosion products have lifted layers of relatively non-corroded aluminum and caused stresses that have caused crack propagation in the lateral direction.

Figure 5.19 shows how successive layers of exfoliation and intergranular attack can result in an increasing corrosion depth. When layers of non-corroded aluminum are raised from the substrate, additional grain boundaries are exposed to the corrosion environment and a new layer of exfoliation corrosion can be initiated. This process will eventually result in the entire top surface of the aluminum plate corroding away in layers with a gradual increasing depth of

corrosion. The depth of this example of exfoliation corrosion was measured at approximately 0.18 mm. This behavior was consistent with the depths of corrosion observed in the single clad spot panels in the regions not considered protected by the clad spot.

Figure 5.20 shows the propagation of the exfoliation corrosion in the lateral direction with no corrosion apparent on the aluminum surface. The long crack in the middle of the image is the edge of the progressing exfoliation corrosion. Given more time in the corrosion environment, a blister would have formed at this location raising a large section from the aluminum thickness.

Figure 5.21 shows a well-defined pit in the aluminum plate. This was an example of obvious pitting observed in the analyzed cross-sections. The explanation for this may be that the corrosion initiated as well defined pits such as in Figure 5.21, but then propagated into exfoliation corrosion caused by intergranular attack of the large number of grain boundaries exposed by the pits. This process would eradicate the pit as exfoliation corrosion propagated radially.
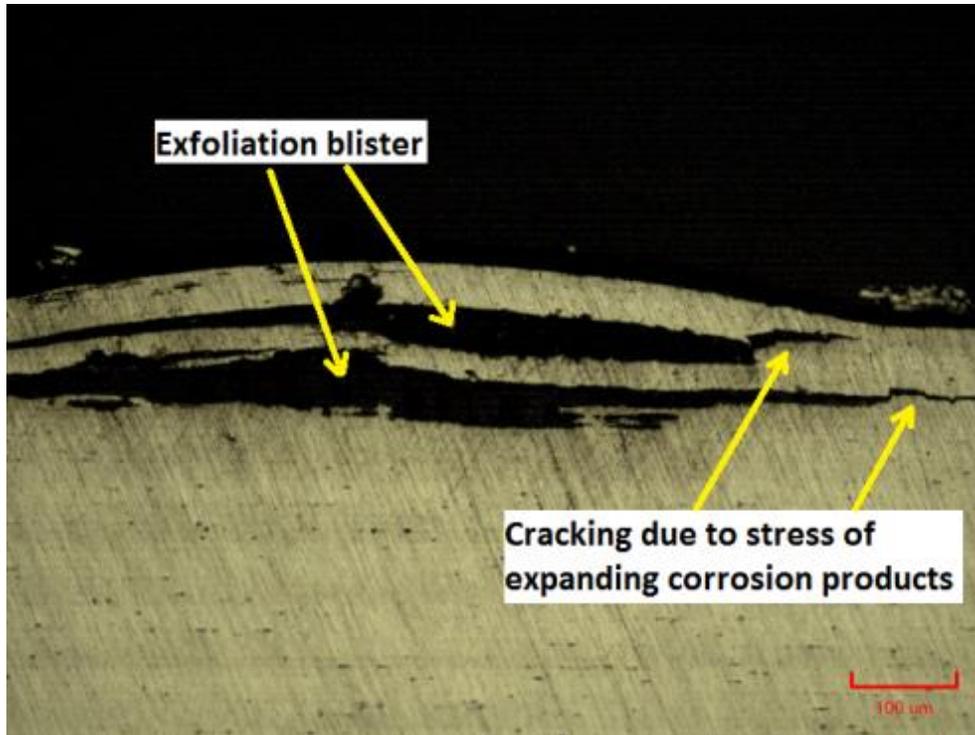
Figure 5.18: Unclad panel, exfoliation bulge, 100x magnification
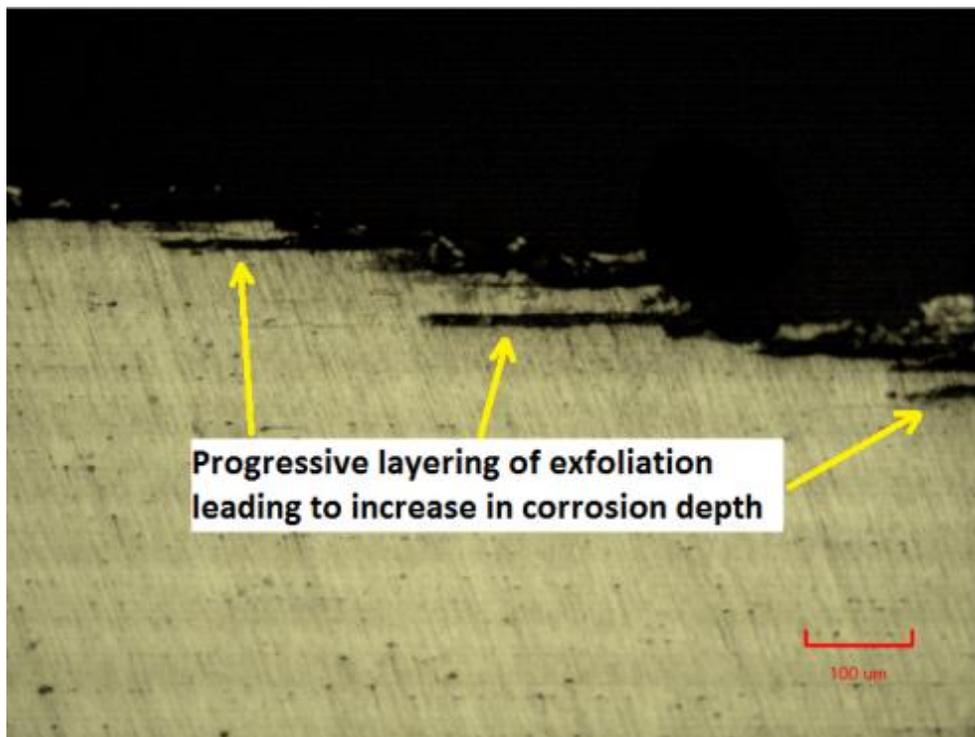
Figure 5.19: Unclad panel deep exfoliation damage, 100x magnification
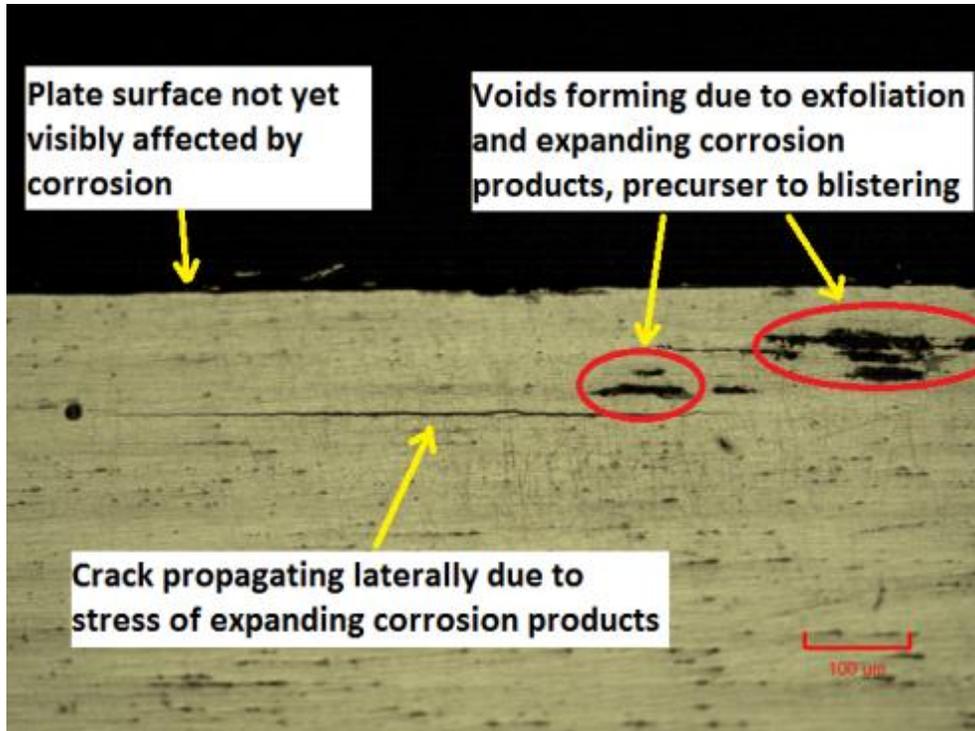
Figure 5.20: Unclad panel, crack propagation due to exfoliation, 100x magnification
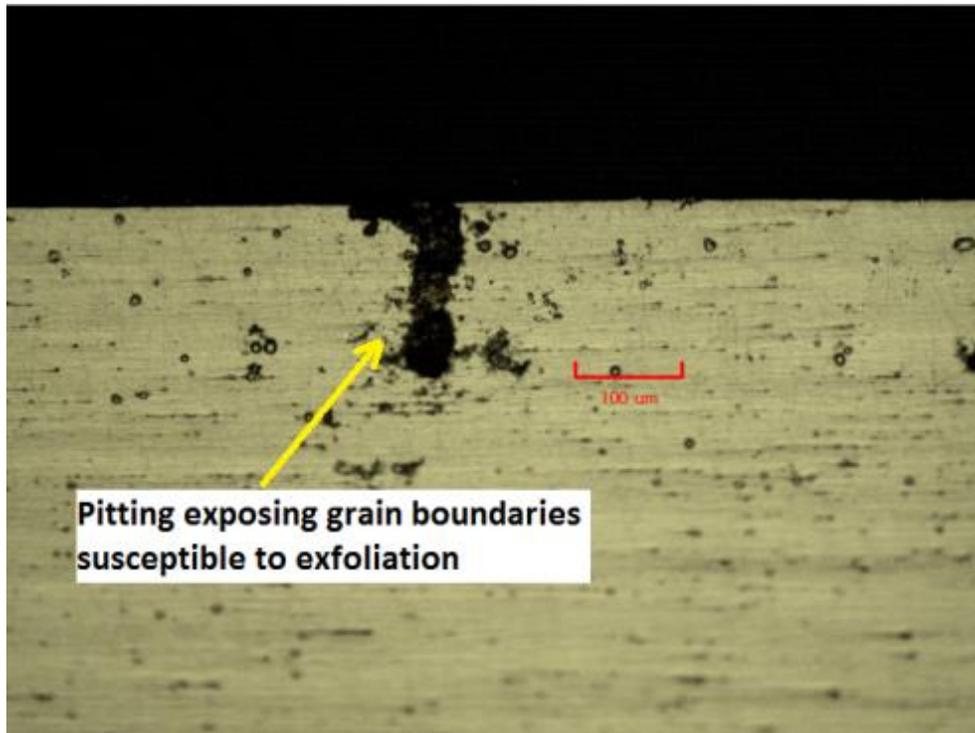
Figure 5.21: Unclad panel, evidence of pitting, 100x magnification

Figures 5.22 and 5.23 are representative cross-sections of the partially clad test panel. After cleaning the test panels with nitric acid, the red coloring on the upper surface of the partially clad aluminum panel did not remain. No appreciable difference was observed between the cross-sections of the protected milled surface, the middle region of light general corrosion and the upper red colored corroded surface.

Figure 5.22 shows the edge of a clad spot and an example of a very shallow pit beginning to propagate as exfoliation corrosion. Several examples of this shallow corrosion were found in the examined cross-sections but the majority of the aluminum surface was smooth and unaffected by corrosion. It can be seen that all of cladding layer from the clad spot has corroded away, leaving the aluminum core below unaffected. The small instances of corrosion combined with all of the cladding layer having been corroded implies that the clad spots have reached the limit of their ability to protect the partially clad panel after 300 hours of acidic salt spray exposure.

Figure 5.23 shows the typical surface not affected by corrosion observed over the majority of the partially clad test panel. No appreciable difference in surface appearance was observed between the surface affected by light general corrosion and the fully protected surface.
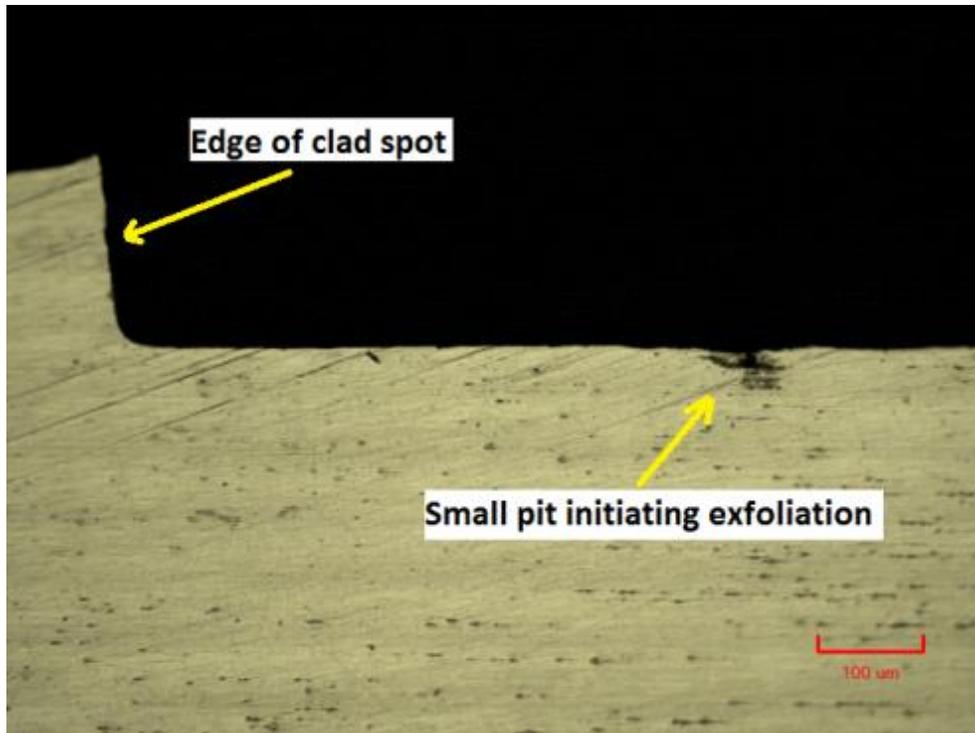
Figure 5.22: Spot clad panel, edge of clad spot with evidence of mild exfoliation
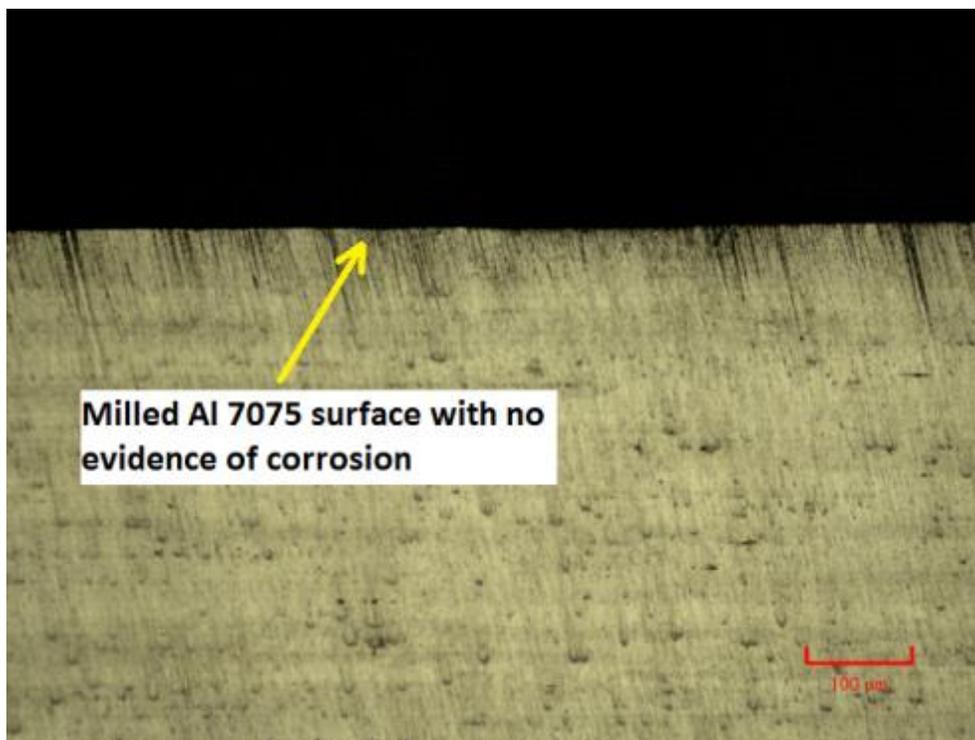
Figure 5.23: Spot clad panel, milled surface with no corrosion damage

5.2.4 Tensile Tests

Tensile specimens were machined from the corroded medium sized panels and tested in accordance to ASTM B557 [27]. Non-corroded tensile specimens were produced and tested in the same fashion for comparison of tensile properties. The results of this comparison are summarised in Figures 5.24, 5.25, 5.26 and 5.27.
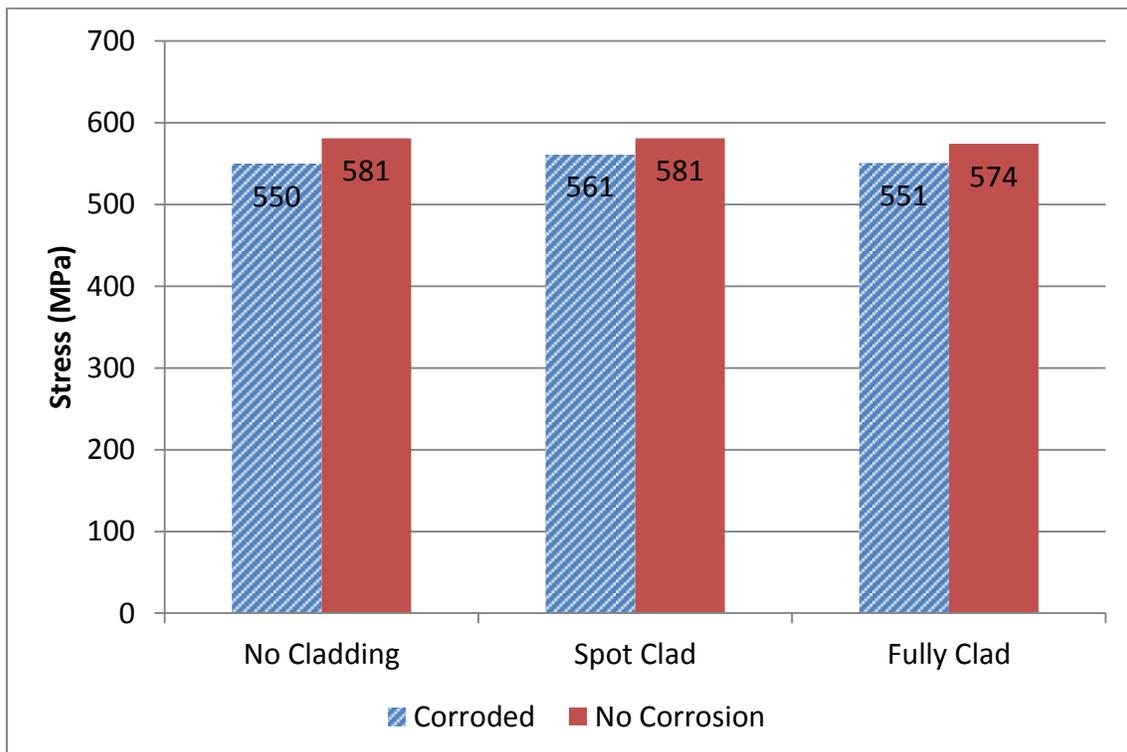
Figure 5.24: Tensile strength summary

The test panels with cladding removed, spot cladding and full cladding each showed a decrease in tensile strength after corrosion exposure. The partially clad test panel exhibited the smallest decrease in tensile strength with a percentage decrease of 3.4%, calculated by the following equation:

$$Percent\ Decrease = \frac{(Corroded\ Value - Uncorroded\ Value)x100}{Uncorroded\ Value}$$

This was followed by the fully clad test panel with a tensile strength percentage decrease of 4.0%. Finally, the cladding removed panel showed a percentage decrease in tensile strength of 5.3%. These values show that the fully clad and partially clad test panels were better protected from the corrosion environment when compared to the test panel with the cladding removed. These values are however more closely distributed than what would have been expected based on the corrosion observed on the test panel surfaces. It was expected that the unprotected test panel would have performed considerably worse than the two protected panels. This is an indication that the exfoliation corrosion damage observed on the test panel with the cladding removed was superficial when compared to the overall plate thickness of 6.35 mm.
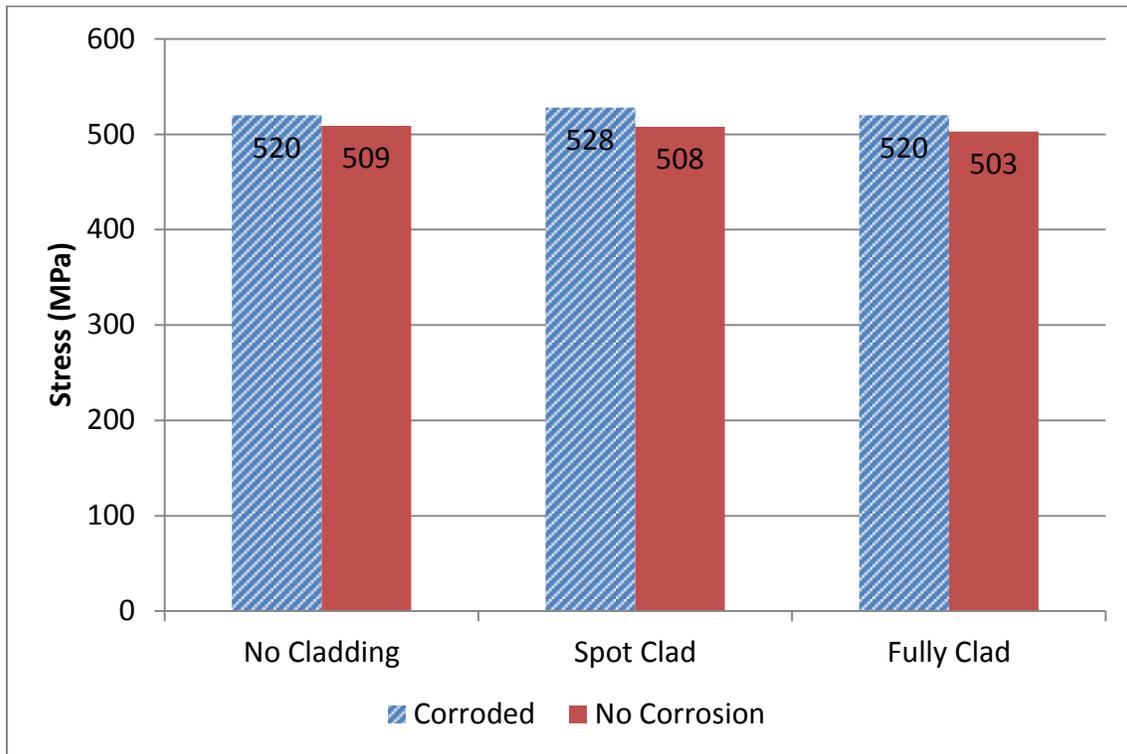
Figure 5.25: Yield strength summary

The yield strength of the three test panels each increased after exposure to the corrosion environment. The spot clad, fully clad and cladding removed test specimens showed a percent increase in yield strength of 3.9%, 3.4% and 2.2% respectively. This trend is not easily explained, as it is expected the yield strength would decrease with corrosion exposure.
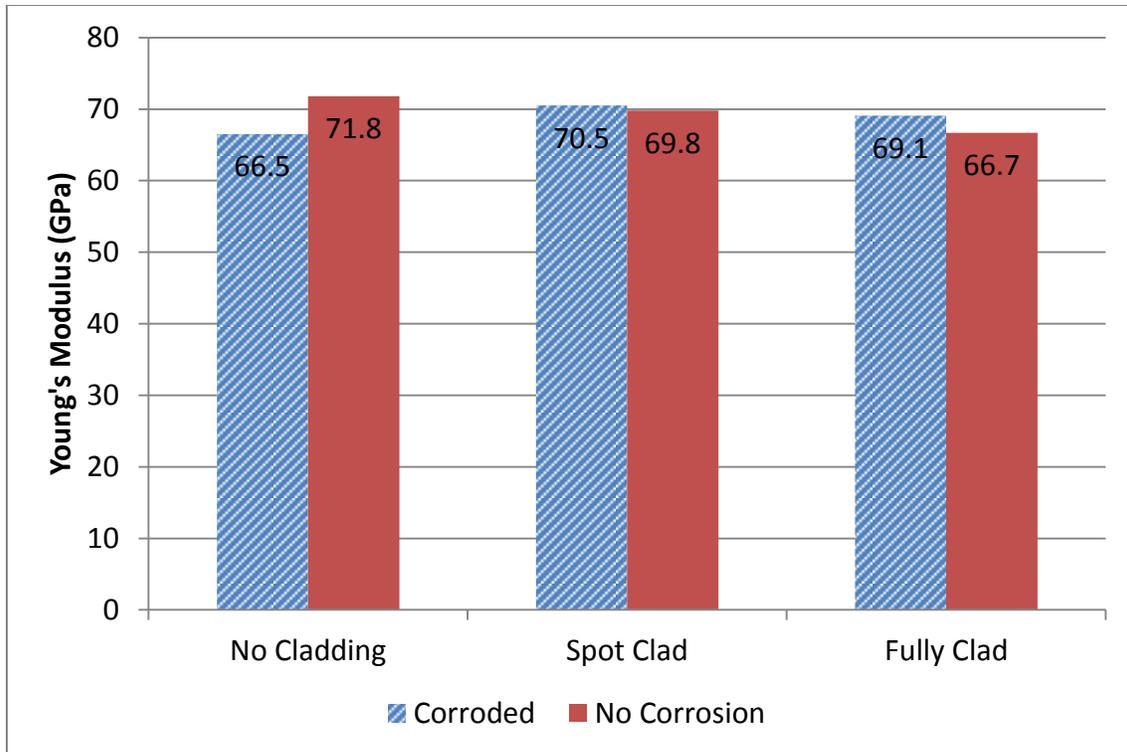
Figure 5.26: Young's modulus summary

The Young's modulus of the spot and fully clad test panels appeared to increase after corrosion exposure while it decreased for the panel with the cladding removed. The percentage increase in Young's modulus for the spot clad and fully clad test panels was 1.0% and 3.6% respectively. The percentage decrease in Young's modulus for the unprotected panel was 7.4%. The decrease in Young's modulus observed for the cladding removed panel when compared to the smaller increases for the spot clad and fully clad panels implies that the cladding removed panel was influenced to a greater extent by the corrosion environment.
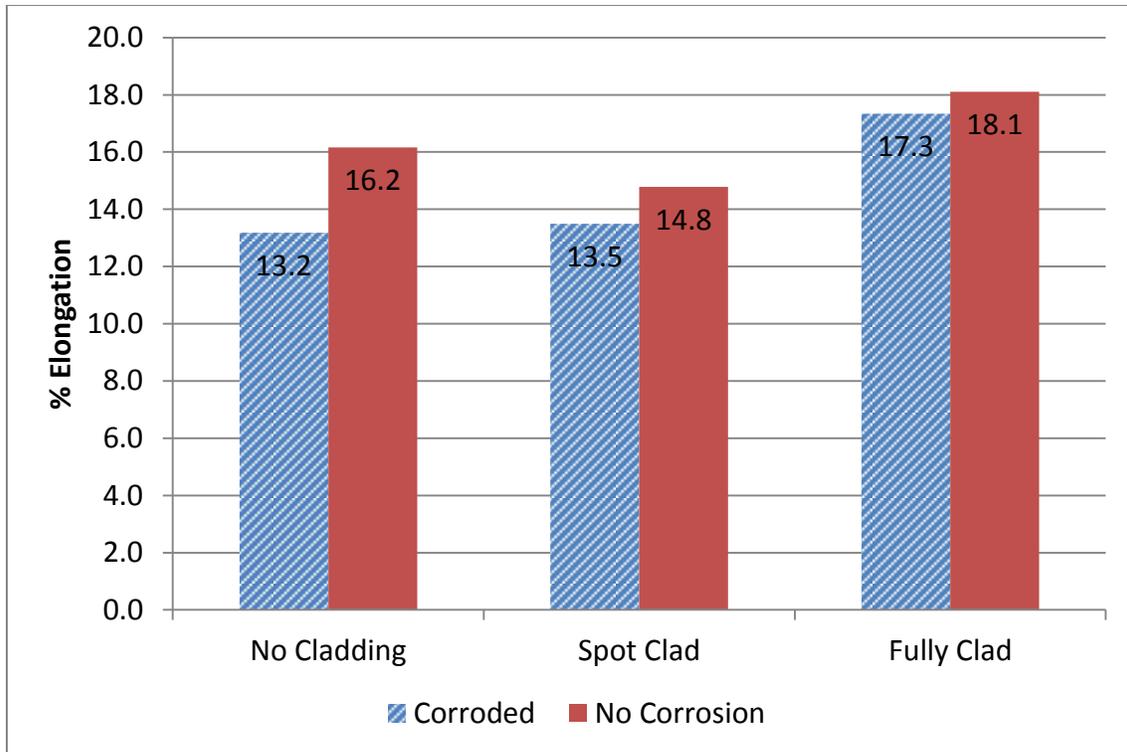
Figure 5.27: % Elongation summary

The percent elongation, calculated with a gauge length consisting of the 72.1 mm reduced section of the tensile specimens, of the cladding removed, spot clad and fully clad test panels all decreased after corrosion exposure. The percent decrease in percent elongation for the cladding removed, spot clad and fully clad test specimens was 18.4%, 8.7% and 4.2% respectively.

The percent decrease in mechanical properties for the medium scale test panels are summarized in Table 5.3. It can be seen from this summary that the spot clad and fully clad test panels resisted corrosion damage causing a decrease in mechanical properties similarly well when compared to the poorer performance of the test panel with the cladding removed.

Table 5.3: Summary of percent decrease in mechanical properties for medium scale test panels, negative values indicate a percent increase in mechanical properties

	No Cladding	Spot Clad	Fully Clad
Tensile Strength	5.3%	3.4%	4.0%
Yield Strength	-2.2%	-3.9%	-3.4%
Young's Modulus	7.4%	-1.0%	-3.6%
% Elongation	18.4%	8.7%	4.2%

5.2.5 Fatigue Tests

The results of the corroded specimen fatigue tests have been summarised in Figure 5.28. As expected, all of the fatigue specimens fail at a lower number of cycles when subjected to a larger maximum stress. What was not expected was the very poor performance of the corroded partially clad test panel. Based on the corrosion observed on the surface of each of the panels, the partially clad and fully clad panels were expected to perform equally well, while the unclad panel was expected to perform poorly due to the exfoliation corrosion acting as stress raisers and locations for crack initiation. It is possible that the geometry of the partially clad fatigue specimens contributed to the early failure under the cyclic loading. It was desired that only the clad layer be removed over the panel surface with the exception of the clad spots. During the machining process this was not accomplished, a significant thickness of approximately 0.6 mm of the core aluminum alloy was also removed. This resulted in the clad spots having a larger thickness than desired and the spots remaining after the corrosion process consumed most of the Alclad layer. The edge of the clad spots likely acted as stress raisers reducing the sample's resistance to cyclic loading. The poor fatigue performance of the corroded partially clad specimens is likely due to the specimen geometry and not a greater

susceptibility to corrosion when compared to the fully clad and cladding removed fatigue specimens.
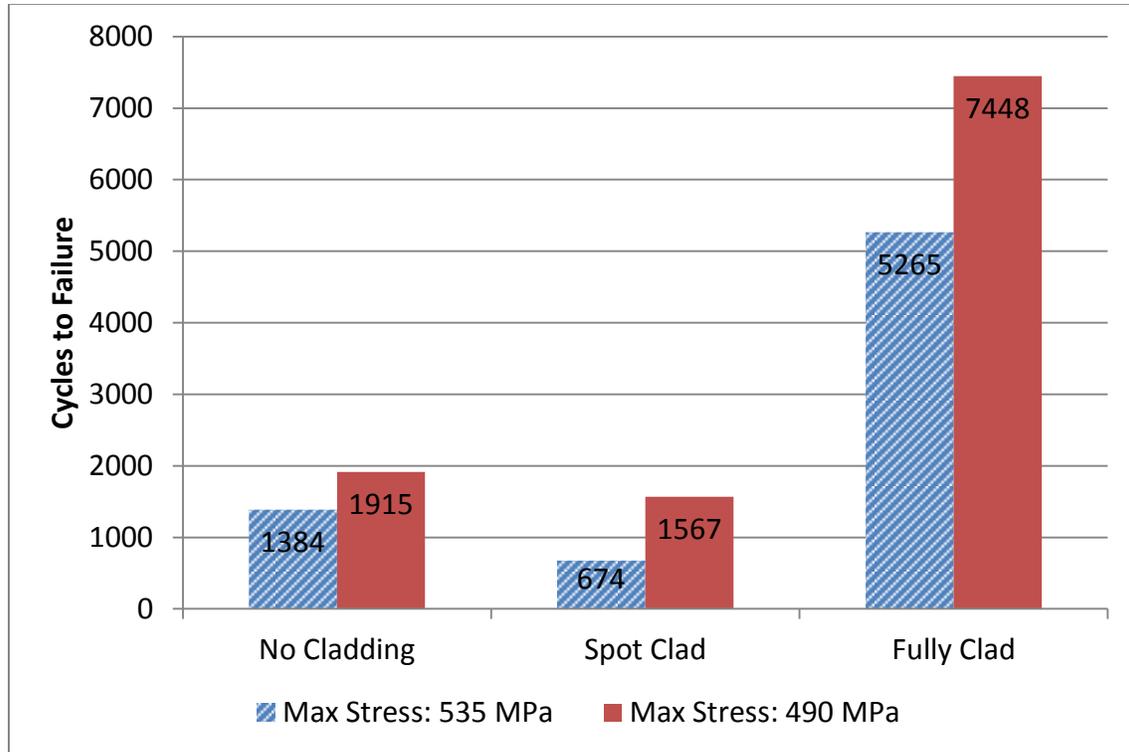
Figure 5.28: Corroded sample fatigue test summary (R=0.1)

Non-corroded fatigue specimens were produced and tested in the same fashion described above at a maximum stress of 490 MPa and the results were compared with the corroded specimens. The results of this comparison are summarised in Figures 5.29. The percent decrease in cycles to failure after corrosion exposure for the unclad, spot clad and fully clad panels was 78.8%, 28.6% and 23.9% respectively. This confirms that the geometry of the clad spot fatigue specimens contributed greatly to the low number of cycles to failure. If we consider the percent decrease in cycles to failure after corrosion exposure, it is confirmed that the fully clad and spot clad panels resisted corrosion damage to a similar degree. The fatigue

resistance of the unclad panel was greatly influenced by the corrosion exposure and failed at a

very low number of cycles when compared to non-corroded specimens.
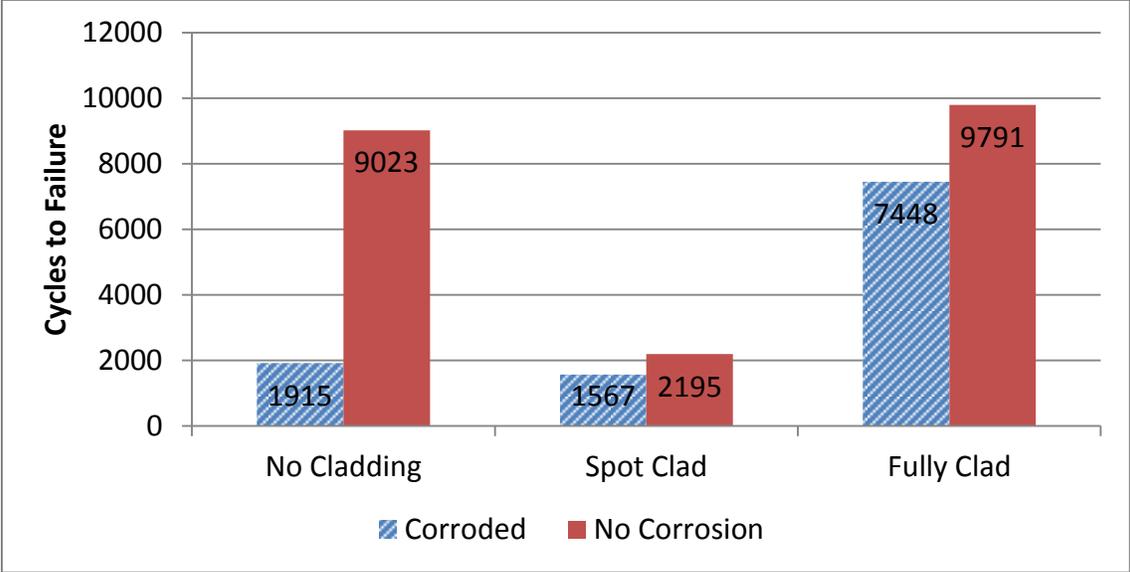
Figure 5.29: Corroded vs no corrosion fatigue test summary (R=0.1, max stress = 490 MPa)

6. Analysis of Results

6.1 Effect on Mechanical Properties

6.1.1 Tensile Strength

The non-corroded Alclad test specimens had a tensile strength of 574 MPa, this was 1.21 %

lower than the non-corroded partially clad and cladding removed panels both having a tensile

strength of 581 MPa. This decrease in strength can be explained by the presence of the

cladding layer on the Alclad test specimens. The cladding layer is assumed to carry no load and

on one side has a thickness of 1.25 % of the aluminum plate. The loss in strength due to the

Alclad layer not carrying any load agrees well with the 1.21 % decrease in tensile strength

observed in the tensile test. This same result can be seen in the corroded Alclad and partially

clad test specimens. If it is assumed that the tensile strength of both cases were affected by

the corrosion environment in a similar fashion, the 1.8% higher tensile strength of the corroded

spot clad test specimens could again be attributed to the 1.25% thickness of cladding layer on

the Alclad specimens that is not carrying a load.

The percent decrease in tensile strength of the Alclad, partially clad and no cladding tests

specimens were 4.0%, 3.4% and 5.3% respectively. This shows that the tensile strength of the

partially clad and fully clad test specimens was less affected by the corrosion environment than

the unprotected test specimens. Interestingly the partially clad specimens outperformed the

Alclad specimens.

75

6.1.2 Yield Strength

The non-corroded Alclad test specimens similarly had slightly lower yield strength than both the non-corroded spot clad and cladding removed test specimens. Also, the corroded Alclad test specimens had lower yield strength than the corroded spot clad specimens. Both of these lower yield strengths can again be likely be attributed to the cladding layer of the Alclad specimens not carrying any load.

The yield strength of all of the test specimens increased after corrosion exposure. The percent increase in yield strength of the Alclad, partially clad and bare tests specimens were 3.4%, 3.9% and 2.2% respectively. The Alclad and partially clad test specimens increased yield strength to a similar degree while the cladding removed test specimens had less of an increase to yield strength after corrosion exposure. This trend of increasing yield strength after corrosion exposure is not easily explained and may require further investigation to better determine the cause.

6.1.3 Young's Modulus

The effect of corrosion exposure on the Young's modulus of the test panels was not considered significant. The presence of corrosion damage generally does not affect the elastic behavior of a metal unless there is a cyclic stress or a significant loss in the effective material thickness due to localized corrosion [31].

6.1.4 Percent Elongation

The ductility of the test panels appears to be negatively affected by both the corrosion environment and machining process used to produce the physical geometry of the test panels.

For the non-corroded test specimens, the as-received Alclad specimens showed the greatest ductility with a percent elongation of 18.1%. The non-corroded test specimens with the cladding removed showed a lower ductility with a percent elongation of 16.2%. This lower percent elongation could be explained by a work hardening of the milled surface or perhaps by a rough surface finish from the milling process resulting in a lower ductility. The non-corroded spot clad test panel samples had the smallest percent elongation at 14.8%. It is believed that this was because of geometry of the raised clad spots. Shown in Figure 6.1, it was observed that the reduction in cross-sectional area occurred primarily along the length of the tensile specimen where there the clad spots were not present. The larger thickness of the clad spots reinforced the tensile specimens and reduced plastic deformation at their locations. As a result, the locations without a clad spot plastically deformed until fracture while the elongation at the clad spots remained relatively small, resulting in an overall lower percent elongation.
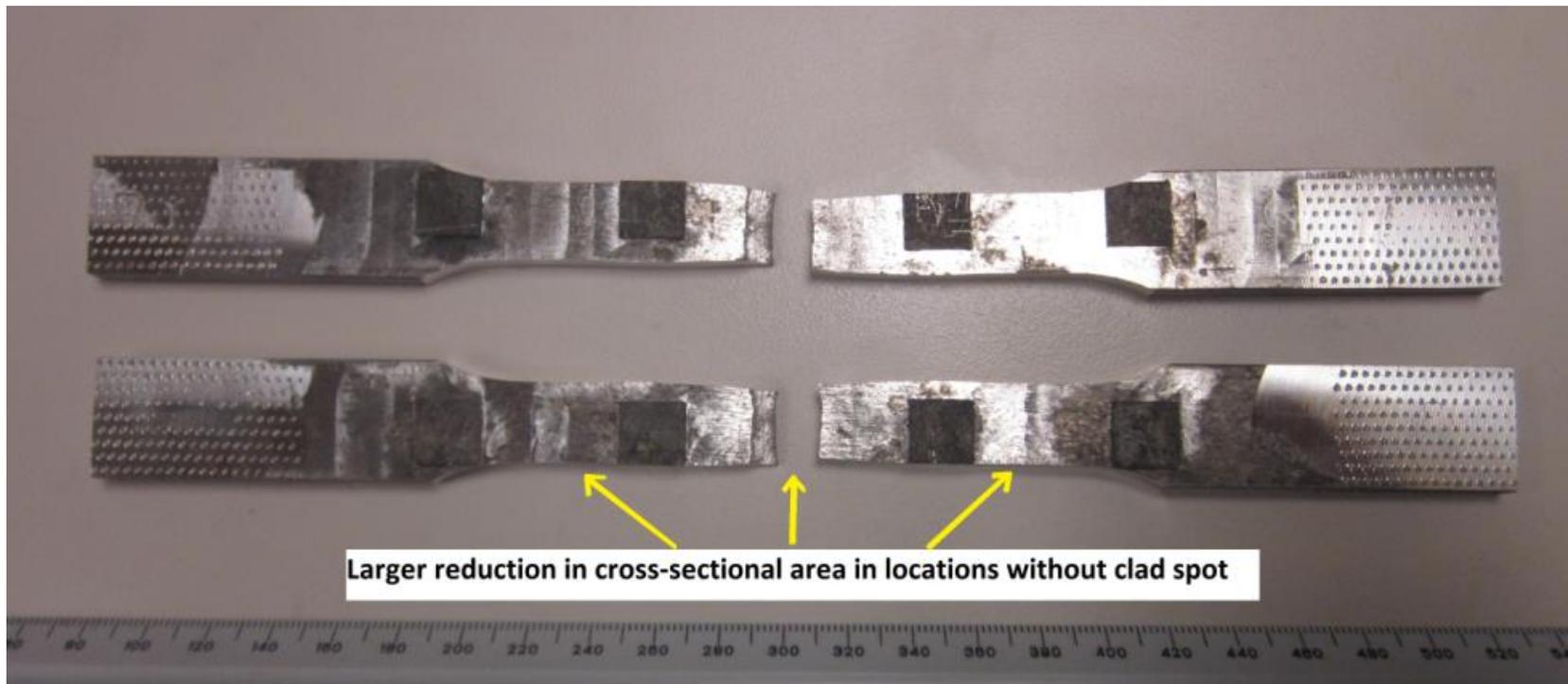
Figure 6.1: Partially clad tensile test specimens showing necking limited to areas without clad spot

The effect of corrosion on the ductility of the bare test panel was the most pronounced with a percent decrease in percent elongation of 18.4%. This was due to the loss of panel thickness caused by exfoliation and the presence of sharp intergranular corrosion that facilitated crack initiation and propagation. The loss in ductility of the Alclad test panel due to corrosion was markedly lower with a decrease in elongation of 4.2%. The Alclad layer successfully protected the panel from a loss in Al 7075 core thickness and prevented any sharp intergranular corrosion. The loss in ductility due to corrosion for the partially clad test panel was somewhat higher than the Alclad panel but much lower than the cladding removed panel with a decrease in elongation of 8.7%. This loss in ductility was likely caused by the small patches of corrosion observed adjacent to the clad spots where a small degree of intergranular corrosion occurred.

6.1.5 Fatigue Tests

It has been stated in other works that the presence of an Alclad layer is detrimental to the fatigue resistance of aluminum sheet and plate because cracks will initiate in the cladding layer under cyclic loading and propagate into the higher strength aluminum core to cause premature failure [32]. This was not observed during the fatigue tests conducted in this study, likely because all of the samples had a cladding layer on the back surface and the extra cladding layer on the front surface of the Alclad test specimens did not significantly increase the fatigue susceptibility.

When considering only the corroded fatigue samples tested under cyclic loading with maximum stresses of 490 and 535 MPa the partially clad test specimens performed the worst, failing after 1567 cycles (at 490 MPa) and 674 cycles (at 535 MPa). The cladding removed samples did

better, failing after 1915 cycles (at 490 MPa) and 1384 cycles (at 535 MPa). The Alclad samples far exceeded the other two by failing after 7448 cycles (at 490 MPa) and 5263 cycles (at 535 MPa). This result was not consistent with the observed corrosion damage on the test panels, where the cladding removed panel would be expected to perform the worst due to the exfoliation corrosion acting as stress raiser facilitating crack propagation during cyclic loading.

After comparing the number of cycles to failure of the corroded samples with the non-corroded samples (at 490 MPa), it became apparent that the presence of the raised clad spots were more detrimental to the fatigue resistance of the tests specimens than the exfoliation corrosion. The raised clad spots are an artifact of the machining process. During the production of the medium sized partially clad test panel, not only the clad layer was removed but also a significant amount of the high strength aluminum core. This resulted in the clad spots being composed of a plateau of aluminum core with cladding at the top. After corrosion exposure the raised part of the clad spot consisting of the aluminum core remained. This did not significantly affect the corrosion resistance of the partially clad panel because the clad layer was still exposed to the corrosive electrolyte and electrically connected to the core. It did however affect the fatigue resistance of the partially clad test specimens due to either varying thickness of the fatigue specimen or due to the stress raiser caused by the edge of the clad spot. As shown in Figure 6.2, the partially clad fatigue specimens failed at an edge of a clad spot where the clad spot appeared to be sheared from the surface of the test specimen.
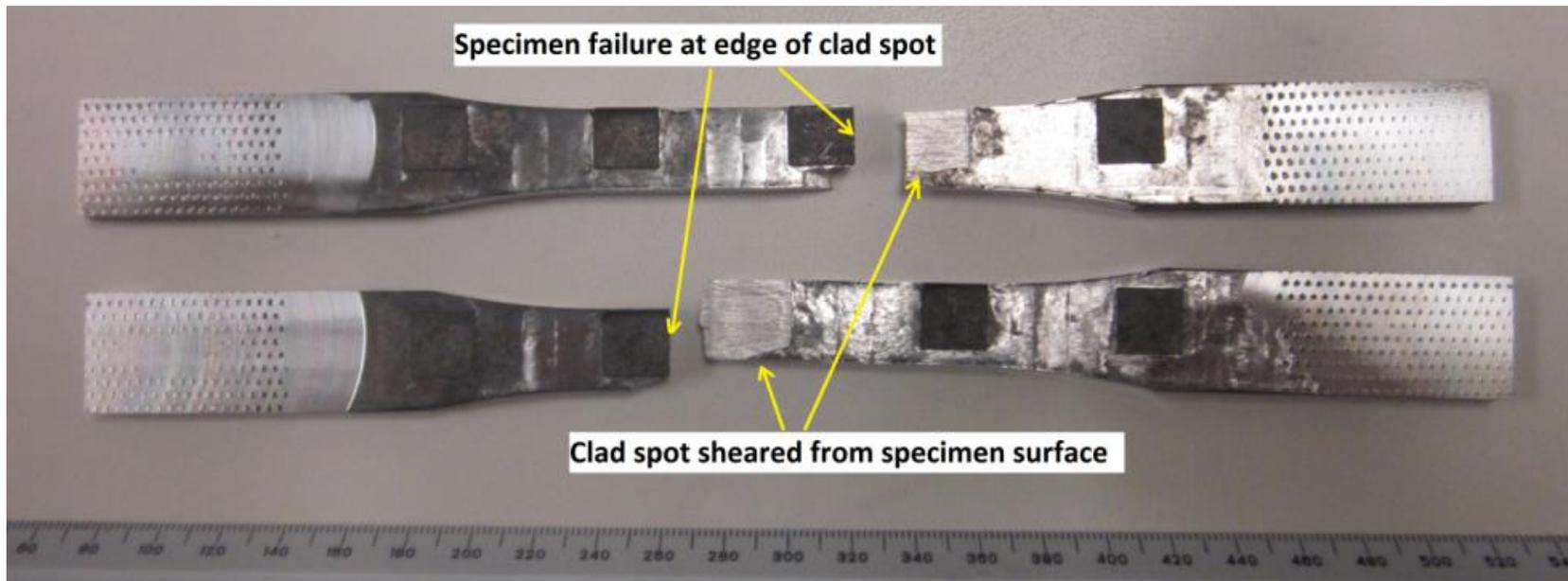
Figure 6.2: Partially clad fatigue test specimens shown to fail at sheared clad spot edge

To determine the relative resistance to corrosion damage deteriorating the fatigue resistance of the three medium test panels, the cycles to failure of the corroded tests specimens were compared to the cycles to failure of the non-corroded tests specimens at a maximum stress of 490 MPa. The decrease in the number of cycles to failure for the Alclad, partially clad and cladding removed tests specimens after corrosion exposure were 23.9%, 28.6% and 78.8% respectively. This confirms that raised part of the clad spots composed of the core were the cause of the premature failure of the partially clad test specimens. It also shows that the Alclad and the partially clad tests specimens had a similar resistance to corrosion detrimental to the fatigue resistance of the test specimens while the cladding removed test specimens exhibiting exfoliation corrosion that was extremely detrimental to resisting fatigue crack propagation.

6.2 Corrosion Environment

The acetic acid salt spray environment used during this experiment resulted in exfoliation corrosion on the medium sized test panel with the Alclad layer removed and mild general corrosion on certain regions of the partially clad medium sized panel. Large amounts of pitting were not observed on either of these panels. This was expected because pitting occurs primarily in the presence of the thin oxide film that passivates aluminum in most environments but this film becomes unstable at very high and low pH [10, pp. 106-108]. The pH of acetic acid salt spray test was between 3.1 and 3.3, at this pH the oxide film just begins to become unstable. Some pitting was observed on the test panel with the cladding removed but the majority of these sites became initiation points for exfoliation corrosion that destroyed evidence of the pit. The Alclad medium sized test panel showed corrosion of the cladding layer that resembled pitting while corroding as a sacrificial anode. These pits deepened until they reached the protected aluminum core of the Alclad plate and then widened, progressing laterally.

The red colored corrosion products primarily observed on the bare medium sized test panel, seen in Figure 5.14 and observed to a lesser extent on the upper region of the partially clad medium sized test panel, seen in Figure 5.15, were not initially expected. This was because the corrosion products of aluminum alloys are known to be white in color [10, pp. 12-13]. After some literature review, it was discovered that during the corrosion of aluminum alloys containing high concentrations of alloyed copper in the presence of chloride ions, it is possible for copper to dissolve into the solution and plate onto the aluminum alloy surface [33], [34]. During the corrosion of aluminum alloys containing copper as a major alloying element, copper

containing intermetallic particles found in Al 7075 T651 such as $MgCu_2$ or Al_2CuMg can be subjected to dealloying where magnesium and aluminum are selectively dissolved, leaving behind a microporous region consisting primarily of elemental copper. These high surface area regions of copper then act as a local cathode and cause pitting and trenching to the alloy adjacent to the copper. It is then possible for the copper region to detach from the aluminum alloy, dissolve into the corrosive electrolyte and electrically plate back onto the alloy surface. It is believed that this is the source of the red coloring observed on the upper region of the medium sized partially clad test panel and over the entire surface of the bare panel. The galvanic cell created by the copper plated at the top surface of the partially clad medium sized test panel is believed to be the cause of the general corrosion observed between the red copper region and the non-corroded region of the test panel as well as the smaller corrosion spots observed adjacent to the clad spots. Copper ion contamination from water and salt used during the experiment can be ruled out because special precautions were taken to limit copper content detailed in Section 4.3.

Energy dispersive spectroscopy (EDS) using a scanning electron microscope (SEM) was used to confirm the composition of the red corrosion products. This characterization technique is not ideal for this task because EDS generates X-rays to a depth of microns on a sample surface [35] and the copper layer is believed to be very thin. In spite of this, EDS did confirm an elevated concentration of copper in the samples covered in the red corrosion product of 7.7 weight % while the overall alloy copper composition was measured as 1.5 weight % for non-corroded samples.

6.3 Materials Selection

For partial cladding to become a viable alternative to Alclad products two major issues would still need to be addressed. The first is the question of how partially clad plate and sheet could be produced in an economically equivalent process when compared to current methods for producing Alcald products after taking into consideration the savings due to lower aircraft weight. Currently Alclad plate and sheet are formed by hot rolling a high strength aluminum core sandwiched between cladding layer sheets, metallurgical bonding them together. One possible production method for partially clad products could be to use a thermal spray coating. Thermal spray coatings are applied by heating a coating material until fully or partially melted and spraying it onto a substrate with a hot gas [36, p. 18.48]. Using this process it may be possible to apply a fine distribution of cladding droplets to the high strength aluminum core before or after the rolling process. This production technique could also address the second issue with partial cladding which is how effectively will partial cladding resist corrosion when used in conjunction with typical aerospace coating systems. For a sacrificial cladding layer to protect the core aluminum both the cladding layer and the area to be protected need to be exposed to the corrosive electrolyte and be electrically connected. This may become an issue if the partial cladding pattern selected has a wide spacing between clad spots. Aerospace aluminum coating systems effectively isolate their aluminum substrate from the corrosive aerospace environment. The sacrificial Alclad layer only protects the aluminum when the coating system fails in a specific location due to damage such as a scratch of filiform corrosion. For a partial cladding layer to be effective in this situation, the spacing between clad spots would have to be small enough that any damage to the coating system exposes both the

unprotected alloy and one or more clad spots. Using a thermal spray production procedure

that applies a fine distribution of clad spots may be effective at solving this issue.

Another consideration about partial cladding is deciding when it should be selected over Alclad

products. If after continued study, partial cladding is confirmed to be equivalently resistant to

corrosion attack as Alclad products and can be produced in an economically comparable

process, partial cladding may still not always be the optimal material selection. Partial cladding

would be best suited for applications where weight reduction of plate or sheet is critical. From

an aircraft maintenance point of view, partial cladding may only be viable in locations that are

easily inspected or when the application is not structurally critical. In applications where a

coating system is not applied, Alclad products may be a better choice for long term corrosion

protection. Some of these considerations have been summarized in a materials selection

decision tree seen in Figure 6.3.
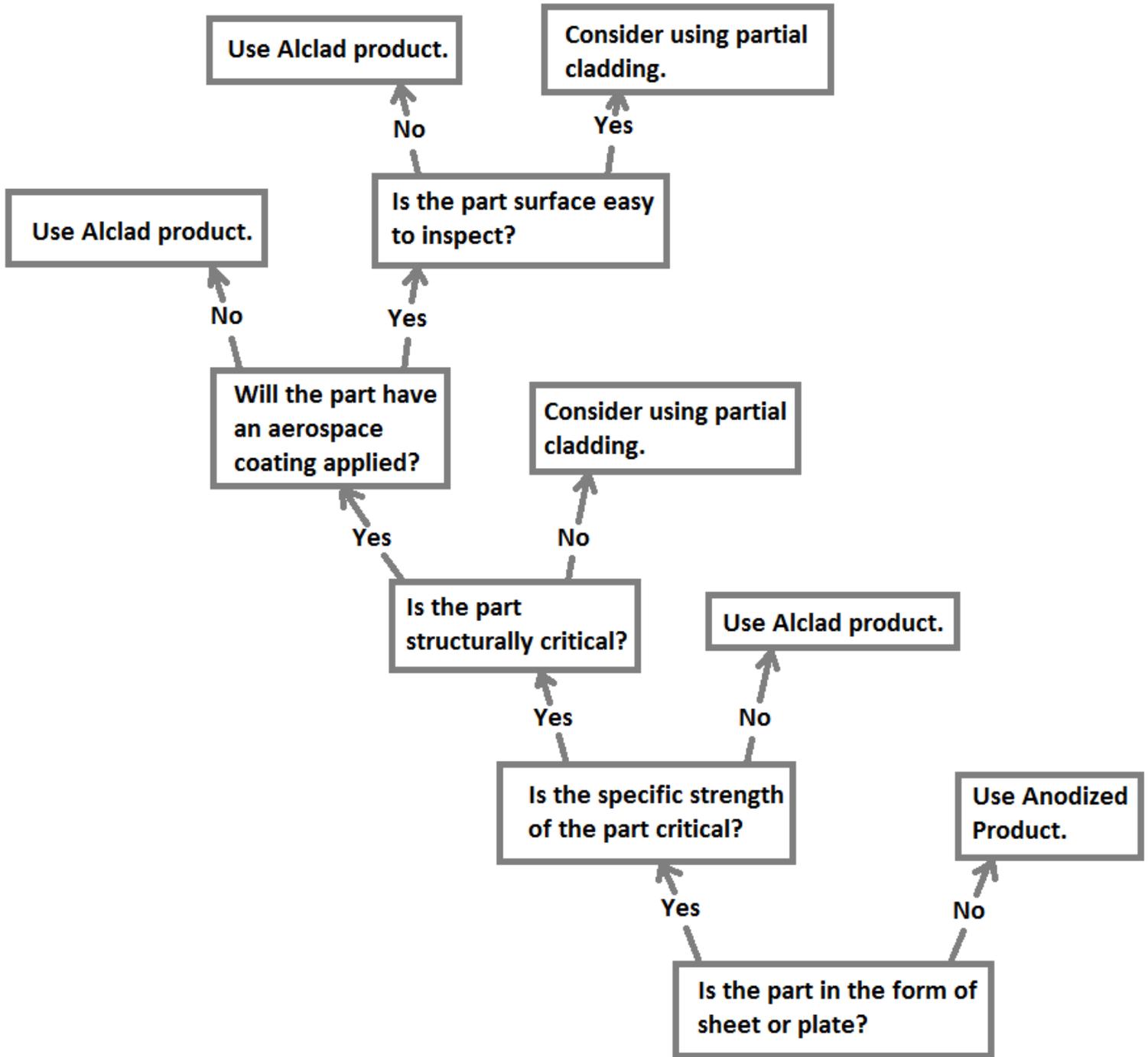
Figure 6.3: Decision tree for the selection of partial cladding in the aerospace industry

Partial cladding may find applications in aircraft maintenance. Currently when exfoliation

corrosion is detected in aging aircraft, the repair procedure is to grind away the aluminum

substrate to a depth where no more signs of exfoliation are present [31]. The ground section is

then repainted with aerospace coatings. The drawback of this procedure is that any Alclad

layer that remained in the ground section would also be removed. If a partial cladding thermal

spray procedure was applied to the affected region before painting, it would result in increased

corrosion resistance of the repaired area. This could prevent or delay the need for future

maintenance and would be especially beneficial because future grinding in the same location

could result in a loss of part thickness that would require it be replaced at a higher expense.

6.4 Analysis of Central Clad Spot Panels

6.4.1 First 1 cm^2 Central Clad Spot Panel

In an effort to numerically analyze the data used to produce the surface plots, the data was

converted into polar coordinates. A value for the distance from the center of the test panel

was calculated for each data point. The angle from the origin of each data point was not

considered to be important for comparing the overall extent of the corrosion damage on each

test panel and determining what central circular regions of the test panels were protected by

the central clad spots. The area of the test panels that was considered during this analysis was

a 50 mm radius circle centered on the clad spot. The data from the four corners of the test

panels were not considered.

The data was represented in two major ways. First, Figure 6.4 depicts the average percentage

of the aluminum surface that exhibits signs of corrosion damage within regions defined by

rings. The rings emanate from the center of the test panels and each has a thickness of 5 mm.

Second, Figure 6.5 shows the change in the average percentage of surface corrosion in a

varying area defined by a circle centered on the clad spot with an increasing radius.

The results for the initial 1 cm^2 central clad spot panel depicted by Figures 6.4 and 6.5 show

four major regions of interest. The area within 5 mm from the center of the clad spot shows

virtually no signs of exfoliation corrosion. This was expected because this region essentially

overlaps the clad spot and the high strength aluminium core receives the full protection of the

sacrificial cladding. Next, the area between 5 and 20 mm from the center of the test panel

shows a good level of corrosion protection. Evidence of corrosion was observed on

approximately 5% of this surface and did not penetrate to a depth of 0.17 mm. This area

coincides with the protected area initially estimated using the surface plot and that was used to

determine the dimensions for the medium scale partially clad test panel. The area between 20

and 40 mm from the center of the test panel show the region where the central clad spot is no

longer protecting the surface of the aluminium from corrosion. In this area, the depth of

corrosion damage extends beyond 0.17 mm. The final region of interest is the area between 40

and 50 mm from the center of the test panel. Here, the extent of the corrosion damage reduces

with increasing distance from the protective central clad spot. This was not expected but could

be explained by interaction between the front of the test panel exposed to the corrosion

environment and the fully clad back of the panel that was isolated from the corrosion

environment by corrosion protective tape. This may be an indication that the method used to

isolate the back of the test panels was insufficient to fully prevent interactions with the

corrosion environment.
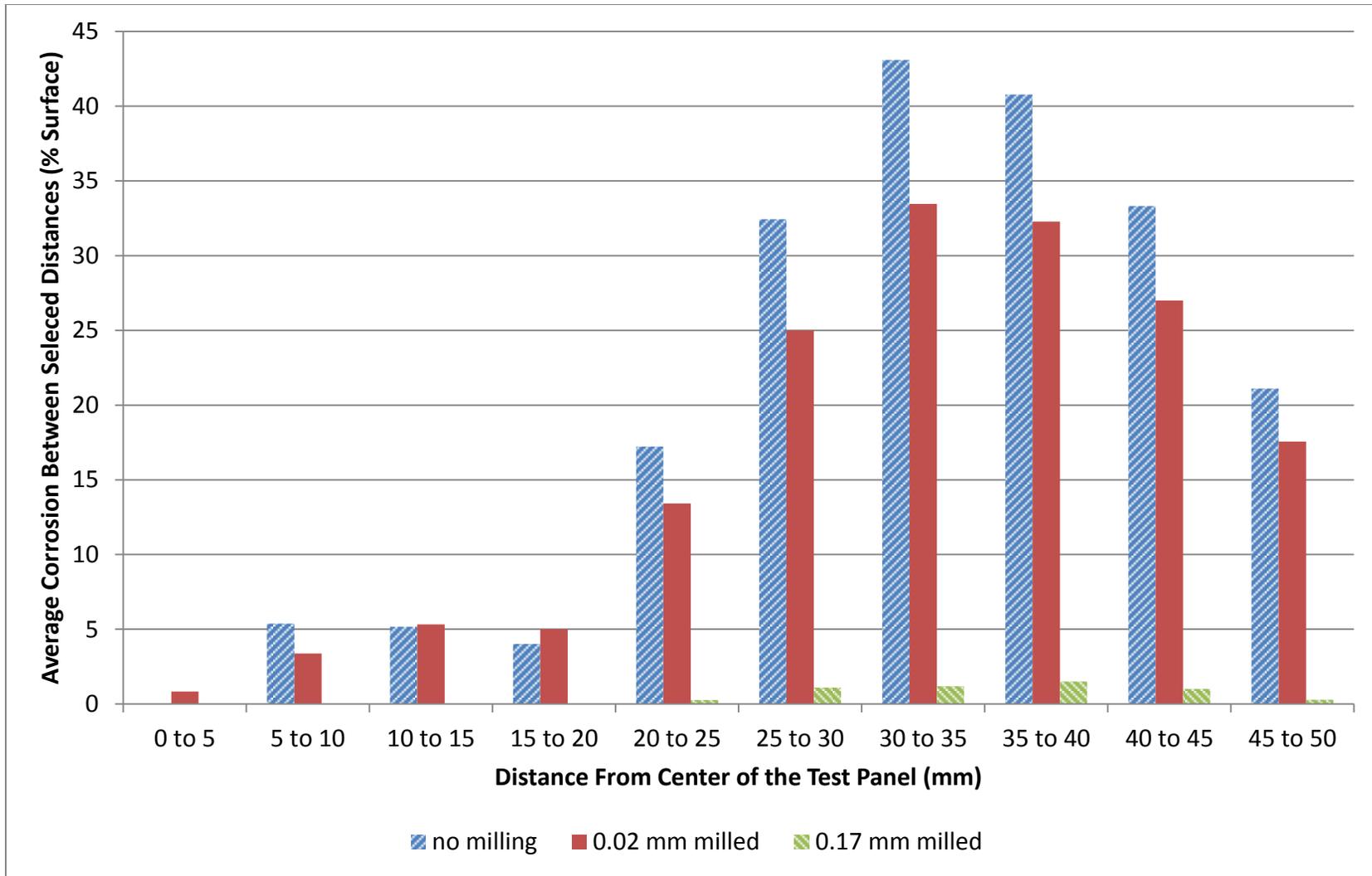
Figure 6.4: Average percentage of corrosion damage observed on the surface of regions defined by rings emanating from the center of the initial 1 cm^2 central clad spot test panel, three milled depths are shown representing the minimum corrosion penetration
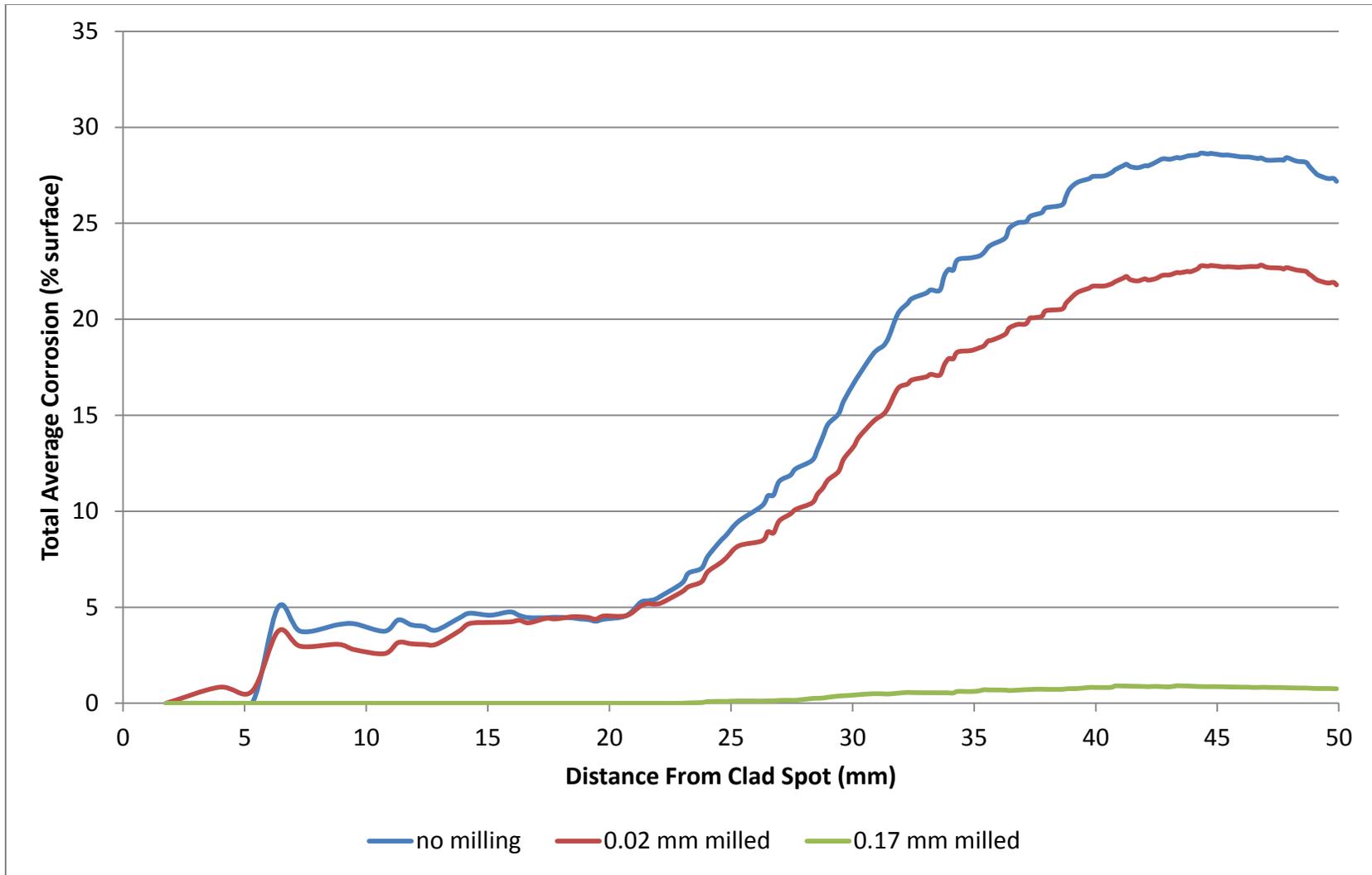
Figure 6.5: Cumulative average percentage of corrosion damaged observed on the surface of an increasing circular area having a radius defined by the distance from the center of the initial 1 cm² central clad spot test panel, three milled depths are shown representing the minimum corrosion penetration

6.4.2 Varying Clad Spot Dimensions

After conducting the initial 1 cm^2 central clad spot panel experiment, a series of three additional central clad spot panels were produced having varying clad spot areas of 0.5 cm^2, 1 cm^2 and 2 cm^2. This was done to explore the relationship between clad spot area and the area and extent of corrosion protection. The panels were exposed to the same corrosion environment and prepared in the same fashion with one significant difference. The second set of central clad spot panels did not have the milling marks from the machining process removed by sanding.

The results of the second set of varying central clad spot area test panels are summarized in Figures 6.6, 6.7, 6.8 and 6.9. The goal of this analysis was to experimentally determine the relationship between the area of the test panel protected and the size of the clad spot and the relationship between the depth of corrosion attack and the size of the clad spot.

From Figures 6.6 and 6.7 it can be seen that the distribution of the corrosion damage on the surface of the aluminium test panels for the second set was much more uniform than for the first test panel. This can likely be attributed by small crevices and increased surface area from the milling process facilitating corrosion initiation. The surface of the 0.5 cm^2 central clad spot panel is the first instance that shows virtually no corrosion protection from the clad spot. The 1 cm^2 and 2 cm^2 central clad spot panels show very similar resistance to corrosion on the panel surface after corrosion exposure. The four regions of corrosion behavior observed on the first central clad spot test are much less apparent on the 1 cm^2 and 2 cm^2 clad spot test panels, but can still be seen. The overall average surface corrosion observed between the 1 cm^2 and 2 cm^2

clad spot test panels is very similar at 30.5% and 29.3% respectively. While the overall average

surface corrosion observed on the 0.5 cm^2 clad spot panel is significantly lower at 26.2%. From

Figure 6.6 it is apparent that the lower average corrosion of the 0.5 cm^2 panel is attributed to

the decrease in corrosion on the outer perimeter of the test panel. This decrease implies a

large degree of interaction between the front corrosion surface of the panel and the clad back

surface that should be isolated from the corrosion environment. It is possible that this has

occurred because the application of the corrosion resistant tape to the 0.5 cm^2 panel was

flawed when compared to the other panels.
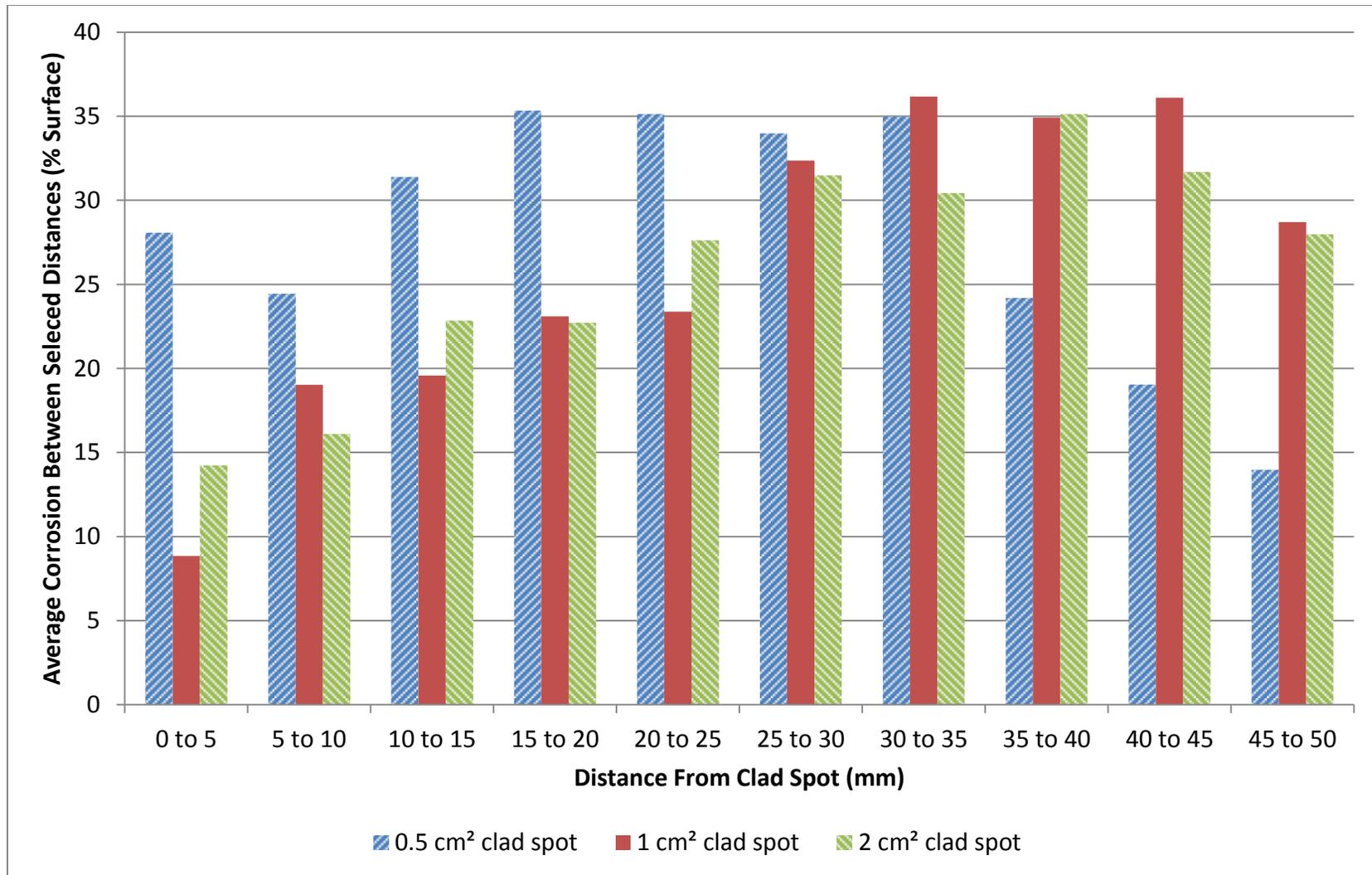
Figure 6.6: Average percentage of corrosion damage observed on the surface of regions defined by rings emanating from the center of the second set of central clad spot test panels (0.5 cm^2, 1 cm^2 and 2 cm^2), milling marks remain, no milling after corrosion exposure
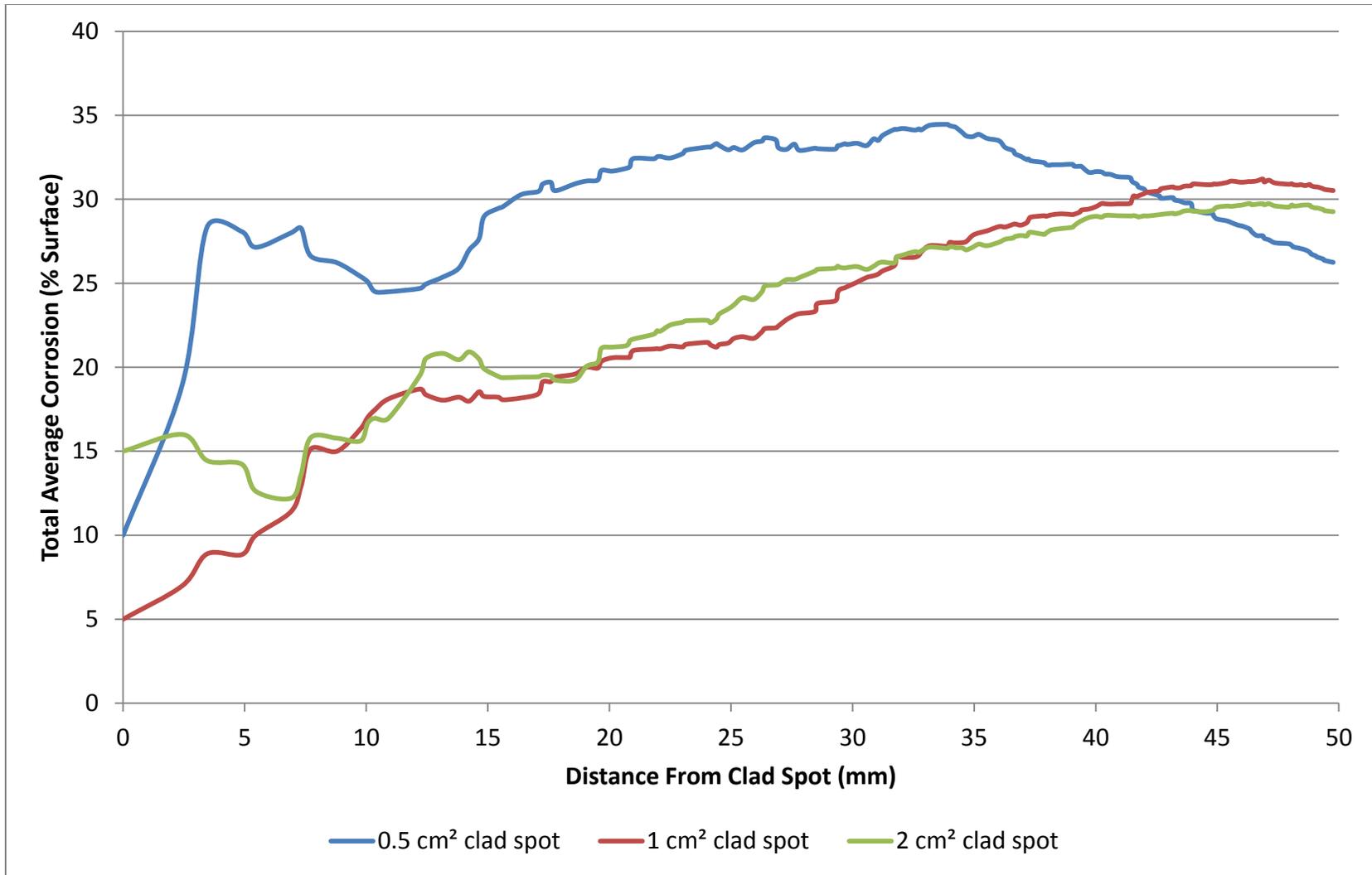
Figure 6.7: Cumulative average percentage of corrosion damaged observed on the surface of an increasing circular area having a radius defined by the distance from the center of the second set of central clad spot test panels (0.5 cm², 1 cm² and 2 cm²) milling marks remain, no milling after corrosion exposure

From Figures 6.8 and 6.9 it can be seen that the size of the clad spot directly affects the

protection of the test panel surface from corrosion penetrating depths larger than 0.17 mm.

The 1 cm^2 and 2 cm^2 clad spots are both similarly effective at protecting the aluminium surface

from corrosion at a distance of 20 mm from the center of the test panel. The 0.5 cm^2 clad spot

is insufficient to protect the aluminium surface at any distance. The level of corrosion

protection in the region between 20 and 50 mm from the center of the panel appears to be

approximately proportional to the size of the clad spot. Again, the drop in the average

corrosion damage in the outside region of the test panel implies some interaction with the clad

back surface of the panels.
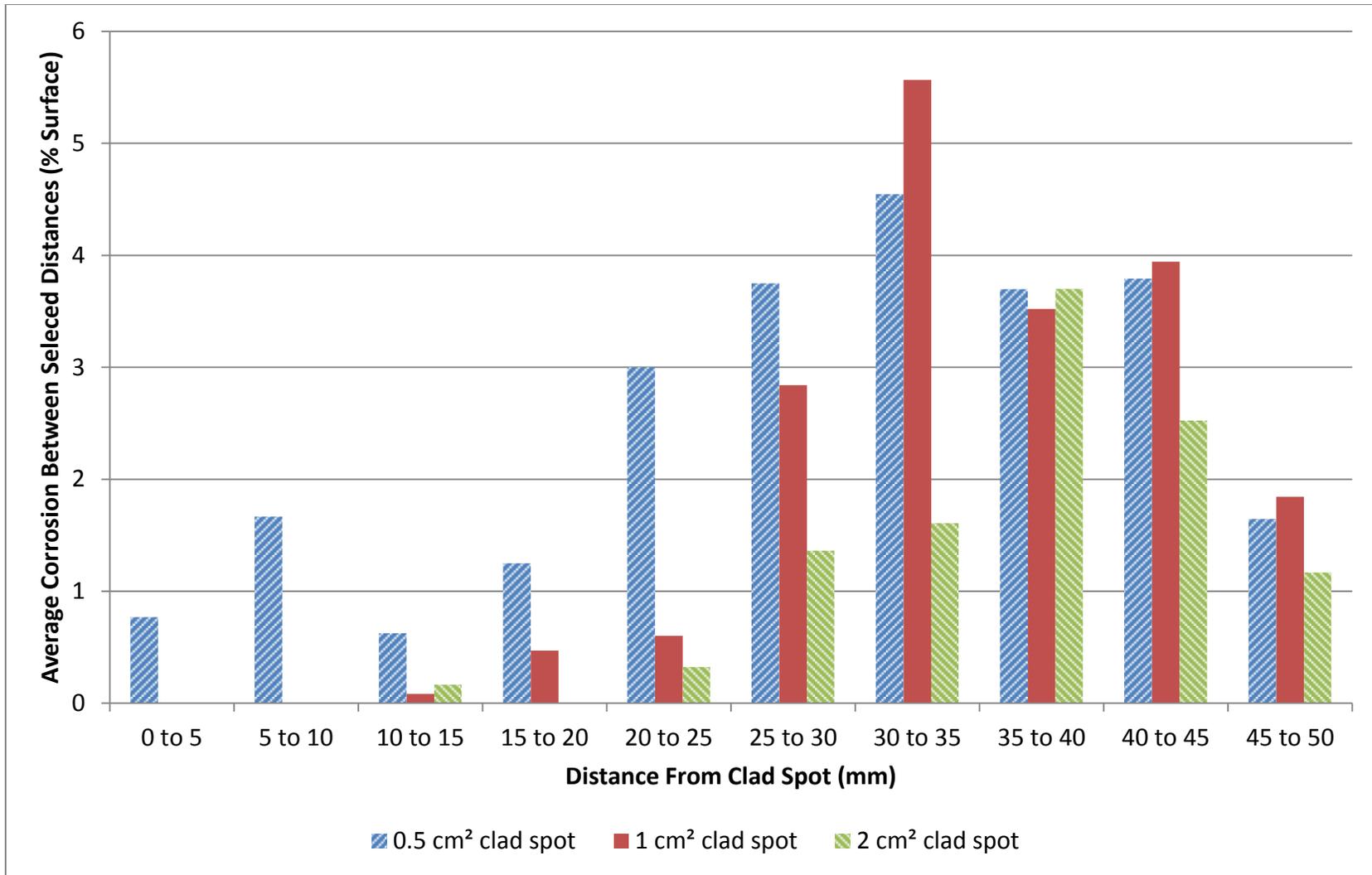
Figure 6.8: Average percentage of corrosion damage observed on the surface of regions defined by rings emanating from the center of the second set of central clad spot test panels (0.5 cm^2, 1 cm^2 and 2 cm^2), milling marks remain, the surfaces were milled to a depth of approximately 0.17 mm after corrosion exposure
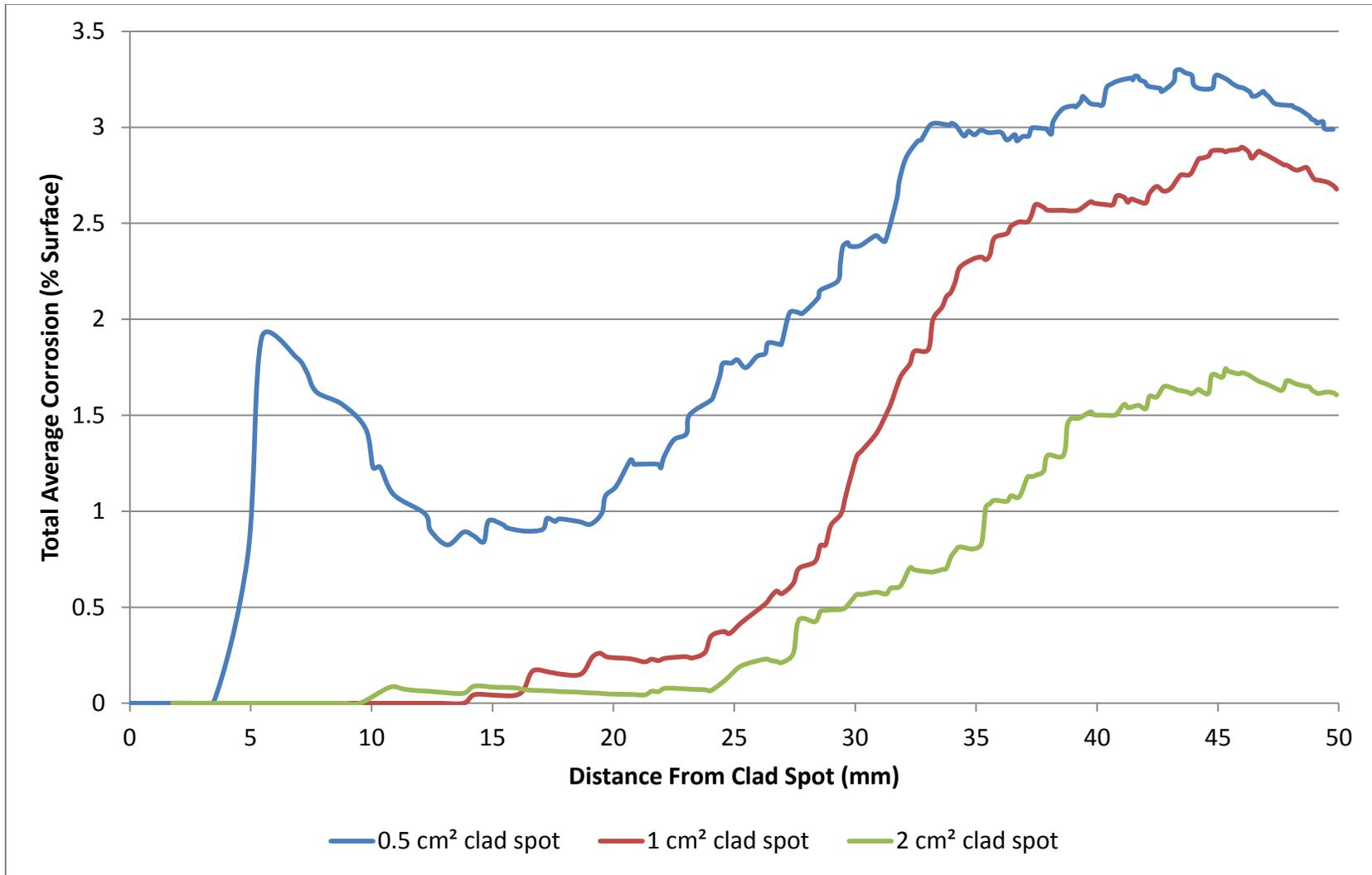
Figure 6.9: Cumulative average percentage of corrosion damaged observed on the surface of an increasing circular area having a radius defined by the distance from the center of the second set of central clad spot test panels (0.5 cm^2, 1 cm^2 and 2 cm^2), milling marks remain, the surfaces were milled to a depth of approximately 0.17 mm after corrosion exposure

6.4.3 Investigating a Critical Radius of Corrosion Protection from a Clad Spot

From the analysis of the spot clad panels it became apparent that after exposure to a corrosive environment there were generally two regions of interest. The area adjacent to the clad spot where low levels of corrosion were observed due to the cathodic protection of the clad spot and the region outside this area where higher levels of corrosion were observed where the clad spot was not able to protect the panel. To better define these two regions of interest, the 50 mm radius circular area of the corroded single clad spot test panels considered for analysis was split into two areas. First, an area (A1) consisting of a circle in the middle of the considered area and an area (A2) consisting of the ring making up the remainder of the analyzed area. A term, critical radius (R_c), was defined as the radius of A1 where the difference in the average percentage of surface corrosion between A2 and A1 is at a maximum. Figure 6.10 illustrates the above described areas and radii.
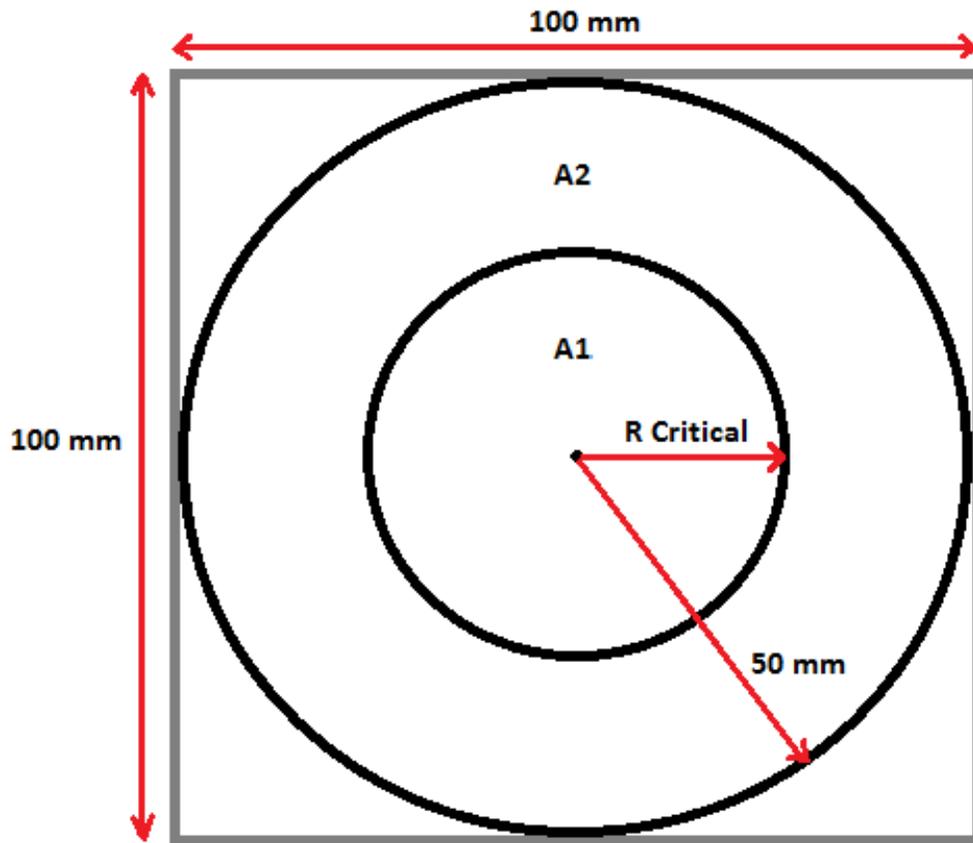
Figure 6.10: Diagram showing the areas A1 and A2 used to determine the critical radius of each of the single clad spot test panels

Figure 6.11 is an example of the graphs produced by varying the radius of A1 and calculating

the maximum difference in percent surface corrosion between A2 and A1 to determine the

critical radius of each of the central clad spot test panels.
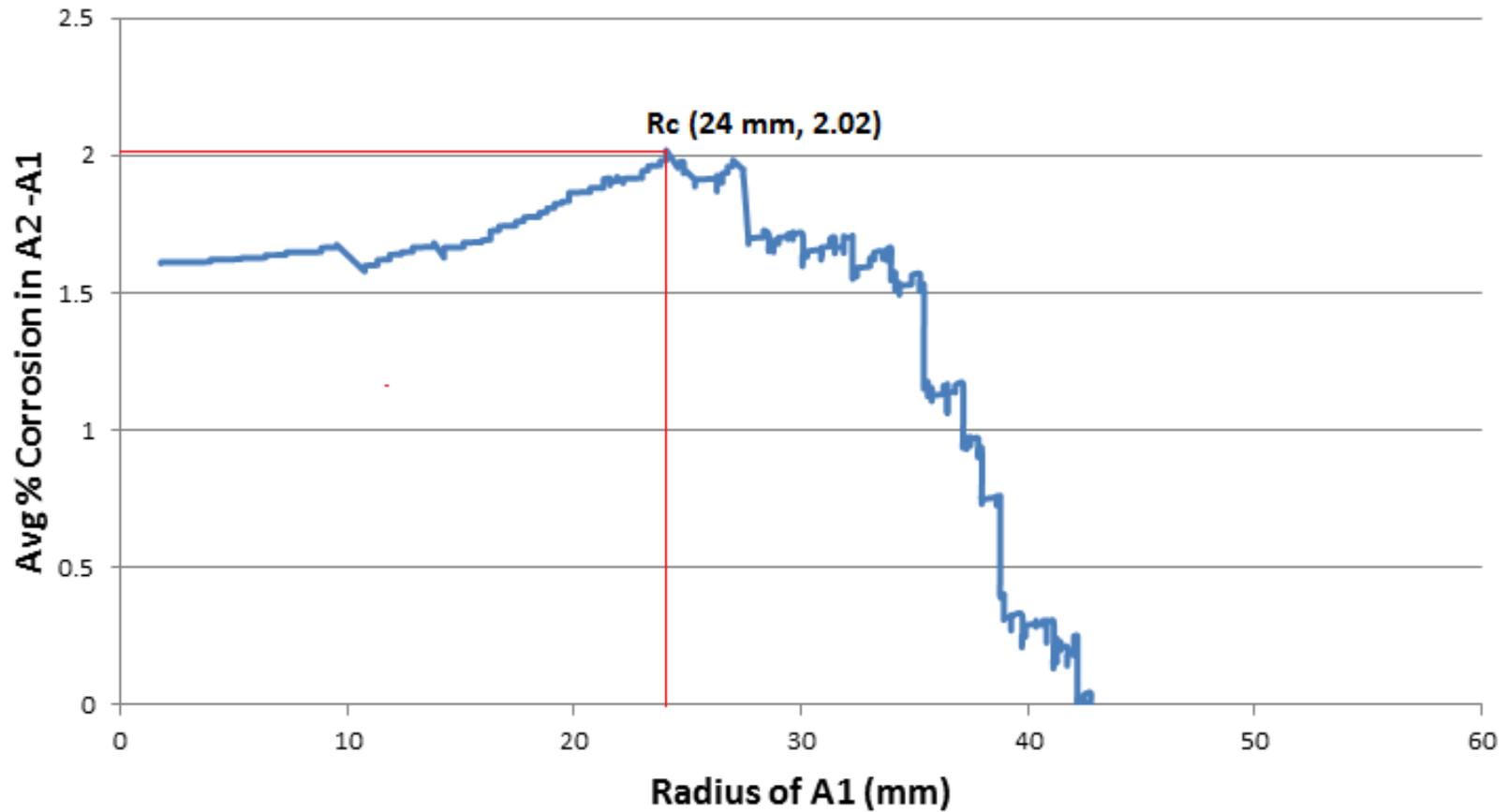
Figure 6.11: Critical radius graph for the 2 cm^2 central clad spot panel after 0.17 mm milled from the surface, indicated point is the critical radius determined by the radius of A1 where the difference in percent surface corrosion between A2 and A1 is at a maximum

The area A1 defined by the radius R_c can be considered the area of the test panel surface that has been protected from the corrosion environment by the central clad spot. The degree of protection provided by the clad spots can be compared by considering the magnitude of the percentage of corrosion observed in the area A1 as well as by the percent difference between the corrosion observed in A1 and A2. Table 6.1 summarizes the values for the critical radius, the average percentage of surface corrosion for areas A1 and A2 and the percent difference of surface corrosion for the two areas for each of the varying central clad spot panels.

Table 6.1: Summary of the critical radius data for the varying central clad spot panels, no milling and milled at a depth of 0.17 mm

	Critical Radius (mm)	Avg Corrosion Inside Circle (%)	Avg Corrosion Outside Ring (%)	% Difference
0.5 cm^2 spot (no milling)	12.2	23.5	26.4	12
1 cm^2 spot (no milling)	16.4	18	32	56
2 cm^2 spot (no milling)	18.6	19.2	30.9	47
0.5 cm^2 spot (0.17 mm milled)	19.5	0.9	3.4	116
1 cm^2 spot (0.17 mm milled)	23.8	0.23	3.4	175
2 cm^2 spot (0.17 mm milled)	24	0.067	2.1	188

From Table 6.1, it can be concluded that the area protected by the central clad spot is increased by increasing the size of the clad spot. The degree of protection from the corrosion environment is also improved with increasing the area of the clad spot. The improvement in corrosion resistance between the 2 cm^2 and 1 cm^2 clad spots is less drastic than the improvement between the 1 cm^2 and 0.5 cm^2 clad spots. This implies that the most efficient clad spot size may be between 2 cm^2 and 1 cm^2 for the protection of an area with a radius of

approximately 20 mm for a panel with a cathodic area of approximately 100 cm^2. This helps

validate the choice for using 1 cm^2 clad spots arranged 2 cm from each other for the medium

sized partially clad panel and implies that this arrangement is a conservative choice as the ratio

between the cathodic and anodic areas will be lower. The clad spots are more effective at

preventing corrosion at depths of 0.17 mm at larger distances than corrosion at the surface of

the panels but the same trends for increasing clad spot size are observed.

7. Discussion

After completing the experiments described in this work, some observations have been made that could be important to future work and experimental procedures used in similar experiments.

7.1 Issues with Machining Test Panels

During the machining process, more material was removed from the plate thickness than desired. Instead of removing 0.19 mm from the plate thickness an average of 0.69 mm was removed. This occurred because the aluminum plate used was not perfectly flat as well as because of difficulties in affixing the plate to the CNC clamping device. This imperfection in the machining stage of the spot clad test panel should not affect the overall corrosion resistance of the plate because the primary goal was to remove the cladding layer and this was achieved. The raised spots did however have a detrimental effect the ductility of the partially clad test panel, discussed in Section 6.1.4 and the fatigue resistance of the partially clad test panel, discussed in Section 6.1.5. In future experiments, if the problem of accurately machining the partial cladding pattern persists, smaller clad spot dimensions in combination with wider tensile and fatigue specimens may minimize the detrimental effect of the clad spot edge on the results for panel ductility and fatigue resistance.

7.2 Effect of Milling Marks on Corrosion Susceptibility

To check for the repeatability of the first 1 cm^2 central clad spot panel and to investigate the effects of milling marks on the corrosion resistance of the panel, the 1 cm^2 central clad spot panels in both the first and second tests were compared in Figures 7.1, 7.2, 7.3 and 7.4. From

Figures 7.1 and 7.2 it is apparent that the presence of the milling marks greatly increases the susceptibility of the aluminium surface to corrosion. The Four regions of different corrosion behavior (very low corrosion at the clad spot, a region of corrosion protection extending to 20 mm from the clad spot, a region of high corrosion damage between 20 and 50 mm from the clad spot and a region of decreasing corrosion damage between 40 and 50 mm from the center of the test panel), discussed in Section 6.4, observed during the first test were again observed during the second test. The major differences being that second test panel with the milling marks has a higher degree (approximately 14% more) of corroded surface area in the protected region. While the first test panel without milling marks has more corrosion (approximately 6%) concentrated in the region between 30 and 40 mm from the center of the panel. The overall percentage of the aluminium surface showing signs of corrosion in the first and second tests were similar at 27.2% and 30.5% respectively.
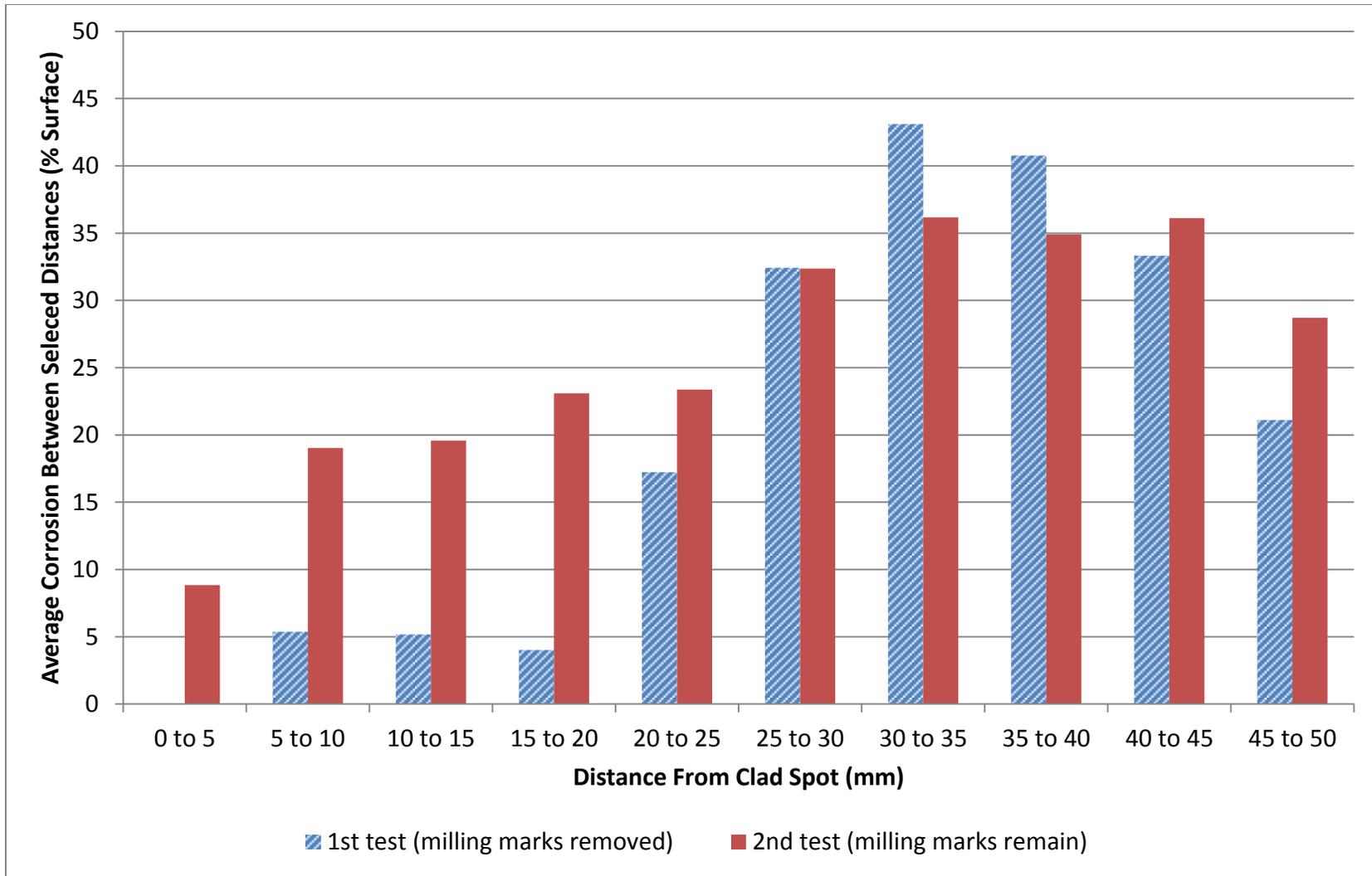
Figure 7.1: Average percentage of corrosion damage observed on the surface of regions defined by rings emanating from the center of the initial and second 1 cm^2 central clad spot test panels, no milling was applied to the surfaces
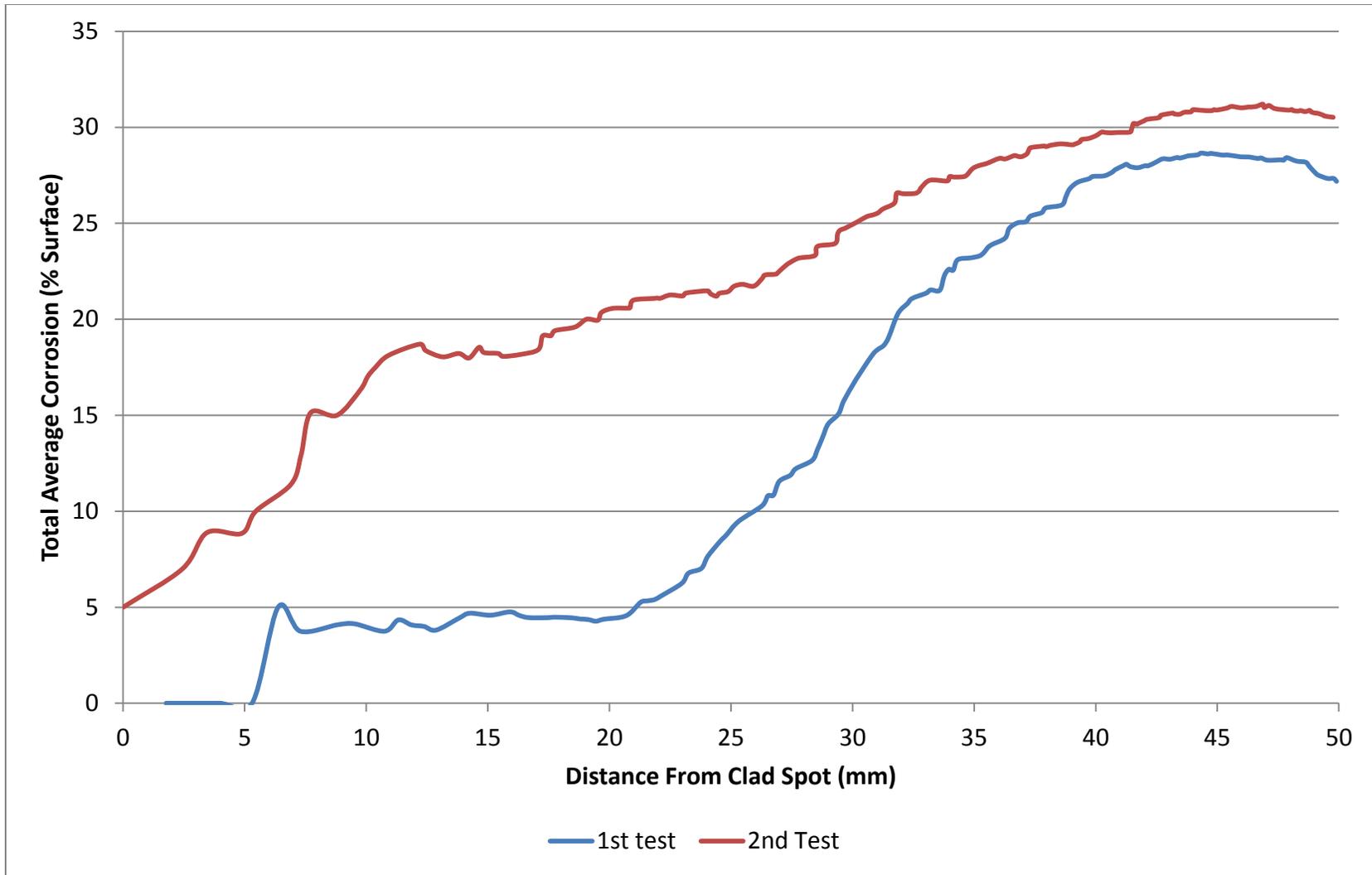
Figure 7.2: Cumulative average percentage of corrosion damaged observed on the surface of an increasing circular area having a radius defined by the distance from the center of the initial and second 1 cm^2 central clad spot test panels, no milling was applied to the surfaces

To compare the depth of corrosion attack between the first and second 1 cm^2 central clad spot test panels, the corroded surfaces were compared after milling approximately 0.17 mm from the panel thickness in Figures 7.3 and 7.4. The four regions of corrosion behavior initially observed on the first 1 cm^2 panel are more apparent on the second test panel when considering corrosion with a minimum penetration depth of 0.17 mm. The second test panel, with the milling marks, was much less effective at preventing corrosion at a depth of 0.17 mm in the region between 20 and 50 mm from the center of the panel. However, the second panel resisted corrosion at this depth similarly as well as the first panel without milling marks in the region extending 20 mm from the center of the panel.

The surface finish of the aluminium panel greatly affects the susceptibility to corrosion. This was already known but it was not known if the protection of the clad spot would make the varying surface finish insignificant in the tested corrosion environment.
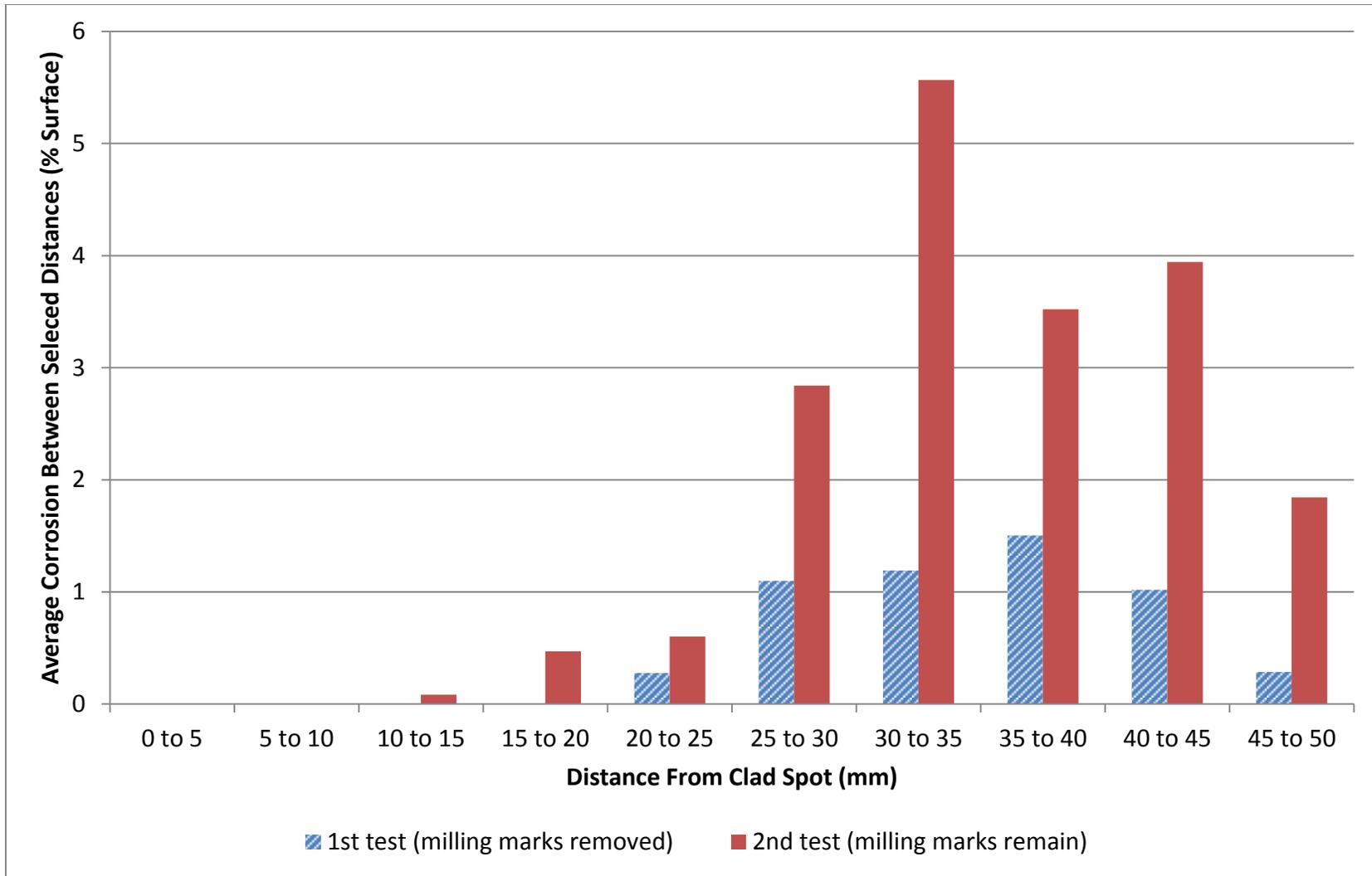
Figure 7.3: Average percentage of corrosion damage observed on the surface of regions defined by rings emanating from the center of the initial and second 1 cm^2 central clad spot test panels, the surface was milled to a depth of approximately 0.17 mm after corrosion exposure
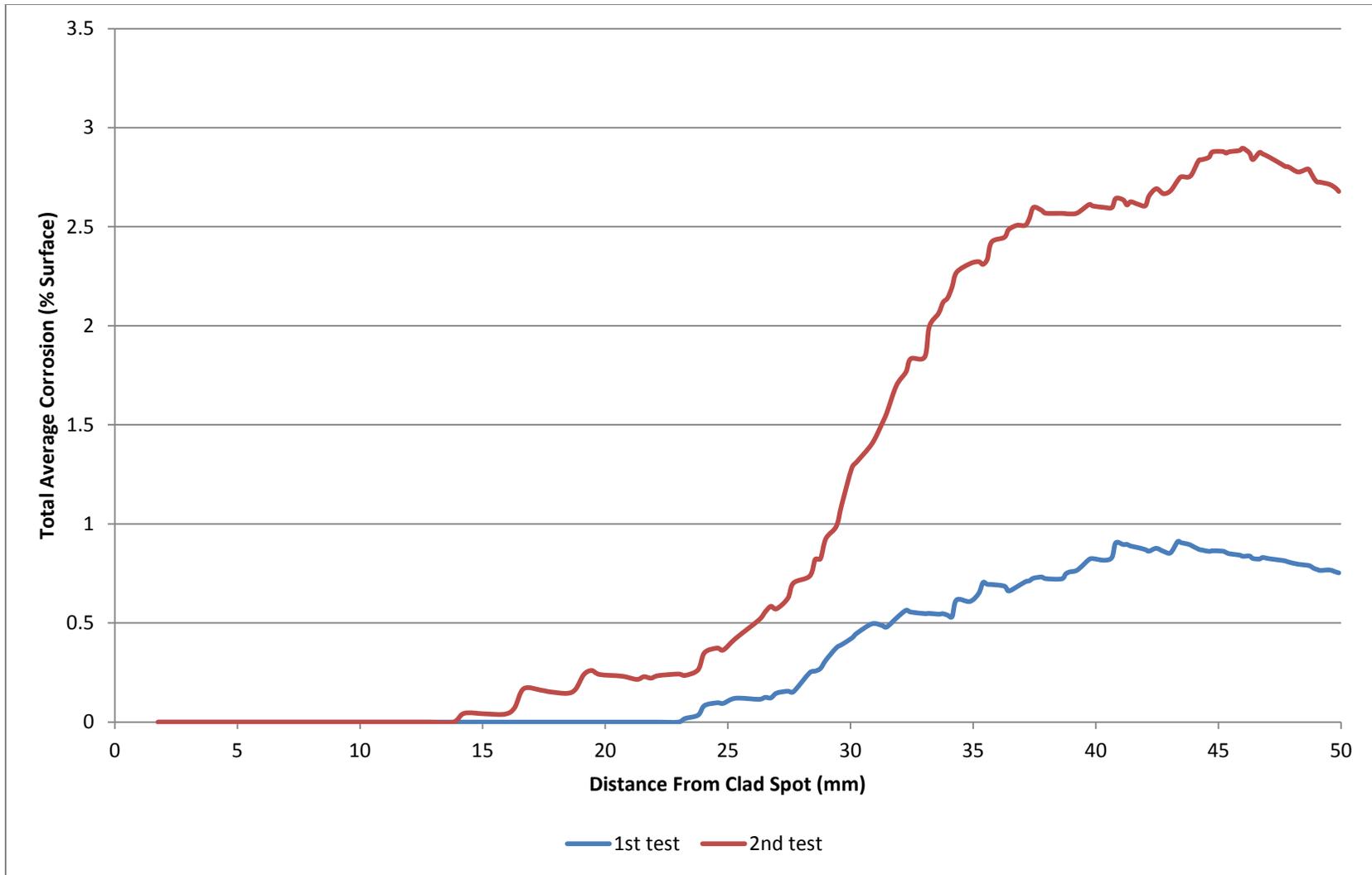
Figure 7.4: Cumulative average percentage of corrosion damaged observed on the surface of an increasing circular area having a radius defined by the distance from the center of the initial and second 1 cm^2 central clad spot test panels, the surface was milled to a depth of approximately 0.17 mm after corrosion exposure

7.3 Effectiveness of Corrosion Resistant Tape

The procedure used to isolate the clad back surface of the test panels from the front surface intended to be exposed to the corrosion environment seems to be insufficient. The outside region of all of the test panels exhibited decreasing corrosion damage that implies electrical interaction between the cladding on the back surface, reducing corrosion through cathodic protection of the outside region. In the future instead of using corrosion resistant tape that requires the seams to be sealed a better choice would likely to dip the back surface and edges of a clad panel into a corrosion resistant polymer or to use a continuous layer of a natural wax.

8. Conclusions

1. For the varying clad spot size test panels, the area directly protected by all of the clad spots was consistent at a distance of approximately 20 mm from the center of the panel. The degree of protection was affected by the surface finish. There was no significant difference in the protection between the 1 cm^2 and 2 cm^2 clad spots at this distance, while the 0.5 cm^2 was significantly worse. This validates the clad spot dimensions used to produce the medium scale partially clad test panel.

2. For the varying clad spot size test panels, in the region not directly protected by the clad spot (between 20 mm and 50 mm from the panel center) the size of the clad spot is inversely related to the area of corrosion penetrating depths beyond 0.17 mm.

3. For the medium scale test panels, the decreases in mechanical properties of the partially clad and fully clad test panels were similar after corrosion exposure. Both the partially clad and fully clad test panels outperformed the cladding removed test panel.

4. For the medium scale test panels, the fatigue resistance of cladding removed test panel was greatly reduced by exfoliation caused by the corrosion environment exposure. The fatigue resistance of the partially clad and fully clad test panels were both detrimentally affected by exposure to the corrosive environment to a similar degree, but to a much lesser degree than the cladding removed panel.

9. Future Work

For partial cladding to become a viable alternative to Alclad products, several major hurdles must still be overcome. The first is that thus far the only forms of corrosion that have been investigated in combination with partial cladding are pitting in previous work [5], and exfoliation in this work. The more catastrophic forms of corrosion where a corrosion environment is present in combination with a stress such as stress corrosion cracking or corrosion fatigue have not yet been investigated in any detail. The effectiveness of partial cladding for protecting against these forms of corrosion must still be established before partial cladding can be considered for any structurally critical applications on aircraft.

Next, the effectiveness of partially clad aluminum alloys must be investigated in combination with aerospace coating systems. It is likely that the cladding patterns investigated in this work and in previous work [5] involve clad spots spaced at distances too large to be effective when considering the area of aluminum exposed to corrosive environments by a scratch or flaw in a coating system. If the scratch or flaw only exposes the aluminum core and does not also expose a clad spot, the partial cladding pattern will not offer any protection. This is because the clad spot must be exposed to the corrosive environment to corrode preferentially and provide cathodic protection. It is likely that cladding patterns with smaller clad spots more closely arranged will be necessary to effectively protect the high strength aluminum core when considering a small flaw in a coating system to maintain equivalent corrosion protection and achieve an overall weight savings when compared to Alclad products.

Finally, an economically comparable production method to the currently established Alclad aluminum sheet products must be investigated for partially clad products. For partial cladding to become a viable alternative, any increase in the cost of producing partially clad aerospace components must be surpassed by the economic potential of fuel savings or increased payload gained from decreased component weight.

One potential avenue for the production of partially clad components may be to use a thermal spray to apply a fine distribution of small clad spots to the aluminum surface. This method of producing a partial cladding pattern would not result in square shaped clad spots; it would likely result in clad spots with a cylindrical or hemispherical shape. Future work in investigating the possibility of using thermal sprays to produce partial cladding patterns could include testing single clad spot panels with cylindrical or hemispherical shaped clad spots.

It may also be worth investigating more complex partial cladding geometries that could be produced with techniques such as laser cladding. Potential Future work may include testing panels with annular clad spots or a partial cladding pattern with a crosshatch geometry.

10. References

[1]   E. A. Starke and J. T. Staley, "Application of modern aluminum alloys to aircraft," *Progress in Aerospace Sciences,* vol. 32, no. 2, pp. 131-172, 1996.

[2]   A. Merati, "Materials replacement for aging aircraft," in *Corrosion Fatigue and Environmentally Assisted Cracking in Aging Military Vehicles*, NATO Science and Technology Organization, 2011.

[3]   W. Tsai, "The economics of maintenance," in *The Standard Handbook for Aeronautical and Astronautical Engineers*, New York, McGraw-Hill, 2003, pp. 18.2-18.19.

[4]   ALCOA Mill Products Inc., *Alloy 7075 sheet and plate,* SPD-10-037 datasheet, 2001.

[5]   S. G. Pantelakis, A. N. Chamos and D. Setsika, "Tolerable corrosion damage on aircraft aluminum structures: local cladding patterns," *Theoretical and Applied Fracture Mechanics,* vol. 58, no. 1, pp. 55-64, 2012.

[6]   Bombardier Inc., "Bombardier 415 | Amphibious and Firefighting Aircraft," [Online]. Available: http://www.bombardier.com/en/aerospace/amphibious-aircraft/bombardier-415.html. [Accessed 2 September 2015].

[7]   A. A. Adjorlolo and J. A. Marceau, "Commercial aircraft," in *Corrosion Test and Standards: Application and Interpretation*, West Conshohocken, ASTM International, 2005, pp. 687-692.

[8]   G. M. Scamans, N. Birbilis and R. G. Buchheit, "Corrosion of aluminum and its alloys," in *Shreir's Corrosion, vol. 3, Corrosion and Degradation of Engineering Materials*, Amsterdam, Elsevier, 2010, pp. 1974-2010.

[9]   N. Birbilis and B. Hinton, "Corrosion and corrosion protection of aluminium," in *Fundamentals of Aluminium Metallurgy: Production, Processing and Applications*, Cambridge, UK ; Philadelphia, Woodhead Publishing Ltd., 2011, pp. 574-604.

[10] C. Vargel, Corrosion of Aluminium, Burlington: Elsevier Science, 2004.

[11] E. Ghali, Corrosion Resistance of Aluminum and Magnesium Alloys Understanding,

Performance, and Testing, Hoboken: John Wiley & Sons, Inc., 2010.

[12] P. K. Rout, M. M. Ghosh and K. S. Ghosh, "Influence of aging treatments on alterations of microstructural features and stress corrosion cracking behavior of an Al-Zn-Mg alloy," *Journal of Materials Engineering and Performance,* vol. 24, no. 7, pp. 2792-2805, 2015.

[13] J. R. Davis, Corrosion of aluminum and aluminum alloys, Materials Park: ASM International, 1999.

[14] E. H. Dix, ""Alclad" a New Corrosion Resistant Aluminum Product," National Advisory Committee for Aeronautics, Washington, 1927.

[15] P. V. Petroyiannis, S. G. Pantelakis and G. N. Haidemenopoulos, "Protective role of local Al cladding against corrosion damage and hydrogen embrittlement of 2024 aluminum alloy specimens," *Theoretical and applied fracture mechanics,* vol. 44, no. 1, pp. 70-81, 2005.

[16] *Standard Test Methods for Tension Testing of Metallic Materials,* ASTM E8M-94a, 1994.

[17] *Standard Test Method for Exfoliation Corrosion Susceptibility in 2XXX and 7XXX Series Aluminum Alloys (EXCO Test),* ASTM G34 - 01(2013), 2013.

[18] C. Vallellano, M. R. Mariscal, A. Navarro and J. Dominguez, "A micromechanical approach to fatigue in small notches," *Fatigue & Fracture of Engineering Materials & Structures,* vol. 28, no. 11, pp. 1035-1045, 2005.

[19] *Standard Test Methods for Tension Testing of Metallic Materials,* ASTM E8/E8M - 15a, 2015.

[20] *Standard Practice for Conducting Force Controlled Constant Amplitude Axial Fatigue Tests of Metallic Materials,* ASTM E466-07, 2007.

[21] M. Tiryakioglu and J. T. Staley, "Physical metallurgy and the effect of alloying additions in aluminum alloys," in *Handbook of Aluminum Physical Metallurgy and Processes*, vol. 1, Boca Raton, Taylor & Francis Group, 2003, pp. 81-209.

[22] J. R. Kissell, S. G. Pantelakis and G. N. Haidemenopoulos, "Aluminum and aluminum alloys," in *The Handbook of Advanced Materials Enabling New Designs*, Hoboken, Wiley, 2004, pp. 321-463.

[23] *Standard Practice for Modified Salt Spray (Fog) Testing,* ASTM G85-11, 2011.

[24] *Standard Specification for Reagent Water,* ASTM D1193-06(2011), 2011.

[25] *Standard Practice for Operating Salt Spray (Fog) Apparatus,* ASTM B117-11, 2011.

[26] P. V. Strekalov, G. K. Dzhincharadze, Z. G. Egutidze, G. G. Penov and V. N. Shirokolobov, "Influence of surface roughness on atmospheric corrosion of copper and aluminum alloys," *Protection of Metals (English translation of Zaschita Metallov),* vol. 21, no. 3, pp. 354-358, 1985.

[27] *Standard Test Methods for Tension Testing Wrought and Cast Aluminum- and Magnesium-Alloy Products,* ASTM B557 - 14, 2014.

[28] *Standard Practice for Preparing, Cleaning, and Evaluating Corrosion Test Specimens,* ASTM G1 - 03(2011), 2011.

[29] *Standard Guide for Examination and Evaluation of Pitting Corrosion,* ASTM G46 - 94(2013), 2013.

[30] J. A. Ellor and J. Repp, "Uniform Corrosion," in *Corrosion tests and standards : application and interpretation*, West Conshohocken, ASTM International, 2005, pp. 205-210.

[31] M. Liao, G. Renaud and N. C. Bellinger, "Fatigue modeling for aircraft structures containing natural exfoliation corrosion," *International Journal of Fatigue,* vol. 29, no. 4, pp. 677-686, 2007.

[32] A. Merati, "A study of nucleation and fatigue behavior of an aerospace aluminum alloy 2024-T3," *International Journal of Fatigue,* vol. 27, no. 1, pp. 33-44, 2005.

[33] M. B. Vukmirovic, N. Dimitrov and K. Sieradzki, "Dealloying and Corrosion of Al Alloy 2024 T3," *Journal of The Electrochemical Society,* vol. 149, no. 9, pp. B428-B439, 2002.

[34] H. M. Obispo, L. E. Murr, R. M. Arrowood and E. A. Trillo, "Copper deposition during the corrosion of aluminum alloy 2024 in sodium chloride solutions," *Journal of Materials Science,* vol. 35, no. 14, pp. 3479-3495, 2000.

[35] B. Hafner, "Energy Dispersive Spectroscopy on the SEM: A Primer," 10 May 2007. [Online]. Available: http://www.charfac.umn.edu/instruments/eds_on_sem_primer.pdf. [Accessed 27 Aug 2015].

[36] L. Straus, "Aerospace paints and protective coatings," in *The Standard Handbook for*

Aeronautical and Astronautical Engineers, New York, McGraw-Hill, 2003, pp. 18.45-18.51.

Appendix A: Central Clad Spot Panel Salt Spray Chamber Test Logs

	Start Date: July 18	Pump Speed: 30		Air Pressure: 14		Comments:
Date:	Test Hours:	Vol. Far Collector:	Vol. Close Collector:	Sol^n temp:	Sol^n PH:	Sol^n SG:	
July18th	0 (0)	-	-	23	3.22	1.032	Bulk fill
July 21st	70 (70:00)	85	63.5	27.5	3.26	1.034	
July 21st	-	-	-	23	3.22	1.032	Bulk fill
July 22nd	92:15 (22:15)	38	22	25	3.20	1.033	Air pressure 14 to 13
July 23	117:22 (25:07)	50	27	27	3.24	1.032	Air pressure 13 to 15.
July 24	139:00 (21:38)	42	22	23	3.41	1.032	Pump Speed 30 to 27. Recalibrated PH meter
July 24	-	-	-	23	3.19	1.032	Bulk Fill
July 25	166:00 (27:00)	39	27	27.5	3.26	1.034	Pump speed 30
July 25	-	-	-	23	3.21	1.030	Bulk fill
July 28	232:08 (66:08)	125	67	28	3.29	1.032	
July 28	-	-	-	24	3.20	1.028	Bilk Fill
July 29	254:20 (22:12)	40	23	26	3.22	1.030	Pressure 15 to 13
July 30	277:57 (23:30)	45	25	26	3.24	1.032	Pump Speed 30 to 25
July 31	301:27 (23:30)	45	25	27	3.25	1.030	Panel Removed

Appendix B: Varying Central Clad Spot Size Panels and Medium Sized Test Panels Salt Spray Chamber Test Logs

	Start Date: August 27, 2014		Pump Speed: 25		Air Pressure: 13		Comments:
Date:	Test Hours (hrs:mins)	Vol. Far Collector (mL):	Vol. Close Collector (mL):	Sol^n temp (°C):	Sol^n PH:	Sol^n SG:	
Aug 27	-	-	-	21	3.20	1.028	Bulk solution
Aug 28	18:30 (18:30)	18.5	17.5	26	3.33	1.028	Pump speed increased from 25 to 30. pH low, possibly due to residual water in machine.
Aug 29	41:44 (23:14)	24	23	25	3.26	1.033	
Aug 29	-	-	-	22	3.19	1.032	Bulk solution
Sep 1	114:31 (72.47)	74.5	73	26	3.28	1.034	Pump speed increased from 30 to 34
Sep 1	-	-	-	21	3.20	1.035	Bulk solution
Sep 2	138:21 (23:50)	24	25	25	3.27	1.035	Pump speed: 30, Air pressure: 15
Sep 3	159:26 (21:05)	21	21	23	3.26	1.035	Pump speed: 33, Air pressure: 16
Sep 4	181:38 (22:12)	24	23	27	3.26	1.034	
Sep 4	-	-	-	22	3.18	1.030	Bulk solution
Sep 5	205:07 (23:29)	24.5	23	27	3.21	1.032	
Sep 7	259:04 (53:57)	54.5	53	28	3.26	1.033	
Sep 7	-	-	-	24	3.18	1.035	Bulk solution
Sep 8	276:41 (17:37)	19	17.5	25	3.20	1.036	
Sep 9	300:01 (23:20)	25	24	25	3.18	1.035	Test complete.

Appendix C: ALCOA Al 7075 Technical Specifications

ALLOY 7075

DESCRIPTION

Introduced by Alcoa in 1943, alloy 7075 has been the standard workhorse 7XXX series alloy within the aerospace industry ever since. It was the first successful Al-Zn-Mg-Cu high strength alloy using the beneficial effects of the alloying addition of chromium to develop good stress-corrosion cracking resistance in sheet products. Although other 7XXX alloys have since been developed with improved specific properties, alloy 7075 remains the baseline with a good balance of properties required for aerospace applications.

Alloy 7075 is available in bare and alclad sheet and plate product forms in the annealed state as well as several tempers of the T6, T73 and T76 types.

APPLICATIONS

Alloy 7075 sheet and plate products have application throughout aircraft and aerospace structures where a combination of high strength with moderate toughness and corrosion resistance are required.

Typical applications are alclad skin sheet, structural plate components up to 4 inches in thickness and general aluminum aerospace applications.

CHEMICAL COMPOSITION LIMITS (WT. %)

Si . . . . 0.40   Zn 5.1-6.1
Fe . . . . 0.50   Ti. 0.20
Cu . . . . 1.2-2.0 Others, each 0.5
Mn. . . . . 0.30   Others, total 0.15
Mg. . . . . 2.1-2.9   Balance, Aluminum
Cr 0.18-0.28

Note: Value maximum if range not shown.

MECHANICAL PROPERTIES

ALLOY 7075 All values are minimum long transverse mechanical properties except where noted.

TEMPER	THICKNESS in. (mm)	TENSILE STRENGTH ksi (MPa)	YIELD STRENGTH ksi (MPa)	ELONGATION %
0 Sheet & plate	0.015-2.00 (0.38-50.80)	40 (max) (276)	21 (max) (145)	9-10
T6 Sheet	0.008-0.249 (0.203-6.32)	74-78 (510-538)	63-69 (434-476)	5-8
T651 Plate	0.250-4.000 (6.35-101.60)	78-67 (538-462)	67-54 (462-372)	9-3
T76 Sheet	0.125-0.249 (3.18-6.32)	73 (503)	62 (427)	8
T7651 Plate	0.250-1.000 (6.35-25.40)	72-71 (496-490)	61-60 (421-414)	8-6
T73 Sheet	0.040-0.249 (1.02-6.32)	67 (462)	56 (386)	8
T7351 Plate	0.250-4.000 (6.35-101.60)	69-61 (476-421)	57-48 (393-331)	7-6

ALCLAD 7075

Two side cladding. Nominal cladding thickness is 4% on gauges under 0.062 in. (1.57 mm); 2.5% on gauges over 0.062 in. (1.57 mm). Property values for one side clad material are similar (not shown). All values are minimum long transverse mechanical properties except where noted.

TEMPER	THICKNESS in. (mm)	TENSILE STRENGTH ksi (MPa)	YIELD STRENGTH ksi (MPa)	ELONGATION %
0 Sheet & plate	0.008-1.000 (0.203-6.32)	36-40 (max) (248-276)	20-21 (max) (138-145)	9-10
T6 Sheet	0.008-0.249 (0.203-6.32)	68-76 (469-524)	58-65 (400-448)	5-9
T651 Plate	0.250-4.000 (6.35-101.60)	75-67 (517-462)	65-54 (448-372)	9-3
T76 Sheet	0.125-0.249 (3.18-6.32)	68-70 (469-482)	57-59 (393-407)	8
T7651 Plate	0.250-1.000 (6.35-25.40)	69-71 (476-490)	58-60 (400-414)	8-6
T73 Sheet	0.040-0.249 (1.02-6.32)	63-66 (434-455)	51-54 (352-372)	8
T7351 Plate	0.250-1.000 (6.35-25.40)	66-69 (455-476)	54-57 (372-393)	8-7

FRACTURE TOUGHNESS

Alloy 7075 sheet and plate products offer moderately good strength/toughness relationships and are the standard of comparison for more recent 7XXX series alloy developments. Alloy 7075 sheet and plate products are not offered with guaranteed minimum fracture toughness values.

TYPICAL FRACTURE TOUGHNESS VALUES Alloy 7075 Plate

ALLOY	TEMPER	K_{IC}:ksi$\sqrt{}$in. (MPa$\sqrt{}$m)*	
		L-T	T-L
7075	T651 T7351	26 (28.6) 30 (32.0)	22 (24.2) 26 (28.6)

*Compact specimen (ASTM E399)

FATIGUE PROPERTIES

COMPARISON OF AXIAL-STRESS NOTCH-FATIGUE DATA FOR ALLOYS 7075-T73XXX 2024-T351 AND 7475-T7351 PRODUCTS

The fatigue behavior of alloy 7075 plate products is shown in the accompanying figure comparing axial-stress notch-fatigue data of 2XXX and 7XXX series alloys.
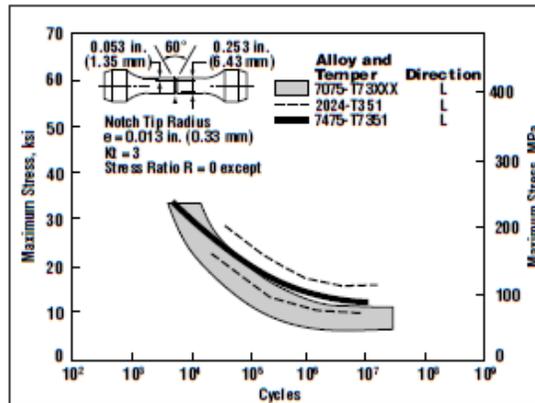
ALLOY 7075

FATIGUE CRACK GROWTH

Fatigue crack growth rates for plate products of 7075-T6 in constant amplitude tests are compared with products of alloys 2024, 7050, and 7475.

COMPARISON OF FATIGUE CRACK GROWTH RATE DATA FOR ALLOY 7075-T651, 2024-T351 AND 7475-T651 PLATE
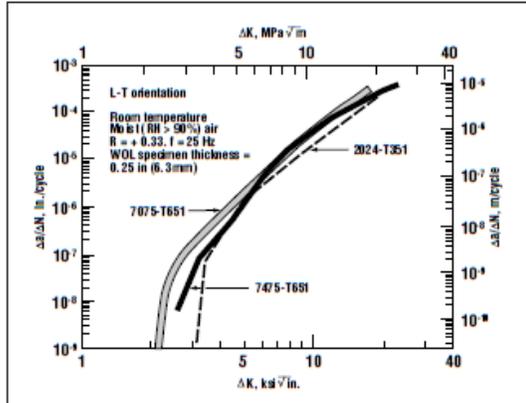
Fatigue crack growth behavior under spectrum loading is becoming increasingly important in the selection of alloys for fatigue critical aircraft structures. Various high strength aerospace alloys are compared for life prediction in flight hours using two types of fatigue spectrums; a wing root application (tension dominated), and a horizontal tail application (tension-compression).

SPECTRUM FATIGUE RANKING
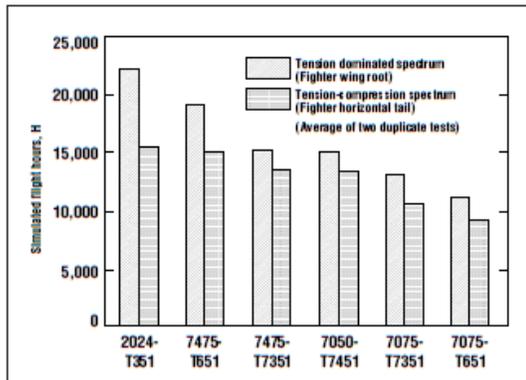
Source: U.S. Navy Contract N00019-81-C-0550/Northrop Corp.

CORROSION RESISTANCE

Alloy 7075 has been thoroughly evaluated for corrosion resistance of atmospheric weathering, stress-corrosion cracking and exfoliation in all currently available tempers. These values have been used as a standard for comparison in the development of more recent high strength aerospace alloys. Within the 7XXX series of alloys, resistance to general corrosion attack, SCC and exfoliation improves significantly in the overage tempers (T7 type) compared with peak strength tempers (T6).

Generally, the T76 type temper is considered the exfoliation resistant temper, while the T73 type temper is considered the SCC resistant temper. It should be noted that T73 is as resistant to exfoliation as T76, but at lower strength levels.

For applications where good surface appearance is required or in corrosive environments, alclad 7075 sheet and plate products are recommended.

THERMAL TREATMENT

Many heat treatments and heat treating practices are available to develop optimum strength, toughness and other desirable characteristics for proper application of alloy 7075 sheet and plate products. Refer to MIL-H-6088, *Heat Treatment of Aluminum Alloys* for additional information.

## PROCUREMENT SPECIFICATIONS

PLATE

Temper	T651	T7651
Specification	QQ-A-250/13	QQ-A-250/24
MIL-HDBK-5	Approved	

BARE SHEET		**ALCLAD SHEET**
Specification	QQ-A-250/12,24	QQ-A-250/13,25,26
MIL-HDBK-5	Approved	Approved

OTHER PRODUCT FORMS

Other product forms of alloy 7075 are extrusions, forgings, wire rod and bar, and rivets.

REFERENCES:

1. The Aluminum Association, *Standards and Data*.
2. The Aluminum Association, *Position on Fracture Toughness Requirements and Quality Control Testing T-5*.
3. MIL-H-6088, *Heat Treatment of Aluminum Alloys*.

PRODUCT SPECIFICATIONS ARE SUBJECT TO CHANGE WITHOUT NOTICE

ALCOA MILL PRODUCTS

P.O. BOX 8025 • BETTENDORF, IOWA 52722 • (800) 523-9596 • www.millproducts-alcoa.com

SPD-10-037

Appendix D: Salt Certificate of Analysis

cer·am

INNOVATION | SUSTAINABILITY | QUALITY

CERTIFICATE OF ANALYSIS

Test Reference: (134495)–19575/Ref1

Issue Date: 20 September 2013

Product

Sodium Chloride (Corro-Salt) - Batch Reference: 300813

Client

Ascott Analytical Equipment Ltd
Unit 6 Gerard
Lichfield Road Industrial Estate
Tamworth
B79 7UW

Test Results

Analyte	Method	Client Specification	Result	Outcome
Aluminium (Al)	C12	<0.001%	<0.001%	Pass
Arsenic (As)	C12	<0.001%	<0.001%	Pass
Barium (Ba)	C12	<0.001%	<0.001%	Pass
Iron (Fe)	C12	<0.001%	<0.001%	Pass
Lead (Pb)	C12	<0.001%	<0.001%	Pass
Nickel (Ni)	C12	<0.001%	<0.001%	Pass
Copper (Cu)*	C12	<0.3ppm	<0.3ppm	Pass
Halides (Sum of Br, I, and F)	-	<0.1%	<0.1%	Pass
- Bromide (Br)	C18	-	<0.01%	-
- Fluoride (F)	C18	-	<0.01%	-
- Iodide (I)*	C12	-	<0.01%	-
Total Impurities	-	<0.3%	<0.1%	Pass

All samples were analysed using UKAS accredited tests; tests which are not covered by this accreditation are marked with an asterisk (*).

The supplier states that anti-caking agents were not added to the product.

Authorised by:

George Jones
Laboratory Supervisor

www.ceram.com

Registered Office: Queens Road Penkhull Stoke on Trent ST4 7LQ
Ceram is the trading name of Ceram Research Limited. Registered in England No. 1960455

UKAS
TESTING
0013

Appendix E: Acetic Acid Certificate of Analysis

Certificate of Analysis

Alfa Aesar®
A Johnson Matthey Company

Product No.:   36289

Product: Acetic acid, glacial, ACS, 99.7+%

Lot No.:   J10Z048

Test	Limits	Results
Assay	99.7 % min	99.93 %
Acetic anhydride	0.01 % max	0.01 %
Chloride	1 ppm max	< 1 ppm
Sulfate	1 ppm max	< 1 ppm
Color (APHA)	10 max	2
Dilution test	To pass test	Passes
Heavy metals (as Pb)	0.5 ppm max	< 0.5 ppm
Iron	0.2 ppm max	0.1 ppm
Residue after evaporation	0.001 % max	< 0.001 %
Substances reducing permanganate	To pass test	Passes
Substances reducing dichromate	To pass test	Passes
Titrable base	0.0004 meq/g max	< 0.0004
Identification	Passes	
Nonvolatile residue	< 0.001 %	
Readily oxidizable substances	Passes	
Congealing temperature	Passes (not lower than 15.6ºC)	
Solidification point	Passes (not lower than 15.6ºC)	

This document has been electronically generated and does not require a signature.

www.alfa.com

Appendix F: Nitric Acid Certificate of Analysis

Certificate of Analysis — Alfa Aesar
A Johnson Matthey Company

Product No.:	87920
Product:	Nitric acid, 65-70%, 99.999% (metals basis)
Lot No.:	Q01A001

Assay   69 %
Color (APHA)   < 7

Al	< 0.5	Sb	< 0.1	As	< 0.1	Ba	< 0.1
Be	< 0.1	Bi	< 0.1	B	< 0.5	Cd	< 0.1
Ca	< 0.5	Ce	< 0.1	Cs	< 0.1	Cr	< 0.5
Co	< 0.1	Cu	< 0.2	Dy	< 0.1	Er	< 0.1
Eu	< 0.1	Gd	< 0.1	Ga	< 0.1	Ge	< 0.1
Au	< 0.1	Hf	< 0.1	Ho	< 0.1	In	< 0.1
Fe	< 0.5	La	< 0.1	Pb	< 0.1	Li	< 0.1
Lu	< 0.1	Mg	< 0.2	Mn	< 0.1	Hg	< 0.02
Mo	< 0.1	Nd	< 0.1	Ni	< 0.5	Nb	< 0.1
Pd	< 0.1	Pt	< 0.1	K	< 0.2	Pr	< 0.1
Re	< 0.1	Rh	< 0.1	Rb	< 0.1	Ru	< 0.1
Sm	< 0.1	Sc	< 0.1	Se	< 0.1	Ag	< 0.1
Na	< 0.3	Sr	< 0.1	Ta	< 0.1	Te	< 0.1
Tb	< 0.1	Tl	< 0.1	Th	< 0.1	Tm	< 0.1
Sn	< 0.1	Ti	< 0.1	W	< 0.1	U	< 0.1
V	< 0.1	Yb	< 0.1	Y	< 0.1	Zn	< 0.2
Zr	< 0.1						

Chloride (Cl^-)	< 0.2
Total Sulphur (S)	< 0.3
Total Phosphorus (P)	< 0.01

Values given in ppb unless otherwise noted

This document has been electronically generated and does not require a signature.

www.alfa.com

NORTH AMERICA
Tel: +1-800-343-0660 or
+1-978-521-6300
Fax: +1-800-322-4757
Email: info@alfa.com

GERMANY
Tel: 00800 4566 4566 or
+49 721 84007 280
Fax: 00800 4577 4577 or
+49 721 84007 300
Email: Eurosales@alfa.com

UNITED KINGDOM
Tel: 0800-801 812 or
+44 (0)1524-850506
Fax: +44 (0) 1524-850608
Email: UKsales@alfa.com

FRANCE
Tel: 0800 03 51 47 or
+33 (0)3 8862 2690
Fax: 0800 10 20 67 or
+33 (0)3 8862 6864
Email: frventes@alfa.com

INDIA
Tel: +91 8008 812424 or
+91 8008 8125 25 or
+91 8008 812626
Fax +91 8418 260060
Email: india@alfa.com

CHINA
Tel: +86 (010) 8567-8600
Fax: +86 (010) 8567-8601
Email: saleschina@alfa-asia.com

KOREA
Tel: +82-2-3140-6000
Fax: +82-2-3140-6002
Email: saleskorea@alfa-asia.com

126

Appendix G: Acetone Certificate of Analysis

ACROS

1 Reagent Lane Fair Lawn, NJ 07410

Certificate of Analysis

This is to certify that units of the above mentioned lot number were tested and found to comply with the specifications of the grade listed. Certain data have been supplied by third parties. Acros Organics expressly disclaims all warranties, expressed or implied, including the implied warranties of merchantability and fitness for a particular purpose. Unless otherwise stated, these products are not intended for dialysis, parenteral, or injectable use without further processing. The following are the actual analytical results obtained:

Catalog Number	16764		Mfg. Date	12/7/2012
Lot Number	B0524762			
Description	ACETONE, 99+%, SPECTROPHOTOMETRIC GRADE			
Country of Origin		United States		

| Result name	Units	Specifications	Test Value
APPEARANCE		REPORT	CLEAR, COLORLESS LIQUID
ASSAY	%	>= 99.0	99.7
EVAPORATION RESIDUE	%	<= 0.001	<0.0001
IDENTIFICATION	PASS/FAIL	= PASS TEST	PASS TEST
OPTICAL ABS AT 330 NM	ABSORBANCE UNITS	<= 1	0.6
OPTICAL ABS AT 340 NM	ABSORBANCE UNITS	<= 0.1	0.03
OPTICAL ABS AT 350 NM	ABSORBANCE UNITS	<= 0.02	0.003
OPTICAL ABS AT 400 NM	ABSORBANCE UNITS	<= 0.01	<0.001
WATER (H2O)	%	<= 0.5	0.3

CERTIFIED BY *Joel Boland*

Lab Manager BPF

Note: The data listed is valid for all package sizes of this lot of this product, expressed as a extension of this catalog number listed above. If there are any questions with this certificate, please contact your Acros Organics representative.

Appendix H: EDS Results for the Composition of the Al 7075 Cladding
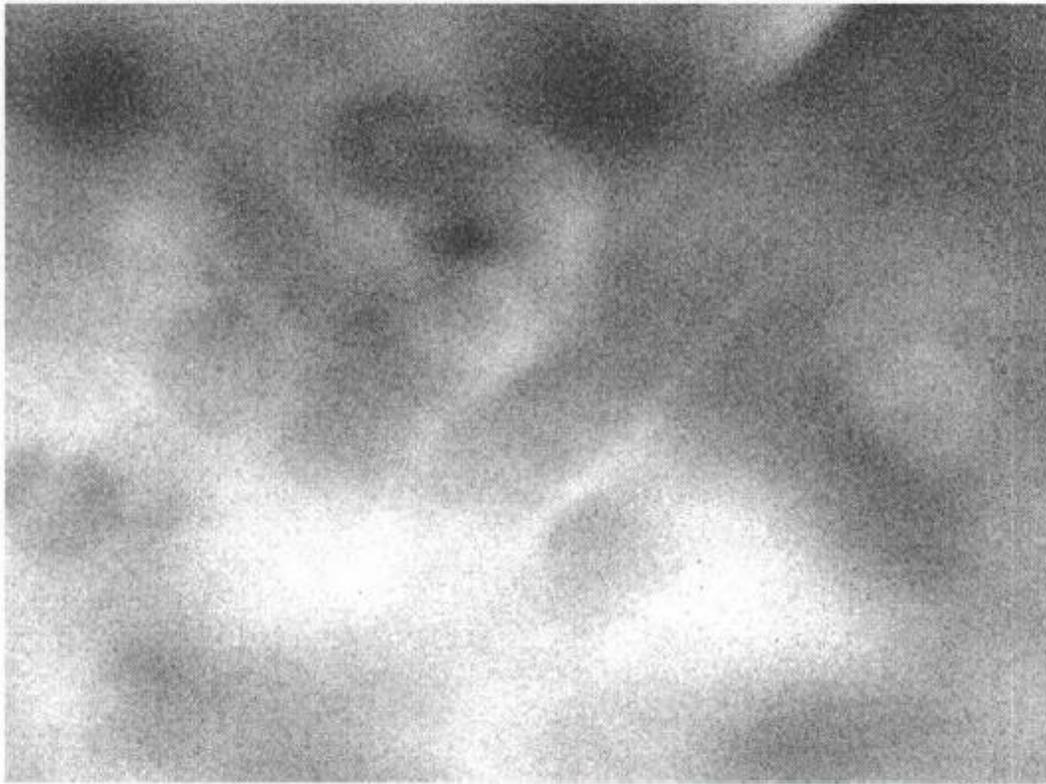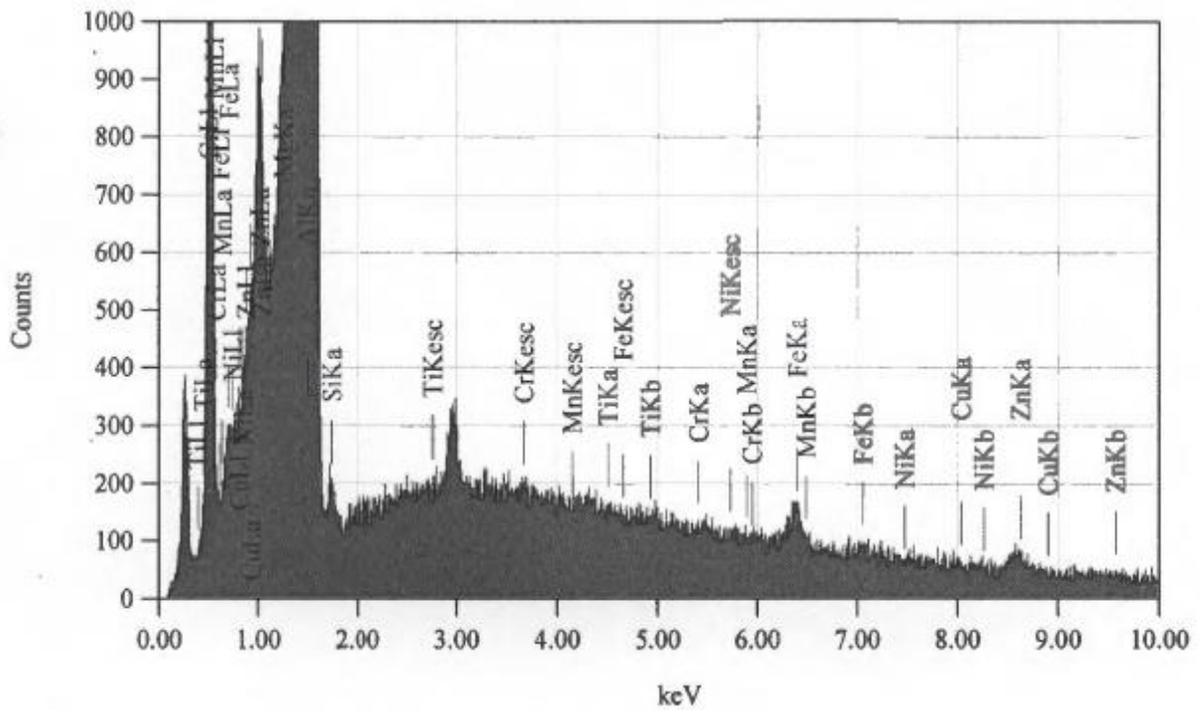
```
ZAF Method Standardless Quantitative Analysis
Fitting Coefficient : 0.0613
Element      (keV)   Mass%  Sigma     Atom%   Compound  Mass%  Cation      K
Al K        1.486   98.06 74312605696.00   98.83                        98.2141
Zn K*       8.630    0.79 28584255488.00    0.33                         0.7694
Fe K*       6.398    0.64 14724759552.00    0.31                         0.6394
Mg K*       1.253    0.33 4485868544.00     0.36                         0.3019
Si K*       1.739    0.16 5821585920.00     0.16                         0.0476
Ti K*       4.508    0.01 1089900416.00     0.00                         0.0061
Cr K*       5.411    0.01 1770146048.00     0.01                         0.0128
Ni K*       7.471    0.01 2114495616.00     0.00                         0.0087
Mn K*
Cu K*
Total              100.00           100.00
```

Title	: IMG1
Instrument	: JCM-6000
Volt	: 15.00 kV
Mag.	: x 2,700
Date	: 2015/02/18
Pixel	: 512 x 384

```
Acquisition Parameter
Instrument   : JCM-6000
Acc. Voltage : 15.0 kV
Probe Current: 1.00000 nA
PHA mode     : T3
Real Time    : 108.83 sec
Live Time    : 100.00 sec
Dead Time    : 8 %
Counting Rate: 9928 cps
Energy Range :  0 - 20 keV
```
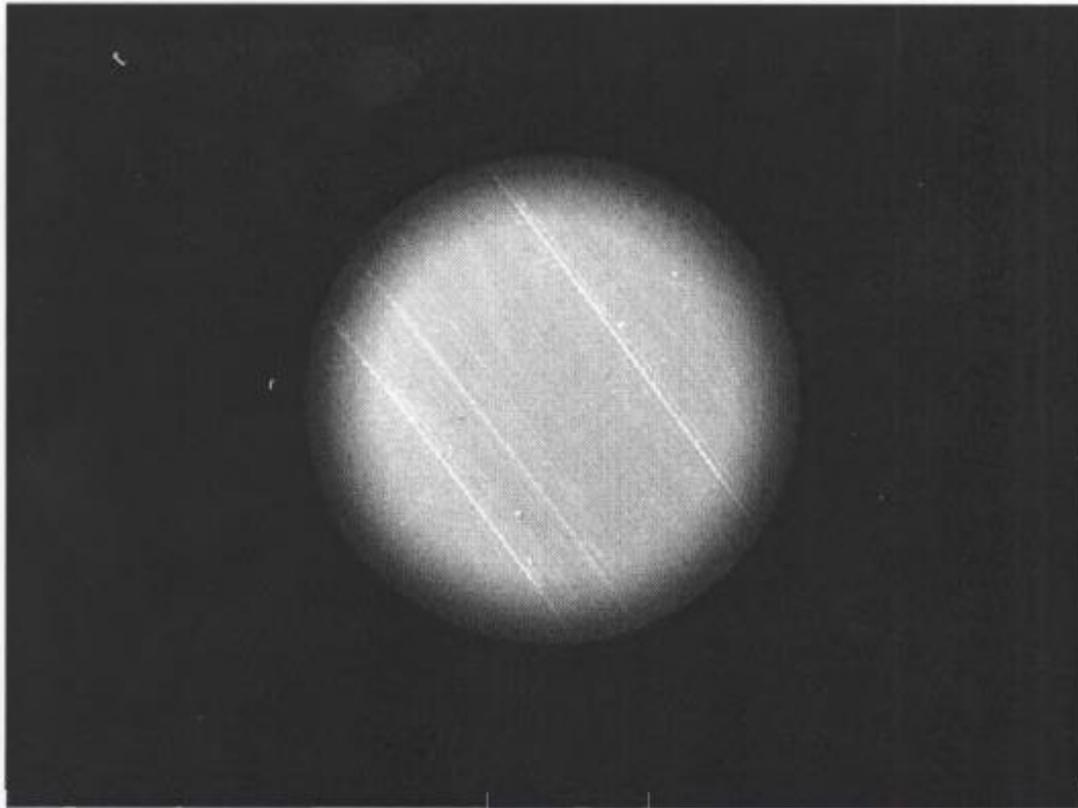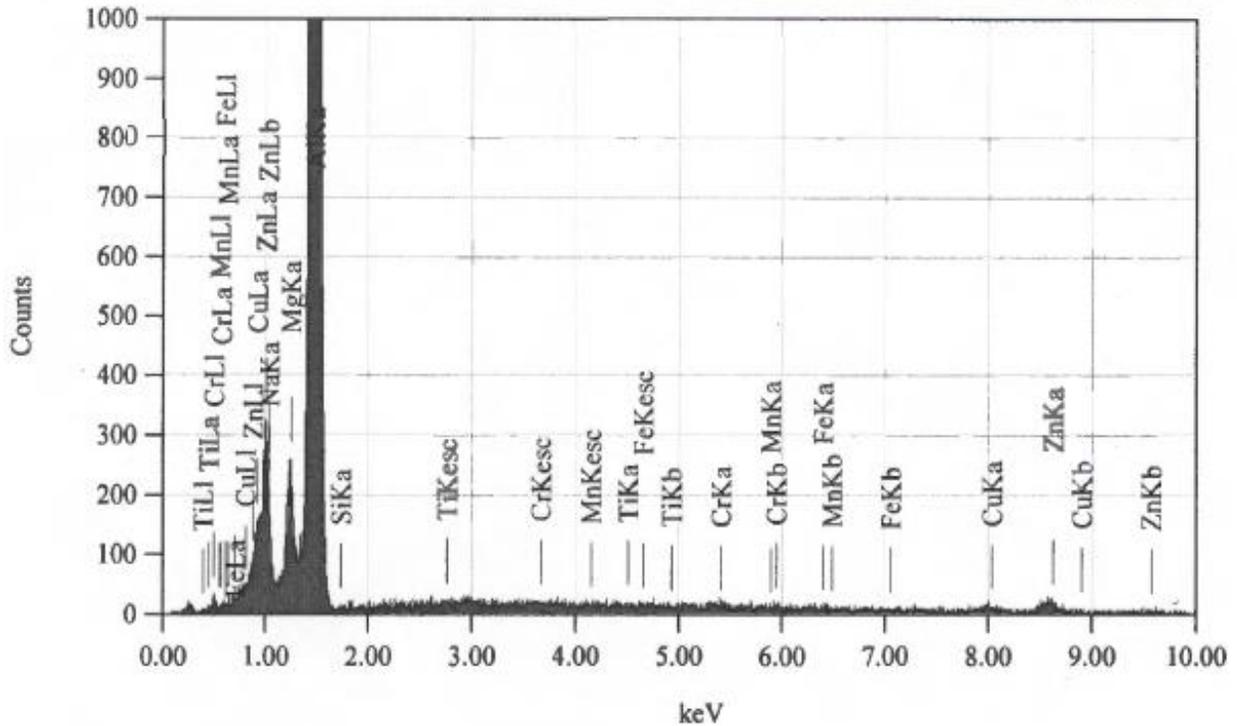
```
ZAF Method Standardless Quantitative Analysis
Fitting Coefficient : 0.0665
Element      (keV)   Mass%  Sigma  Atom%  Compound  Mass%  Cation        K
Al K        1.486   90.78   0.29  93.94                           89.7965
Zn K*       8.630    4.43   0.33   1.89                            5.2734
Mg K        1.253    2.86   0.07   3.29                            2.6362
Cu K*       8.040    1.50   0.20   0.66                            1.7847
Cr K*       5.411    0.30   0.08   0.16                            0.3516
Fe K*       6.398    0.10   0.08   0.05                            0.1215
Mn K*       5.894    0.03   0.09   0.02                            0.0360
Na K
Si K*
Ti K*
Total               100.00        100.00
```

Title	: IMG1
Instrument	: JCM-6000
Volt	: 15.00 kV
Mag.	: x 60
Date	: 2015/02/18
Pixel	: 512 x 384

```
Acquisition Parameter
Instrument    : JCM-6000
Acc. Voltage : 15.0 kV
Probe Current: 1.00000 nA
PHA mode      : T3
Real Time    : 102.03 sec
Live Time    : 100.00 sec
Dead Time    : 1 %
Counting Rate: 891 cps
Energy Range :  0 - 20 keV
```

**Appendix J: EDS Results for the Composition of the Red Corrosion Products**
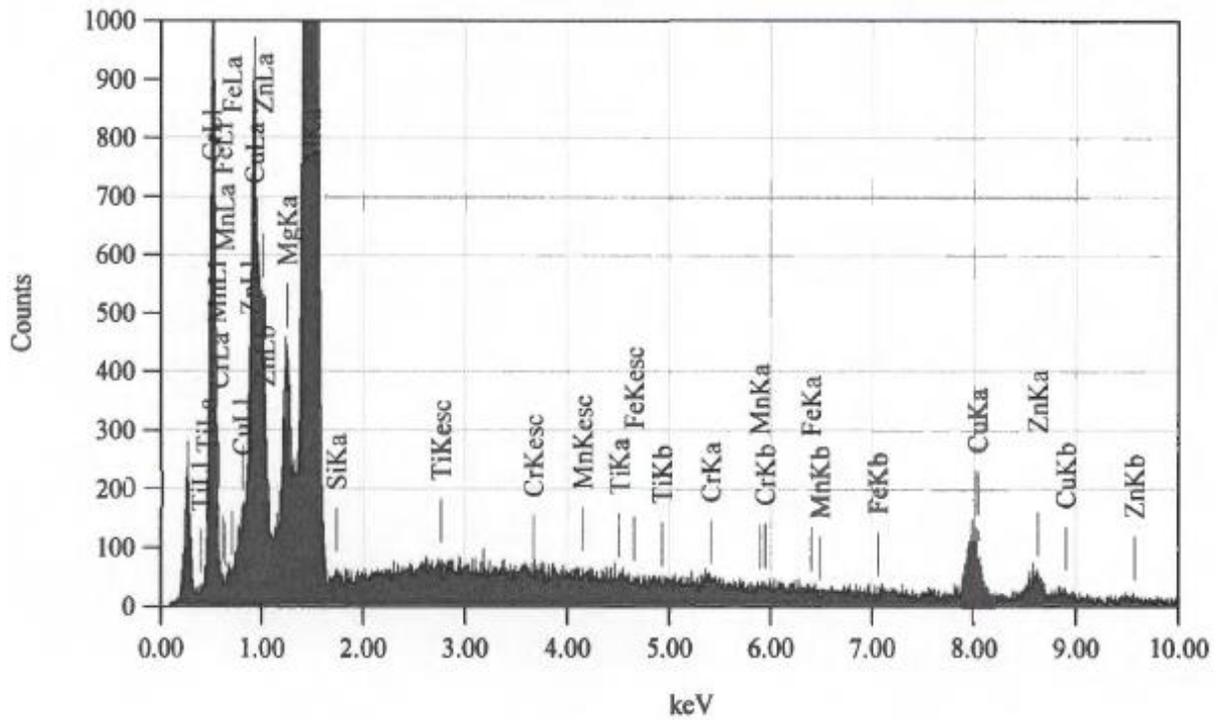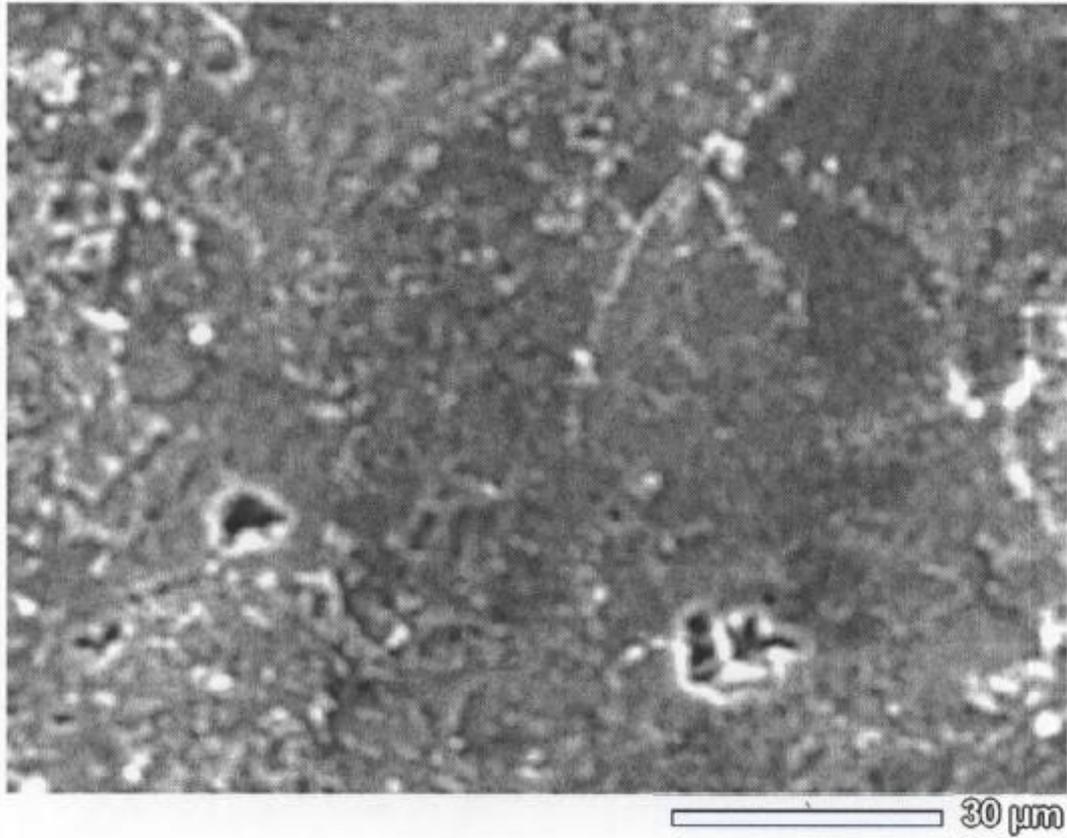
```
ZAF Method Standardless Quantitative Analysis
Fitting Coefficient : 0.1120
Element        (keV)   Mass%   Sigma   Atom%   Compound   Mass%   Cation          K
Al K           1.486   85.40   0.18    91.84                              81.8052
Cu K           8.040    7.71   0.17     3.52                              10.1568
Zn K           8.630    4.39   0.19     1.95                               5.7759
Mg K           1.253    1.99   0.05     2.38                               1.6550
Cr K*          5.411    0.32   0.05     0.18                               0.4183
Si K*          1.739    0.07   0.05     0.07                               0.0272
Ti K*          4.508    0.06   0.03     0.04                               0.0799
Fe K*          6.398    0.06   0.05     0.03                               0.0817
Mn K*
Total                 100.00          100.00
```

Title	: IMG1
Instrument	: JCM-6000
Volt	: 15.00 kV
Mag.	: x 1,000
Date	: 2015/02/20
Pixel	: 512 x 384

```
Acquisition Parameter
Instrument    : JCM-6000
Acc. Voltage  : 15.0 kV
Probe Current : 1.00000 nA
PHA mode      : T3
Real Time     : 102.03 sec
Live Time     : 100.00 sec
Dead Time     : 1 %
Counting Rate : 2216 cps
Energy Range  : 0 - 20 keV
```

Appendix K: Technical Specifications for Ascott S120ip Salt Spray Chamber

Salt spray chamber performance

Temperature range	Adjustable from ambient to +50°C/+122°F
Salt spray fall-out rates	Adjustable from 0.5 to 2.5 ml per 80 cm2 per hour
Wetting mode (Premium chambers only)	Adjustable from ambient to +50°C/+122°F
Drying mode (Premium chambers only)	Adjustable from ambient to +50°C/+122°F

Premium salt spray chambers		S120ip
Chamber Capacity		120 Ltrs/ 4.2cu ft
Mounting Format		Bench top
Loading threshold		280mm/11"
Chamber external dims, max	W	1315mm/51.8"
	D	680mm/26.8"
	H	800mm/31.5"
Chamber internal dims, max	W	715mm/28.2"
	D	490mm/19.3"
	H	490mm/19.3"
Salt solution reservoir ext. dims.	W	n/a (integral)
	D	n/a (integral)
	H	n/a (integral)
Salt solution reservoir capacity for extra capacity, see optional accessory ACC02		40 Ltrs/ 10.5 USgal
Removable slotted sample racks see also optional accessories ACC17/ACC18)		4 racks each with 23 angled slots

Chamber construction	Glass reinforced plastic, Polypropylene & PVC parts
Color	9 standard colors to choose from

Electricity supply
  Standard models
  Premium models
	1 phase
	1 phase
	Voltage (VAC) and frequency (Hz) dependant on country/region of installation

Water	Deionized/distilled for topping up air saturator and making salt solution. Air saturator requires a continuous water connection 0.5-6.0 bar (7.3-87 psi). If air saturator is topped up manually option ACC66 must be ordered
Air	Clean dry & oil free, 4.0 to 6.0 bar (58-87psi) with 240 Ltrs (8.5cu.ft) per minute flow
Exhaust	3m (10ft) exhaust pipe is provided which should be terminated outside building
Drain	3m (10ft) drain pipe provided which should be terminated into floor level drain
Operating environment conditions	+18 to +23°C (+64 to 73°F), 85% max RH (non condensing) ambient

Appendix L: Technical Specifications for Instron 5585H Load Frame

		5585H
Load Capacity	kN	250
	kgf	25000
	lbf	56200
Maximum Speed	mm/ min	500
	in/ min	20
Minimum Speed	mm/ min	0.001
	in/ min	0.00004
Maximum Force at Full Speed	kN	100
	lb	22500
Maximum Speed at Full Load	mm/ min	200
	in/ min	8
Return Speed	mm/ min	500
	in/ min	20
Position Control Resolution	μm	0.060
	μin	2.4
Total Crosshead Travel	mm	1180
	in	46.5
Total Vertical Test Space (Note 5)	mm	1256
	in	49.4
Depth Daylight	mm	NA
	in	NA
Space Between Columns	mm	575
	in	22.6
Height (Note 7)	mm	2092
	in	82.4
Width	mm	1300
	in	51.2
Depth	mm	756
	in	29.8
Weight	kg	952
	lb	2100
Maximum Power Requirement	VA	2850

Common Specifications

Position Measurement Accuracy: ±0.02 mm or 0.05% of displacement (whichever is greater)

Crosshead Speed Accuracy (Zero or constant load): ±0.1% of set speed

Load Measurement Accuracy: ±0.4% of reading down to **1/100** of load cell capacity, ±0.5% of reading down to **1/250** of load cell capacity

Strain Measurement Accuracy: ±0.5% of reading down to **1/50** of full range with ASTM E83 class B or ISO 9513 class 0.5 extensometer

Single Phase Voltage: For 5581, 5582, and 5584 - 100,120, 220, or 240 VAC ±10%; For the 5585H 200/208, 220, 230, 240 VAC ±10%, 47 to 63 Hz. Power supply must be free of spikes, surges or sags exceeding 10% of the average voltage.

Operating Temperature: +10 °C to +38 °C (+50 °F to +100 °F)

Storage Temperature: -40 °C to +66 °C (-40 °F to +150 °F)

Humidity Range: +10% to +90%, non-condensing

Atmosphere: Designed for use under normal laboratory conditions. Protective measures may be required if excessive dust, corrosive fumes, electromagnetic field or hazardous conditions are encountered.

Notes:

5. Total vertical test space is the distance from the top surface of the base platen to the bottom surface of the moving crosshead, excluding load cell, grips and fixtures.

7. Add 295 mm (11.6 in) to 5581, 5582, 5584 and 5585 heights when the optional 2910-061 load frame support base/ extension is included.